Programa de Doctorado en Biotecnología - Universidad Pública de Navarra
Instituto de Agrobiotecnología - Consejo Superior de Investigaciones Científicas

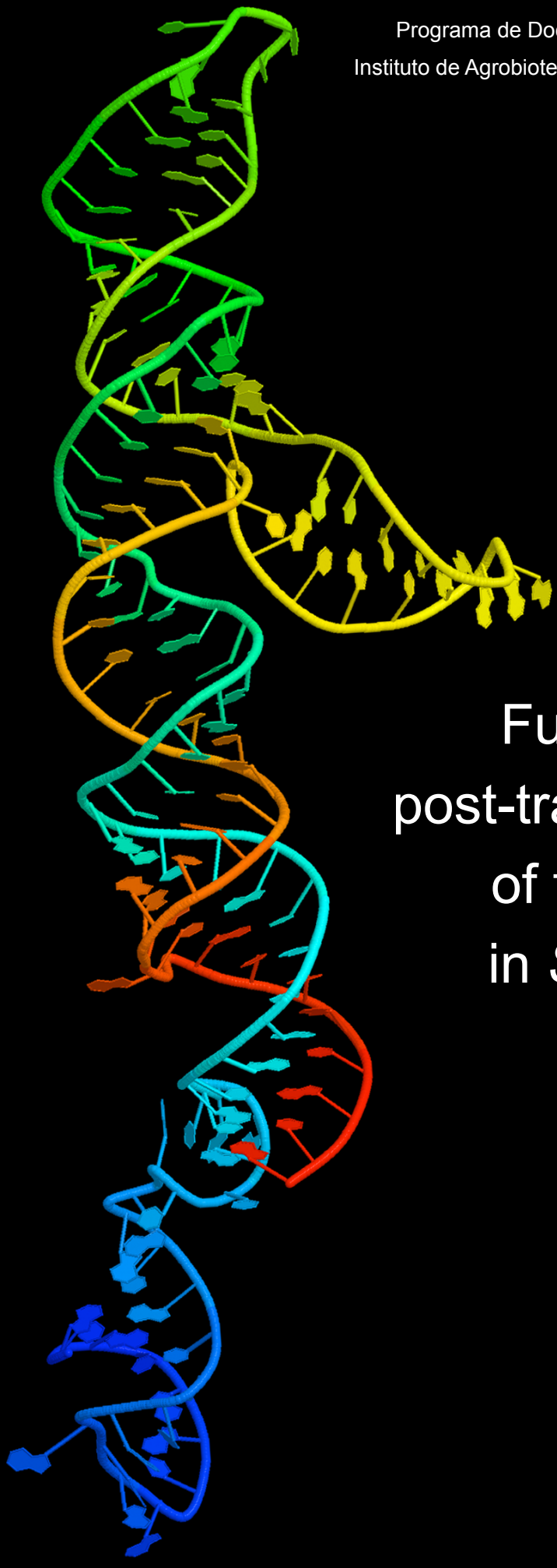

DOCTORAL THESIS

Functional specificity and post-transcriptional regulation of the cold shock proteins in *Staphylococcus aureus*

Arancha Catalan-Moreno

Pamplona, 2020

upna
Universidad Pública de Navarra
Nafarroako Unibertsitate Publikoa

TESIS DOCTORAL

Functional specificity and post-transcriptional regulation of the cold shock proteins in *Staphylococcus aureus*

Memoria Presentada por

ARANCHA CATALÁN MORENO

Para optar al grado de Doctor por la Universidad Pública de Navarra

Director:

Dr. ALEJANDRO TOLEDO ARANA

Pamplona, 2020

Dr. ALEJANDRO TOLEDO-ARANA, Científico Titular del Consejo Superior de Investigaciones Científicas (CSIC), responsable del Laboratorio de Regulación Génica Bacteriana del Instituto de Agrobiotecnología (IdAB, CSIC-UPNA-GN)

INFORMA:

Que la presente memoria de Tesis Doctoral titulada "**Functional specificity and post-transcriptional regulation of the cold shock proteins in *Staphylococcus aureus***" que ha sido elaborada por Doña **ARANCHA CATALÁN MORENO**, ha sido realizada bajo su dirección y que cumple las condiciones exigidas por la legislación vigente para optar al grado de Doctor.

Y para que así conste, firma la presente en Pamplona, a 27 de Mayo de 2020.

Fdo. Alejandro Toledo Arana

“La voluntad es la joya de la corona de la conducta” Enrique Rojas

A mis padres.

AGRADECIMIENTOS

AGRADECIMIENTOS

Todo proceso de creación es un camino arduo, lleno de momentos duros, desesperación e incertidumbre, pero siempre con un final de satisfacción por el trabajo realizado. Así es también la ciencia. Esta tesis no hubiese visto la luz sin la colaboración de un grupo humano incansable y de primera categoría que de una manera u otra han formado parte de este proyecto. Por lo que, me gustaría agradecer a:

La Universidad Púbica de Navarra, el Consejo Superior de Investigaciones Científicas y el Instituto de Agrobiotecnología, gracias a estas tres instituciones se ha podido llevar a cabo dicha tesis.

Alejandro, porque su incansable esfuerzo como director y su humildad han hecho posible este trabajo. Ha sido una suerte poder aprender e investigar a su lado. El ejemplo de lucha, confianza, respeto y adaptación a los problemas son enseñanzas que siempre llevaré presentes. No quiero dejar de agradecer todas las oportunidades brindadas para que poco a poco creciera como persona y científica. Gracias de corazón.

Carlos, Pilar y Naiara con los que empecé este proyecto y que se convirtieron en un apoyo indispensable. Gracias por siempre ofrecerme vuestra mano y estar conmigo en los momentos más difíciles. En especial a Naiara porque su comprensión y positividad han sido esenciales para mi. Marta, Pili, Laurène y Leticia por ayudarme siempre, darme buenas ideas y compartir buenos momentos fuera y dentro del laboratorio. Jaione porque su llegada no hizo más que sumar, gracias por todos los buenos consejos y momentos compartidos.

El grupo de Biofilms Microbianos, Iñigo, Cristina, Begoña, Pedro, Maite y Sonia por compartir tanta buena ciencia y ser ese grupo hermano en el que

tantos congresos, desayunos y buenos ratos hemos podido disfrutar juntos. Beatriz, buena amiga, siempre dispuesta a ayudar, gracias por esos días inolvidables recorriendo Grecia.

Junkal y su grupo por sus buenas aportaciones y comentarios sobre este trabajo durante estos últimos meses.

Mari Jose, Idoia, Elena, Inés, Sara, Anabel, Fernando Armona y todas las personas que han pasado por el servicio de apoyo a la investigación y administración, por su labor incalculable e indispensable.

Todas las personas del Idab que sobrepasan las barreras institucionales y que son verdaderos compañeros. En especial a Edu, Javi, Mikel, Dani, Maite, Adriana, Kike, Arguiñe, Belda, Inés y Ana por todos esos buenos momentos jugando al voleibol, tenis, padel, nuestras comidas y fiestas.

Los amigos que encontré en este centro ¡Que bueno que nuestros caminos se cruzaron! Victor, por ser esa persona tan maravillosa y “tonta” de las que este mundo está necesitado. María A. por trasmitirme siempre tranquilidad y positividad. Lorena y Saioa vuestros consejos y filosofía de vida han sido fundamentales. Espero podamos seguir celebrando juntas todas nuestras pequeñas victorias. Sois únicas.

El grupo de RNA mensajeros y RNA reguladores bacterianos en el IBMC de Estrasburgo, por acogerme durante tres meses y hacerme sentir una más de su grupo Isabelle, Pascale, Stefano, David, Lucas, Laura y Anne-Catherine. Emma y Paula con las que disfrute cada día del Crous y me ayudaron a integrarme en la cultura francesa gracias a las tardes de apéro.

Las chicas del equipo de padel de San Juan, por preocuparse y hacerme olvidar los malos días de trabajo. Todo el equipo de Padel and Foot

Strasbourg, que me acogieron sin conocerme e hicieron que las tardes y los fines de semana volaran.

No quiero olvidarme de mis amigas Irene, Amaya, Iosune, Esti, Isabel y Andrea, esas piezas imprescindibles en mi vida. Gracias por hacerme sentir especial y visitarme cuando he estado lejos de casa.

Toda mi familia, tíos y primos que siempre se preocupan por mi y se alegran de todas las cosas buenas que me pasan. En especial a mis tíos José Luis y María Jesús, por su cariño y preocupación en que todo saliera bien. Mi tío Santi, por su interés en que mis bacterias crecieran bien. Mi segunda familia, Santiago, Pili, Marta y Luis por darme todo su cariño.

Mi abuela Victoria y mi tío Fermín, porque su lucha y resiliencia han sido un ejemplo para mí.

Tengo la suerte de tener a unas pocas personas que siempre están a mi lado. En primer lugar, mi hermano, gracias por ofrecerme siempre tu amor y generosidad por encima de todo. También Marta y mi pequeña Helena por vuestra dulzura y naturalidad ante la vida. Juan, por ser mi mejor complemento, ayudarme a crecer, comprenderme y animarme cuando más lo necesito. Siempre tendré presente tu lema: “10% lo que te pasa, 90% cómo reacciones”. De forma especial a mis padres, porque su esfuerzo y apoyo a lo largo de todos estos años han hecho que pueda conseguir todas mis metas. Mi padre, por ayudarme a pensar y enseñarme con paciencia y prudencia. A ti mamá, mi mejor maestra, por guiarme y moldearme para sacar la mejor versión de mi misma.

Millones de gracias.

Este trabajo ha sido realizado gracias a la financiación recibida a través de los siguientes proyectos de investigación:

European Research Council Consolidator grant ERC-coG-2014-646869: "High-throughput in vivo studies on post-transcriptional regulatory mechanisms mediated by bacterial 3'-UTRs".

Ministerio de Economía y Competitividad. BFU2011-56698-P: "Regulación post-transcripcional mediada por las regiones 3' no traducidas del RNA mensajero en bacterias".

Consejo Superior de Investigaciones Científicas.PIE-201540I013: "Regulación post-transcripcional mediada por RNAs y proteínas de unión a RNA en bacterias patógenas".

TABLE OF CONTENTS

ABBREVIATIONS

CDS	Coding sequence
CLIP	Cross-linking immunoprecipitation
CSP	Cold shock protein
PAGE	Polyacrylamide gel electrophoresis
RBP	RNA-binding protein
mRNA	Messenger RNA
ncRNA	Non-coding RNA
RBS	Ribosome binding site
RIP	RNA immunoprecipitation
RNAT	RNA thermometer
SD	Shine-Dalgarno
sRNA	Small RNA
STX	Staphyloxanthin
UTR	Untranslated region
5'UTR	5' untranslated region
3'UTR	3' untranslated region

SUMMARY

SUMMARY

Staphylococcus aureus is a widespread pathogen that colonizes humans, animals, hospitals and community facilities. Its ability to produce severe diseases, resist to most of the antimicrobials used in healthcare systems and its persistence in a wide range of inanimate surfaces have led to efforts in developing new prevention and treatment strategies. In this regard, understanding how virulence, antimicrobial resistance and environmental survival work in this pathogen are considered crucial. Recent discoveries depict post-transcriptional regulation as a key layer in the control of *S. aureus* gene expression. RNA binding proteins (RBPs) are important players in such layer of regulation. In this thesis, we have explored the functional specificity (Chapter I) and the post-transcriptional regulation (Chapter II) of the cold shock proteins (CSPs), a family of RNA chaperones that are present in all kingdom of life but whose function remains poorly understood.

S. aureus encodes three *csp* genes that share a protein sequence identity higher than 70%. Therefore, discriminating between functional divergence and redundancy between them proved challenging. Previous works of our group showed that the expression of CSPs was subjected to a tight post-transcriptional control that prevented us from comparing their functionalities. Thus, we engineered the *cspA* mRNA to express the CSPs paralogs coding sequences (CDSs) while sharing the same untranslated regions. Although

this strategy ensured similar CSP levels, only CspA could specifically restore the phenotypes in a *ΔcspA* strain indicating a certain degree of functional specificity among CSPs. To determine the amino acid residues responsible for CspA specificity, we created several chimeric CSPs by interchanging the amino acid differences between the CspA and CspC CDSs. We found that CspA Pro58 was crucial for modulating the CspA-associated phenotypes. Interestingly, we were able to transfer CspA specificity to CspC when introducing the E58P substitution. These results highlighted how just one evolutionarily selected amino acid change may be sufficient to modify the functionality of CSP paralogs.

Next, we focused on deciphering what were the post-transcriptional regulatory mechanisms controlling the expression of the CspB and CspC proteins. *In silico* bioinformatic analyses, *in vitro* structural probing experiments and *in vivo* site-directed mutagenesis demonstrated that the CspB and CspC expression was thermoregulated when *S. aureus* transitioned from host-related (37ºC) to ambient temperatures (e.g. 22 and 28ºC). This thermoregulation occurred at the post-transcriptional level through the action of two orthologous thermo-sensitive RNA elements located in the *cspB* and *cspC* 5'UTRs. Depending on the temperature, the 5'UTRs could form two mutually exclusive alternative structures, which behaved as RNA thermoswitches controlling CspB and CspC translation. At host-related temperatures, the 5'UTRs folded into a locked conformation in which the RBS was blocked by an anti-RBS sequence that inhibited CSP translation. In contrast, when *S. aureus* faced ambient temperatures, the 5'UTRs refolded into an open conformation, thereby sequestering the anti-

RBS sequence in an RNA hairpin that, in return, released the RBS and promoted translation. We also showed that the temperature-dependent repression involves the action of CspA. In addition, we demonstrated that the thermoregulation of CspB and CspC proteins is required for *S. aureus* survival when leaving their natural host. These regulatory elements were similar to those recently described in *Escherichia coli* and *Listeria monocytogenes*. Using *in silico* RNA structural comparative analyses, we found that RNA-thermoswitches were also present in other species.

In summary, this thesis has revealed relevant aspects about the functions of *S. aureus* CSPs and their regulation that may apply to other bacteria. Specifically, we demonstrated that just one amino acid might be sufficient to confer CspA specificity in *S. aureus* and that the CSPs may not share the same targets despite their high protein identity. At the same time, we highlighted the importance of RNA-mediated thermoregulation to control CspB and CspC translation when *S. aureus* transitions from the host to the environment, a post-transcriptional regulatory mechanism that seems to be wide-spread in bacteria.

Sections of this Doctoral Thesis have been or will be published in the following articles:

Catalan-Moreno A, Caballero CJ, Irurzun N, Cuesta S, López-Sagaseta J and Toledo-Arana A. One evolutionarily selected amino acid variation is sufficient to provide functional specificity in the cold shock protein paralogs of *Staphylococcus aureus*. **Molecular Microbiology** 113(4): 826-840 (2020)

Catalan-Moreno A, Cela M, Menendez-Gil P, Irurzun N, Caballero CJ, Caldelari I and Toledo-Arana A. Thermoregulation of CspB and CspC proteins is required for *Staphylococcus aureus* growth at ambient temperature. **In preparation**.

Other publications in relationship with this topic in which the candidate has participated:

Caballero CJ, Menendez-Gil P, **Catalan-Moreno A**, Vergara-Irigaray M, García B, Segura V, Irurzun N, Villanueva M, Ruiz de los Mozos I, Solano C, Lasa I and Toledo-Arana A. The regulon of the RNA chaperone CspA and its autoregulation in *Staphylococcus aureus*. **Nucleic Acids Research** 46 (3): 1345-1361 (2018).

Menendez-Gil P, Caballero CJ, **Catalan-Moreno A**, Irurzun N, Barrio-Hernandez I, Caldelari I and Toledo-Arana A**.** Differential evolution in 3'UTRs leads to specific gene expression in *Staphylococcus*. **Nucleic Acids Research** 48 (5): 2544–2563 (2020).

RESUMEN

RESUMEN

Staphylococcus aureus es un patógeno muy extendido capaz de colonizar humanos y animales, y contaminar hospitales y viviendas. Debido a su habilidad para producir enfermedades graves, resistir a la mayoría sino a todos los antibióticos usados en clínica, y a su capacidad para persistir en una gran variedad de superficies, resulta necesario buscar nuevas alternativas para prevenir y tratar las enfermedades asociadas a *S. aureus*. Entender como la virulencia, la resistencia a los antibióticos y la supervivencia en el ambiente son reguladas por *S. aureus* es esencial para avanzar en esta dirección. Descubrimientos recientes muestran que la regulación post-transcripcional es un nivel clave para controlar la expresión génica en *S. aureus*, siendo las proteínas de unión a ARN (RBPs) actores importantes en este proceso.

En esta tesis, hemos estudiado la especificidad funcional (Capítulo I) y la regulación post-transcripcional (Capítulo II) de las *cold shock proteins* (CSPs), una familia de chaperonas del ARN que se encuentran presentes en todos los seres vivos. Sin embargo, la mayoría de las funciones de las CSPs son todavía desconocidas. *S. aureus* codifica tres genes *csp* que comparten una secuencia proteica con una identidad superior al 70%. Por lo tanto, discernir si las CSPs cumplen funciones redundantes o, por el contrario, actúan de manera específica, resulta extremadamente complejo. Estudios previos de nuestro grupo mostraban que la expresión de las CSPs

estaba sujeta a una compleja regulación post-transcripcional que impedía comparar de manera equivalente las funciones de las mismas. Con el fin de solventar este problema, el ARNm de *cspA* fue modificado para que expresase las otras proteínas parálogas manteniendo sus regiones no traducidas. Aunque esta estrategia aseguraba niveles similares de las CSPs, solo CspA pudo restaurar los fenotipos en un mutante de *cspA*, lo que indicaba un cierto grado de especificidad funcional entre las CSPs. Con el fin de determinar qué residuos aminoacídicos eran responsables de dicha especificidad, creamos varias quimeras de las CSPs donde se intercambiaban los amino ácidos que eran diferentes entre CspA y CspC, las dos CSPs con mayor porcentaje de identidad. Así demostramos que la Pro58 de CspA era la responsable de controlar específicamente los fenotipos asociados a esta proteína. Curiosamente, la especificidad de CspA podía ser transferida a CspC cuando únicamente se introducía la mutación E58P. Estos resultados mostraban cómo un solo amino ácido seleccionado evolutivamente podía ser suficiente para modificar la especificidad funcional en los parálogos de las CSPs.

Posteriormente, nos centramos en descifrar cuáles eran los mecanismos de regulación post-transcripcionales que controlaban la expresión de las proteínas CspB y CspC. Estudios bioinformáticos *in silico*, experimentos estructurales *in vitro* y mutagénesis direccionadas *in vivo* demostraron que la expresión estaba termorregulada cuando *S. aureus* pasaba de crecer de temperaturas relacionadas con su huésped (37ºC) a temperaturas

ambientales (por ejemplo, 22 y 28ºC). Esta termorregulación ocurría a nivel post-transcripcional a través de la acción de dos elementos ortólogos de ARN termosensibles localizados en las 5'UTRs de los ARNm de *cspB* y *cspC*. Dependiendo de la temperatura, las 5'UTRs pueden adoptar dos estructuras alternativas, que actúan como ARN termosensores controlando la traducción de CspB y CspC. A temperaturas relacionadas con el huésped, las 5'UTRs forman una conformación cerrada en la que la RBS se encuentra bloqueada por una secuencia anti-RBS, inhibiendo así la traducción. Por el contrario, cuando *S. aureus* crece a temperatura ambiente, las 5'UTRs se reorganizan en una conformación abierta donde la secuencia anti-RBS es secuestrada por una horquilla de ARN, liberando la RBS para inducir la traducción. Demostramos también que esta reorganización estructural requiere la acción de CspA. Además, revelamos que la termorregulación de las proteínas CspB y CspC es necesaria para la supervivencia de *S. aureus* cuando abandona su hospedador natural. Estos ARN termosensores son similares a los descritos recientemente en *Escherichia coli* y *Listeria monocytogenes*. Mediante análisis *in silico* de comparación estructural, encontramos que estos elementos reguladores están presentes en otras especies bacterianas.

En resumen, en esta Tesis se han descifrado aspectos relevantes sobre las funciones de las proteínas CSPs de *S. aureus* y su regulación, que pueden ser extrapoladas a otras bacterias. Específicamente, demostramos que sólo un amino ácido es suficiente para conferir la especificidad funcional de

CspA en *S. aureus* y sugerimos que las CSPs no compartirían las mismas dianas a pesar de tener una gran homología proteica. Al mismo tiempo, destacamos la importancia de la termorregulación mediada por estructuras de ARN que controlan la traducción de las proteínas CspB y CspC cuando *S. aureus* abandona su hospedador y pasa al ambiente, un mecanismo de regulación post-transcripcional que parece estar extendido en el mundo bacteriano.

Secciones de esta Tesis Doctoral han sido o serán publicadas en los siguientes artículos:

Catalan-Moreno A, Caballero CJ, Irurzun N, Cuesta S, López-Sagaseta J and Toledo-Arana A. One evolutionarily selected amino acid variation is sufficient to provide functional specificity in the cold shock protein paralogs of *Staphylococcus aureus*. **Molecular Microbiology** 113(4): 826-840 (2020)

Catalan-Moreno A, Cela M, Menendez-Gil P, Irurzun N, Caballero CJ, Caldelari I and Toledo-Arana A. Thermoregulation of CspB and CspC proteins is required for *Staphylococcus aureus* growth at ambient temperature. **In preparation**.

Otras publicaciones relacionadas con el tema en las que la candidata ha participado:

Caballero CJ, Menendez-Gil P, **Catalan-Moreno A**, Vergara-Irigaray M, García B, Segura V, Irurzun N, Villanueva M, Ruiz de los Mozos I, Solano C, Lasa I and Toledo-Arana A. The regulon of the RNA chaperone CspA and its autoregulation in *Staphylococcus aureus*. **Nucleic Acids Research** 46 (3): 1345-1361 (2018).

Menendez-Gil P, Caballero CJ, **Catalan-Moreno A**, Irurzun N, Barrio-Hernandez I, Caldelari I and Toledo-Arana A**.** Differential evolution in 3'UTRs leads to specific gene expression in *Staphylococcus*. **Nucleic Acids Research** 48 (5): 2544–2563 (2020).

INTRODUCTION

INTRODUCTION

1. *Staphylococcus aureus*, an important life-threating pathogen

Staphylococcus aureus is a Gram-positive pathogen that belongs to the family of *Staphylococcaeae*. It was first isolated from a surgical wound infection in 1880s by Alexander Ogston and described as a spherical bacterium of approximately 1 μm in diameter forming grape-like clusters. *S. aureus* is part of the human microbiota colonizing mainly the nose, the skin and their glands, but also the gastrointestinal (GI) tract flora. Approximately 20-25% of the adult population are persistent nasal carriers and a further 10-30% classified as intermittent carriers (Flaxman *et al.*, 2017; Krismer *et al.*, 2017). *S. aureus* is the leading cause of infective endocarditis, osteomyelitis, skin and soft tissue diseases, as well as pleuropulmonary and device related infections. The presence of this bacterium in the human body increases the risk of infection. In fact, immunocompromised or hospitalized carriers are at high risk of developing bacteraemia. The nasal strain is usually found as the initial cause of the infection (Marchfelder and Hess, 2012; Novick, 2003; Tong *et al.*, 2015).

Aside from humans, *S. aureus* is documented to be a member of farm animals causing mastitis in cows, goats and sheep. These reservoirs also represent a source of colonization for humans. In addition, primates could be oro-pharingeal and faecal carriers (Schaumburg *et al.*, 2013) as well as rabbits, pigs and piglets that can be colonized with similar strains related to

a human clone (Holmes *et al.*, 2016). In high density pig farming areas in Europe, livestock-associated methicillin-resistant *Staphylococcus aureus* (LA-MRSA) strains, particularly the clonal complex CC398, have emerged as relevant zoonotic agents. Normally, professional individuals in contact to livestock are colonized with LA-MRSA and they are usually the source of introduction of LA-MRSA into hospitals and households (Becker *et al.*, 2017).

Despite the fact that mice are not a natural host of *S. aureus*, an outbreak in an animal facility also revealed that the affected animals were persistently colonized with a mouse-adapted *S. aureus* strain (Holtfreter *et al.*, 2013).

Due to the high prevalence of *S. aureus* in humans and animals, the presence of *S. aureus* is usually detected in food and has caused important food poisoning outbreaks. The CC398 was also found in up to 11.9% of meat samples from different parts of the world becoming a potential threat to human health (de Boer *et al.*, 2009). Therefore, hygiene measures during food production processes are essential and extremely recommended to prevent *S. aureus* foodborne diseases (Fetsch and Johler, 2018).

S. aureus is also an important community pathogen being part of households, hospitals, schools and day-care facilities increasing the risk for recurrent infections and transmissibility. It can contaminate environmental surfaces of a wide variety of items including bathroom, sinks, remote controls, toilet seats, computers, towels, telephones among other elements. In recent years, environmental contamination with *S. aureus* has been

recognized as a potential risk and mediator of its transmission to the human host (Knox *et al.*, 2015). Epidemiologic studies suggested that nasal colonization plays a less prominent role in the contagiousness and pathogenesis than environmental contamination (Miller and Diep, 2008; Davis *et al.*, 2012). The main mode of transmission is through direct contact (person-person or fomite-person). Unfortunately, strategies to reduce contamination among household have had no impact due to the multiple areas of re-colonization. Thus, there is an urgent need to develop new and better approaches that contribute to the eradication of resistant *S. aureus* clones. Those strategies will depend on the discovery of different factors that impair their great survival (Knox *et al.*, 2015).

The versatility to invade different niches and cause a wide range of infections can be attributed to its ability to produce a wide set of virulence and stress-resistance genes. Most of these factors include surface proteins necessary for adhesion and invasion of the host, exoproteins for immune evasion or toxins for disseminations and acquisition of nutrients (Novick, 2003; Marchfelder and Hess, 2012). To adapt to the ever changing environment, *S. aureus* encoded multiple regulators. An example is the accessory gene regulator (agr), which controls virulence gene expression by sensing an autoinducing peptide (AIP), which accumulates when bacterial population increase. The agr system consists of two adjacent transcripts RNAII and RNAIII controlled by P2 and P3 promoters, respectively. The RNAII is composed of four genes *agrBDCA* that encode

the machinery of the *agr* system. The RNAIII is a dual mRNA encoding the δ-hemolysin and acting as a post-transcriptional RNA regulator controlling the expression of agr-dependent genes. RNAIII target genes include the α-toxin (Hla), serine proteases (SplA-F), surface proteins (protein A, Spa), leukocidins, lipase or surface receptors (Jenul and Horswill, 2018). Another key regulator controlling the stress response is the sigma factor B (σ^B), which regulates more than 200 genes related to virulence, persistence, antibiotic resistant and biofilm formation (Guldimann *et al.*, 2016; Jenul and Horswill, 2018). For example, the production of the yellowish carotenoid pigment of *S. aureus*, staphyloxanthin (STX), which protects bacteria against oxidative stress and neutrophils killings, is directly induced by the SigB factor (Liu *et al.*, 2008). STX biosynthesis is carried out by the action of the enzymes encoded by the *crt* operon (Figure 1). The promoter of this operon is activated by the alternative SigB factor which is in turn upregulated by the cold shock protein A (CspA) (Katzif *et al.*, 2005) (Figure 1). Concerning biofilm formation, SigB repressed the production of the PIA-PNAG exopolysaccharide (Valle *et al.*, 2003). Interestingly, SigB is also able to repress the transposition of IS256, an insertion sequence present in some staphylococcal strains. In absence of SigB, IS256 transposition is increased, causing the disruption of the *icaADBC* operon in some clones that become unable to form biofilm. Therefore, SigB modulates IS256-mediated phase variation in *S. aureus* (Valle *et al.*, 2019) (Figure 1).

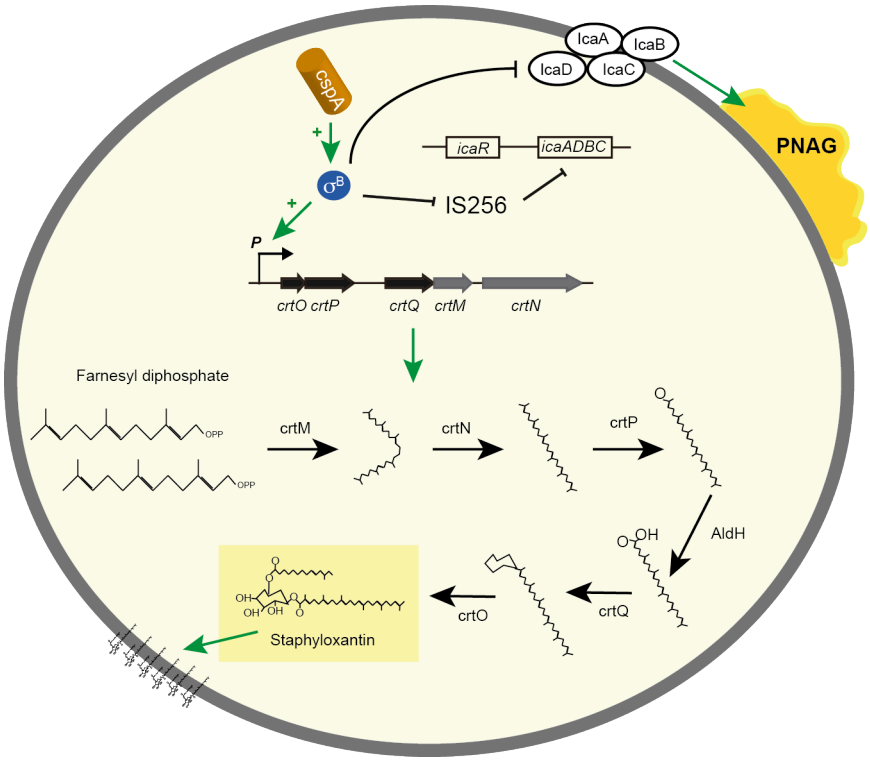

Figure 1. Schematic representation of staphyloxanthin biosynthesis and SigB regulation of *cspA*-associated phenotypes in *S. aureus*. The staphyloxanthin precursors are two molecules of farnesyl diphosphate that undergo multiple chemical reactions due to the action of enzymes encoded by the *crtOPQMN* operon. The cold shock protein CspA, triggers the expression of the sigma factor B (σ^B) that subsequently activates the promoter of the *crtOPQMN* operon producing an increase in staphyloxanthin production. At the same time, SigB is also involved in repressing PNAG production and IS256 transposition to *ica* genes that also affects biofilm formation.

In addition to virulence genes production, the acquisition of antibiotic resistance genes is also a powerful weapon that enhances *S. aureus* mortality. The excessive and inappropriate exposure to antibiotics has led to the emergence of denominated methicillin resistant strains of *S. aureus* (MRSA). Most antibiotics to treat *S. aureus* such as penicillin, streptomycin, tetracycline, erythromycin, chloramphenicol or methicillin have become obsoletes as bacteria have developed different strategies to overcome and survive under antibiotic pressure. A recent report from the World Health Organization (WHO) alerts of the serious situations of antibiotic resistance worldwide being *Staphylococcus aureus* one of the most commonly resistant bacteria. Thus, the understanding of the molecular mechanisms controlling the survival and adaption of *S. aureus* is crucial for developing new antimicrobial therapies.

2. Post-transcriptional regulation in bacteria

Gene expression processes include essential molecular mechanisms facilitating bacterial adaptation in response to changing environments. During many years, mRNA levels were considered as a direct indicator of the protein abundance. Conversely, in the past decades, a huge amount of studies demonstrated that in many cases there is a weak correlation between the mRNA and protein levels. In bacteria, elements usually modulating RNA decay, translation initiation efficiency or transcript

elongation are known as post-transcriptional regulators, and include non-coding (ncRNAs) and RNA binding proteins (Picard *et al.*, 2009).

2.1. Non-coding RNAs

Technological advances in RNA sequencing unveiled diverse ncRNAs from different organisms, including small RNAs, riboswitches, antisense RNAs, and long 5' and 3'UTRs. These ncRNAs were far more abundant than previously anticipated. ncRNAs can be classified in two different categories: *cis*- or *trans*-acting RNAs. The first category is formed by ncRNAs encoded on the opposite DNA strand of their targets and share 100% complementarity. Nevertheless, their ability to bind other RNAs cannot be excluded (Lasa *et al.*, 2012). *Trans*-acting sRNAs are about 50-500 nt long that bind with some complementarity to their target mRNAs, which are often encoded in distinct loci. The mRNA-sRNA interaction usually occurs near the ribosome binding site (RBS) to inhibit ribosome loading. In addition, sRNAs are also able to bind to other mRNA areas including the CDS and the 3' end, affecting mRNA stability. Unlike *cis*-acting, *trans*-acting sRNAs usually require the presence of a RNA binding protein promoting the sRNA-mRNA interaction (Kaberdin and Bläsi, 2006; Waters and Storz, 2009; Picard *et al.*, 2009; Papenfort and Vanderpool, 2015; Bronsard *et al.*, 2017). In addition, the untranslated regions of the mRNAs could also contain *cis*-acting regulatory elements that directly control mRNA expression. For example, riboswitches, RNA thermosensors (heat or cold shock) or pH

sensors can be found in the 5'UTRs (Narberhaus *et al.*, 2006; Waters and Storz, 2009; Nechooshtan *et al.*, 2009). Riboswitches are RNA elements sensing the presence of essential metabolites or ions to control the expression of genes codifying proteins that are usually involved in the metabolism or homoeostasis of these molecules (Winkler and Breaker, 2005). Riboswitches can modulate transcription or translation by changing RNA conformation upon metabolite binding. Inhibition of transcription occurs when RNA structures serve as a Rho-independent terminator while, in the other hand, activation is driven by anti-terminator hairpins that allow transcription. Similarly, translation is activated or inhibited by re-organization of secondary structures that release or sequester the RBS, respectively (Serganov and Nudler, 2013). Examples of riboswitches are found in *Listeria monocytogenes*, *Clostridium acetobutylicum*, *Escherichia coli, Enterococcus faecaclis, Salmonella thyphimurium* among others (Toledo-Arana *et al.*, 2009; Serganov and Nudler, 2013; Bastet *et al.*, 2018). Examples of pH or thermosensors changes will be further discussed below. The 3'UTRs have also been reported to post-transcriptionally regulate diverse states of mRNAs including degradation, localization or translation (Wilkie *et al.*, 2003; Ren *et al.*, 2017). It was shown that long 3'UTRs contain cleavage sites for ribonucleases to initiate mRNA decay (Selinger *et al.*, 2003). Accumulating evidences indicated that these regions are also rich reservoirs of sRNAs (Mayr, 2017) as for example the 3' end of *cpx* mRNA which represses in an Hfq-dependent manner multiple mRNAs encoding

extracytoplasmatic proteins in *E. coli* (Chao and Vogel, 2016). Another described function of 3'UTRs is their ability to overlap with regulatory sRNAs as the case of GadY that binds the 3'UTR of *gadX* gene increasing mRNA stability (Opdyke *et al.*, 2004). In addition, it has been shown that 3'UTRs are able to interact with the 5'UTRs of its own mRNAs to control translation and mRNA processing (Ruiz de los Mozos *et al.*, 2013; Braun *et al.*, 2017).

2.2. RNA-binding proteins

RNA-mediated regulation relies on the action of many RNA binding proteins (RBPs), which are essential players in the complex post-transcriptional regulatory networks. Researchers initially characterizing the heterogeneous nuclear ribobucleoproteins (hnRNP) were the first to realize that this protein contains a particular amino acid sequence responsible for RNA binding (Burd and Dreyfuss, 1994). In the past years, several RNA-binding domains (RBDs) have been characterized including the K-homology (KH) domain (type I and type II); RGG (Arg-Gly-Gly) box; SM domain; DEAD/DEAH box; Zinc finger (ZnF); double stranded RNA-binding domain (dsRBD); cold shock domain; Pumilo/FBF (PUF or Pum HD) domain; and the Piwi/Argonanute Zwille (PAZ) domain (Glisovic *et al.*, 2008) (Figure 2). Depending on their recognition pattern, RBPs can play critical roles affecting RNA structures, interactions or translation of mRNAs.

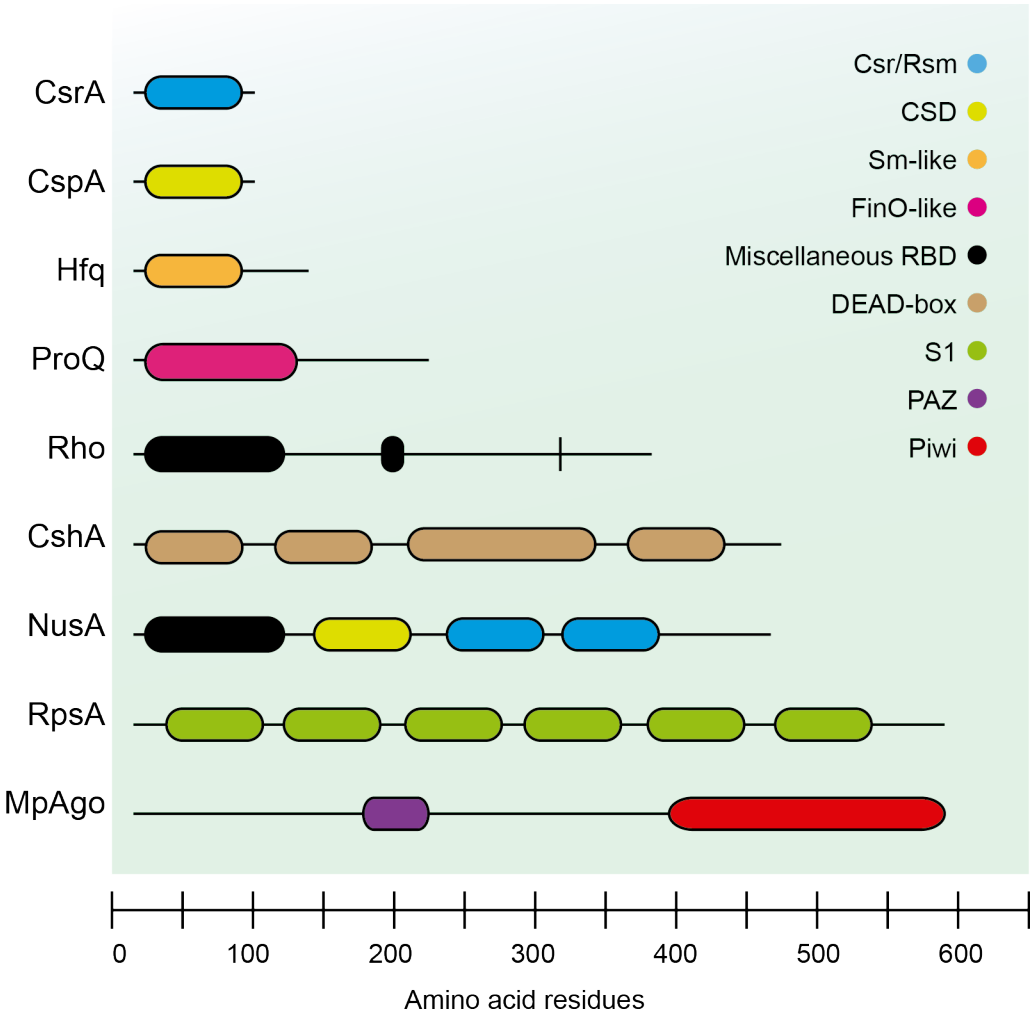

Figure 2. RNA-binding domains of RBPs. Examples of proteins containing different RNA binding domains described so far. The RNA-binding domains showed include the Csr/Rsm (blue), CSD (yellow), Sm-like (orange), FinO-like (pink), Miscellaneous RBD (black), DEAD-box (brown), S1 domain (green), PAZ (purple) and Piwi (red). The approximate size is also indicated in amino acid residues. This figure was adapted from Glisovic *et al.*, 2008.

RBPs have essential roles promoting RNA interactions, structure modifications, turnover, localization, export and translation of mRNAs (Glisovic *et al.*, 2008). The discovery of new RBPs had an enormous importance in eukaryotic and prokaryotic organisms. For example, mutations in the RBP TDP-43 disrupting its correct protein structure were proved to cause amyotrophic lateral sclerosis (ALS) in humans (Hanson *et al.*, 2012).

An increased number of RBPs are also being described in prokaryotes. In fact, between the 2-8% of the genome is predicted to encode RBPs (Glisovic *et al.*, 2008). However, the functions of most of them remain poorly understood, even in relevant Gram-positive pathogens such as *S. aureus*. In general, RBPs can be classified into three large groups: ribonucleases, ribosomal proteins and RNA chaperones. Ribonucleases (RNases) are a family of enzymes involved in RNA processing that recognize a specific sequence and/or structure. Numerous RNases with different processing patterns are encoded in bacteria such as RNase E, PNPase, RNase J1 or J2 (Mathy *et al.*, 2010; Lioliou *et al.*, 2012; Bonnin and Bouloc, 2015). Likewise, ribosomal proteins are structural components of the ribosomes capable of binding RNA and participating in mRNA translation. In bacteria, the ribosomes (70S) are composed of a small subunit 30S (comprised of 21 ribosomal proteins (r-proteins) and 1 ribosomal RNA (rRNAs) 16S) and a large subunit 50S (formed by 34 r-proteins and 2 rRNAS, 23S and 5S) (Wilson and Nierhaus, 2005; Fox, 2010).

Finally, the RNA chaperones belong to a heterogeneous group of proteins that facilitate RNA-RNA interactions, occlude RBS regions or refold specific RNA structures to modulate gene expression. In the following section the functions of the main bacterial RNA chaperones are described.

3. RNA Chaperones

RNA chaperones are RBPs carrying out essential biological functions including RNA misfolding reducement, improvement of the matchmaking between regulatory RNA and targets, and the control of translation by interacting with specific regions of the mRNAs. The loss of RNA chaperone proteins can lead to impaired growth, reduced tolerance to different environmental stresses, and reduced virulence (Woodson *et al.*, 2018).

3.1. RNA chaperones targeting mRNAs to modulate translation

The carbon storage regulator A (CsrA) belongs to the Csr/Rsm protein family, which includes highly conserved RBPs of approximately 7 kDa found in almost all bacterial phyla. CsrA was primarily described as essential for glycolysis activation and gluconeogenesis suppression. However, a new global regulatory role has been recently attributed (Sabnis *et al.*, 1995; Holmqvist *et al.*, 2016; Potts *et al.*, 2017). CsrA forms a dimer that leads to a β-barrel structure composed of 10 antiparallel β -sheets, containing an RNA-biding domain in each terminal and two α-helixes in each side of the protein (Figure 3A).

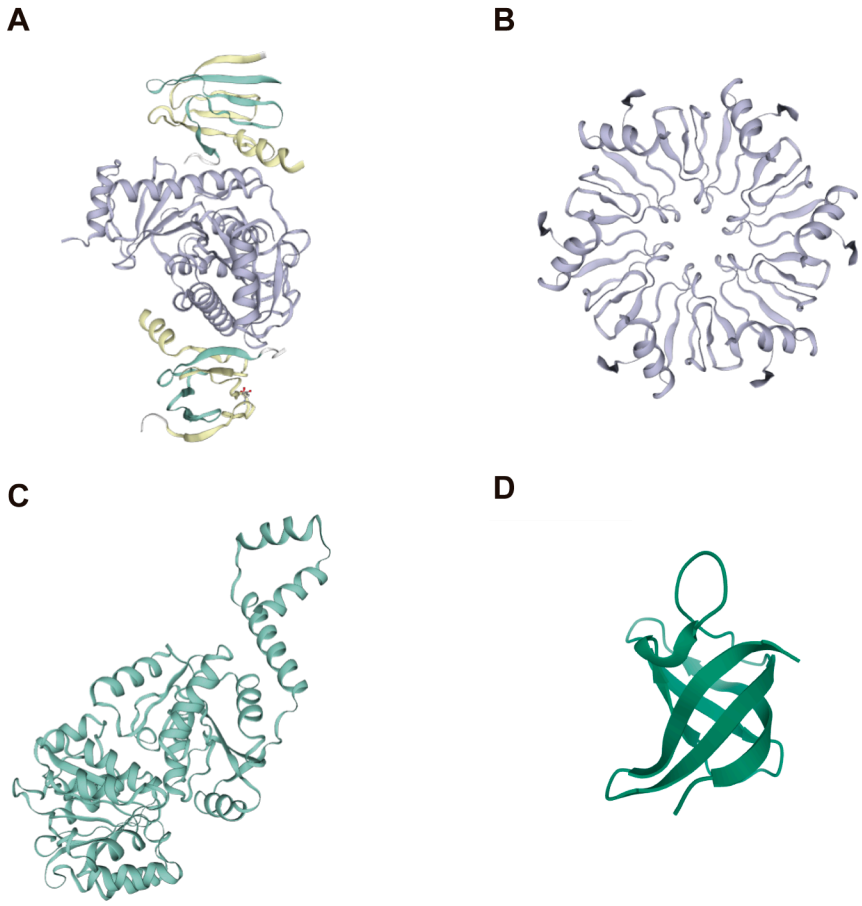

Figure 3. RNA chaperones structure model predicted by SWISS-MODE. (**A**) CsrA protein structure from *E. coli*. CsrA is composed by a dimer that leads to a β-barrel structure. The latter is formed of 10 antiparallel β -sheets and two α-helixes in each side of the protein. (**B**) Hfq protein structure from *E. coli*. The secondary structure is formed by a ring-shaped of six identical monomers. Each monomer comprises five antiparallel β- sheets and an α-helix at the N-terminal. (**C)** RNA helicase CshA from *S. aureus* is a dimer of two RecA like domains and a C-terminal able to bind RNAs. (**D**) CspA protein structure from *S. aureus.* CSPs are formed by a β-barrel composed of five anti-parallel β-strands and two RNA binding domains (RNP1 and RNP2).

Studies using cross-linking immunoprecipitation followed by a deep sequencing (CLIP-seq) revealed that CsrA recognizes AUGGA rich motifs preferentially located at the apical loops of RNA hairpins (Holmqvist *et al.*, 2016). Its canonical mode of action is binding to the 5'UTR to inhibit translation by blocking the RBS. For example CsrA recognizes two singles-stranded GGA triplets in the *glgC* 5'UTR to obstruct the ribosome binding to the *glgC* RBS and subsequent glycogen synthesis is inhibited (Baker *et al.*, 2002). Alternatively, regulatory mechanisms affecting transcription and RNA decay have also been described (Yakhnin *et al.*, 2013; Figueroa-Bossi *et al.*, 2014).

The activity of CsrA can be inhibited by the action of proteins and ncRNAs. On the one hand, the *E. coli* protein CesT binds CsrA, inhibiting mRNA-CsrA complex formation (Katsowich *et al.*, 2017). On the other hand, CsrA activity is also controlled by the interaction with *csrB* and *csrC* sRNAs among others, which sequester CsrA from their mRNAs targets. These sRNAs contain multiples CsrA-recognition motifs, interfering with CsrA protein function and preventing its action (Figure 4) (Liu *et al.*, 1997). CsrA/Rsm protein family is highly conserved among species, however in Gram-positive bacteria, CsrA circuits work without antagonistic sRNAs (Hör *et al.*, 2020). Studies of homologous proteins from distant species showed complementation of each other's function *in vivo* (Agaras *et al.*, 2013).

Although Csr/Rsm homologs seem to play non-redundant roles, it is unknown whether these proteins are auxiliary proteins that modulate the affinity of certain targets in combination with other major RBPs.

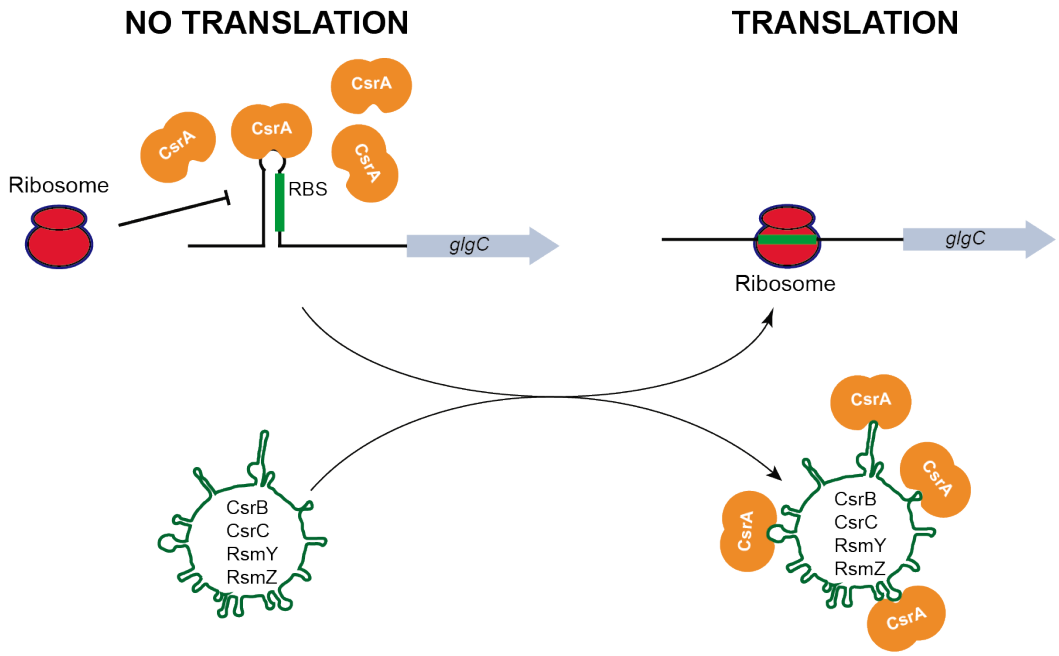

Figure 4. Schematic representation of different CsrA activities. CsrA can inhibit mRNA translation by binding to a specific region of the mRNA 5'UTR. This occludes the RBS and impairs ribosome binding. However, some sRNAs such as CsrB could recognize and bind different motifs in CsrA, blocking its function and ultimately enhancing mRNA translation. Figure was adapted from Toledo-Arana *et al.*, 2007.

3.2. RNA chaperones facilitating sRNA-mRNA interactions

The Host Factor Q (Hfq) is probably one of the best RNA chaperones described so far in bacteria. Since its discovery more than 50 years ago as a host factor that unwinds phage RNA for efficient phage replication (Franze de Fernandez *et al.*, 1968), its functions have been widely reviewed (Vogel and Luisi, 2011; Updegrove *et al.*, 2016). To date, it is known that the main function of Hfq is acting as an RNA chaperone by facilitating the interaction between *trans*-acting sRNAs and mRNAs, which often occur through imperfect base pairings. Hfq can bind to different sRNA such as OxyS, DsrA, RprA and Spot42 RNAs among other identified sRNAs (Sledjeski *et al.*, 1996; Møller *et al.*, 2002; Večerek *et al.*, 2003). This interaction may lead to inhibition of translation by binding to the RBS of the target mRNA. On the contrary, it can promote translation initiation as the Hfq-sRNA complex can base pairs to the 5'UTR of target mRNA to open up an inhibitory stem loop. This is the case of DsrA sRNA that activates the synthesis of RpoS in cooperation with Hfq (Hopkins *et al.*, 2009).

Hfq is organized in a ring-shaped complex formed by the oligomerization of six identical monomers. Five antiparallel β-sheets together with an α-helix define the Hfq monomer structure (Vogel and Luisi, 2011; Updegrove *et al.*, 2016) (Figure 3B). Hfq possesses two conserved Sm domains located in the β-1, -2 and -3 sheets (Sm1 motif) and β-4 and -5 sheets (Sm2 motif). The RNA binding capacities reside in four different places including the

proximal and the distal faces, the rim and the C-terminal tail (Holmqvist and Vogel, 2018). The proximal face preferentially recognizes unpaired U-rich sequences at the 3' ends of the sRNAs, particularly those comprising the Rho-independent terminators found in all Hfq target sRNAs (Updegrove *et al.*, 2016). This motif appeared to be conserved in Hfq from Gram-negative to Gram-positive bacteria. The deletion of the poly U of Rho independent terminators resulted in a deficient binding to Hfq, confirming its essential role in protein interaction (Otaka *et al.*, 2011). By contrast, the distal face interacts with single stranded A-rich sequences present in mRNA 5'UTRs to bring mRNA targets in close proximity to the sRNA-binding proximal face (Lorenz *et al.*, 2010; Peng *et al.*, 2014). Once Hfq is loaded with both sRNA and mRNA, the rim contacts their UA-rich sequences to promote RNA pairing. The arginines from these motifs are conserved in most Gram-negative bacteria whereas they are almost completely absent in Hfq from several Gram-positive species such as *Bacillus anthracis* and *S. aureus* (Updegrove *et al.*, 2016). Therefore, although this is the established mechanism of how Hfq interacts with its targets sRNA and mRNA, the enormous sequence diversity of RNA partners leads to case-to-case variations.

The C-terminal tail of Hfq varies significantly in sequence and length. Since this tail was not included when performing the first structural models of Hfq, the cellular function of this protein region was unclear. New evidences are pointing the C-terminal as a key player in sRNA-Hfq interaction. The novel

crystal structure of Hfq in complex with RydC suggested that the C-terminal is capable of binding certain sRNAs (Dimastrogiovanni *et al.*, 2014). In addition, the deletion of the C-terminal reduced both the *in vivo* RydC half-life and the *in vitro* binding to Qrr sRNA from *Vibrio cholera*, confirming the role of this region in sRNA binding (Dimastrogiovanni *et al.*, 2014; Vincent *et al.*, 2012).

Most of the work to understand Hfq function has been carried out in Gram-negative bacteria. In contrast, the function of Hfq in Gram-positive species is unknown. Interestingly, in most of the sRNAs identified in Gram-positive bacteria, Hfq was dispensable for sRNAs function, indicating different Hfq roles among bacteria.

Recently, a new chaperone promoting sRNA-mRNA interactions was also discovered. ProQ is a homolog of FinO RBP of approximately 25 kDa, which targets several hundreds of cellular transcripts in *Salmonella* and *E. coli* (Holmqvist *et al.*, 2016; Smirnov *et al.*, 2016). These targets include >70 sRNAs that have been associated with stabilization of sRNAs, duplex formation and translation repression (Holmqvist and Vogel, 2018). Higher availability of ProQ in the cell (5-10 times more ProQ monomers that Hfq hexamers) may lead to hold duplex for longer times than Hfq (Smirnov *et al.*, 2016). In addition, recent CLIP-seq studies revealed that ProQ might recognize secondary structures rather than sequence motifs (Holmqvist *et al.*, 2016). Note that ProQ is absent in Gram-positive bacteria (Hör *et al.*, 2020). However, considering the large number of RBPs with unknown

functions that are present in the bacterial genomes, it might be expected that novel RNA chaperones with similar functions to Hfq/ProQ would be discovered in the near future.

3.3 RNA chaperones actively unwinding RNA structures

RNA helicases are RBPs involved in unwinding double stranded RNAs that are usually, but not always, programmed to be degraded. This uncoiling activity normally requires ATP hydrolysis (Hunger *et al.*, 2006; Oun *et al.*, 2014). RNA helicases are classified into six protein families. Most of them belong to superfamily 2 (SF2), which in turn comprises five subfamilies. Among them, the largest subfamily includes DEAD-box proteins, which share nine conserved motifs (Q-motif, motif 1, motif 1a, motif 1b, motif II, motif III, motif IV, motif V, and motif VI). Motif II contains the amino acid sequence D-E-A-D (asp-glu-ala-asp), which gave this family of proteins the name “DEAD box” (Figure 3C). Gram-negative bacteria encode multiple DEAD RNA helicases (e.g. DeaD (CsdA), RhlE or SrmB) that are associated with cold stress, ribosome biogenesis or RNA turnover (Owttrim, 2014).

In Gram-positive bacteria such as *S. aureus* or *B. subtilis*, the DEAD box RNA helicase CshA is part of the degradosome (Lehnik-Habrink *et al.*, 2010; Roux *et al.*, 2011). Recent studies revealed that CshA, is essential for interactions with components of the RNA degradosome, such as the polynucleotide phosphorylase and RNase Y (Lehnik-Habrink *et al.*, 2010;

Giraud *et al.*, 2015). In *S. aureus*, CshA is also important for quorum sensing due to its function in controlling the stability of the *agr* mRNA and therefore virulence factors expression (Oun *et al.*, 2014). In addition, CshA can stabilize target mRNAs and sRNAs *in vivo*. The expression of these mRNAs, including some with housekeeping functions, was decreased in a *ΔcshA* mutant upon MazF activation (an endoribonuclease that cleaves a vast amount of mRNAs *in vivo*) (Kim *et al.*, 2016).

RNA helicases from different species are essential genes in cold-shock conditions, such as CsdA in *E. coli*, ChrC in *Cyanobacterium anabaena* or CshA and CshB in *B. subtilis* (Hunger *et al.*, 2006). After cold shock, mRNAs form RNA secondary structures that inhibit translation initiation. To rescue translation in such conditions, DEAD-box helicases such as *B. subtilis* CshA and CshB unwind the unfavourable secondary structure. Subsequently, other proteins (e.g. cold shock proteins) bind to the unstructured mRNA to prevent its refolding (Hunger *et al.*, 2006) (Figure 5). The relevance of the RNA helicases functions is demonstrated by the fact that at least one RNA helicase should be present in the genome to preserve cell viability (Hunger *et al.*, 2006).

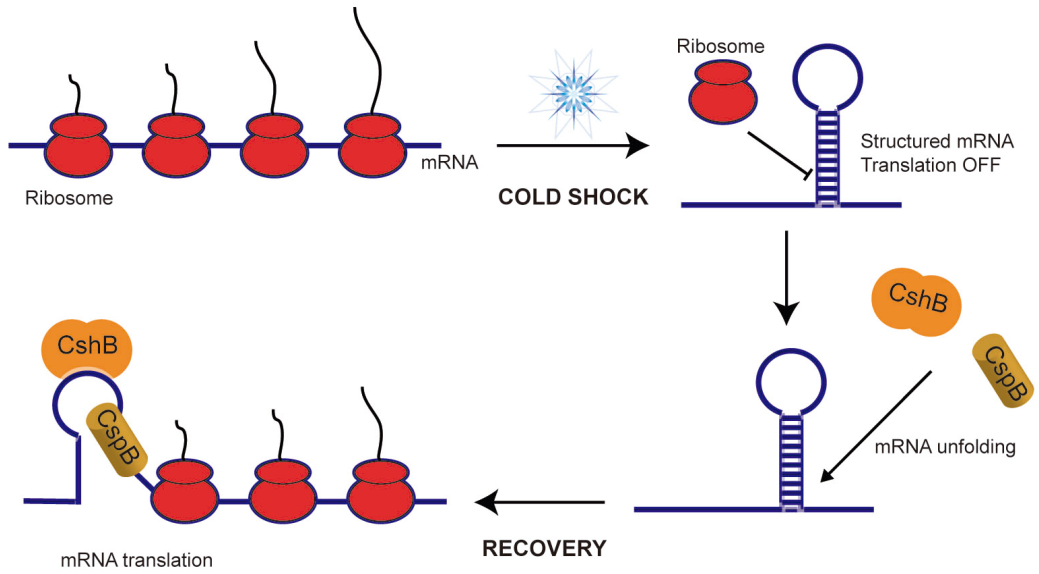

Figure 5. Model of the putative mechanism of RNA helicase CshB and the cold shock protein B in *B. subtilis*. After cold shock, CshB unwinds mRNAs structures, while CspB might prevent the refolding of mRNAs, allowing translation**.** The figure was adapted from Hunger *et al.*, 2006.

3.4. RNA chaperones unfolding RNAs by capturing single-strands

Cold is a physical parameter that severely affects different processes compromising cell viability. As explained above, when bacteria encounter cold temperatures, the mRNAs tend to increase their internal RNA structures inhibiting ribosome progression and leading to growth arrest. In order to protect themselves, most bacteria are able to respond to the cold stress activating the cold-shock proteins (CSPs), which work as holdases maintaining an unfolded state of the mRNAs (Graumann and Marahiel, 1998). The CSPs are a family of small 7.4 kDa proteins, which structure consists of five antiparallel β-sheets that form a β-barrel and constitutes the cold shock domain (CSD) (Figure 3D). The CSD is conserved across all

kingdoms of life, and it is included in numerous proteins such as the eukaryotic Y-box proteins (YBPs), the mammalian Unr proteins, a fraction of the plant glycine-rich protein family (GRPs), the nematode LIN-28 proteins and the bacterial cold shock proteins (CSPs).

Two RNA-binding motifs are present in the CSD, RNAP1 and RNAP2, located at β- 2 and 3 strands, respectively. These motifs are essential for nucleic acid binding. Studies on the structural features of this protein domain revealed additional key amino acids involved in the protein-nucleic acid interaction. According to them, the RNA binding and RNA melting activities seem to be carried out by different amino acids. (Sachs, Max, Heinemann, and Balbach, 2012).

A recent genome-wide study demonstrated that the decrease in protein synthesis after cold-shock is accompanied by a global increase in ORF-wide mRNA structures. During the acclimation phase, cellular translation is recovered by CspA that unfolds mRNA structures and RNase R that degrades mRNAs. This increase in translation correlates with a decrease in ORF-wide mRNA structures (Zhang *et al.*, 2018). Zhang and co-workers suggested that this mechanism is broadly conserved among Gram-positive and Gram-negative bacteria.

CSPs have been found in a wide variety (>50 species) of Gram-positive and Gram-negative bacteria including mesophilic, psycotrophic and thermophilic species. The only exceptions in nature that do not present CSPs are *Helicobacter pylori* and *Mycoplasma genitalium*. Interestingly, the number

of CSPs varies between species, for example, the chromosome and plasmids of *Bacillus megaterium* encode eighteen CSP paralogs while nine, six, three or just one paralog could be found in *E. coli*, *Salmonella*, *B. subtilis* and *Streptococcus pyogenes*, respectively.

Due to the capacity of CSPs to destabilize secondary structures in target RNAs, they can also act as transcription anti-termination modulators by preventing formation of hairpin structures that cause a pause on transcription (Phadtare *et al.*, 1999; Bae *et al.*, 2000). As a consequence of the high percentage of identity shared by the CSPs, it is extremely difficult to establish whether they have the same functions or in the contrary they play specific roles. There are different studies suggesting that both options could be true (Wang *et al.*, 1999; Xia *et al.*, 2001; Michaux *et al.*, 2017; Caballero *et al.*, 2018; Zhang *et al.*, 2018).

The fact that not all CSPs are activated at cold temperatures could insinuate that some of them must drive different functions. Studies in *E. coli* cells showed that CspC and CspE are expressed at 37ºC, whereas CspA, CspB, CspG and CspI were induced after 6 h of exposure to low temperature (15ºC) (Xia *et al.*, 2001). In addition, mutational studies in *E. coli*, *Salmonella spp.* or *B. subtilis* showed that only when deleting a combination of double mutants results in strong phenotypes. However, the single-gene deletion had no effect, attributing redundant functions for some of them (Graumann *et al.*, 1997; Xia *et al.*, 2001; Shenhar *et al.*, 2012; Michaux *et al.*, 2017). Recently, an RNA ligand-centric approach performed in *Salmonella* showed

two different clusters formed by CspA/CspC/CspD and CspC/CspE indicating different set of ligand between the clusters (Michaux *et al.*, 2017). Similarly, in *E. coli* two evolutionary branches separating CspH from the rest of the CSPs were found (Yamanaka *et al.*, 1998) suggesting the possibility that they carried out different functions.

It is important to recall that CSPs are not only expressed during cold stress and a minimum of one *csp* gene is essential for cell viability of *B. subtilis*. However, further roles for CSPs when bacteria is growing in "non-cold shock" conditions are poorly understand (Graumann *et al.*, 1997; Giuliodori *et al.*, 2010; Caballero *et al.*, 2018; Zhang *et al.*, 2018). Interestingly, RNA ligand profiles performed in *Salmonella* indicated that CSPs were generally enriched for RNA targets of general processes such as metabolism and translation. However, only CspC/CspE were associated with stress responses and pathogenicity (Michaux *et al.*, 2017). Therefore, further investigations are needed to determine what are the CSP elements driving the differences of their functions.

In addition, several studies highlighted the role of CSPs on regulating their own translation. For those CSPs involved in cold shock adaption, their expression is controlled through RNA thermosensors located at the *csp* 5'UTRs. This thermosensors are complex RNA structures that could be modulate by the binding of its own CSP (Zhang *et al.*, 2018). Further details about CSP thermoregulation are discussed in the next section.

Regarding the CSPs that are not activated by cold shock conditions, their expression could be also auto-regulated by modifying the structures of long RNA hairpins located in the *csp* 5'UTR. We recently proposed an auto-regulatory mechanism in which a U-rich region within the *cspA* 5'UTR seems to be essential for the control of CspA expression in *S. aureus* (Caballero *et al.*, 2018). In principle, at low intracellular concentrations of CspA, RNase III can process a long hairpin of the *cspA* 5'UTR, leading to a structural mRNA change that facilitates CspA translation (Figure 6). However, in the presence of sufficient levels of CspA protein, it interacts with its own 5'UTR through the U-rich motif avoiding the hairpin folding. As a result, CspA impairs RNAse III cleavage and, consequently, the mRNA is not processed in the form that facilitates translation (Figure 6).

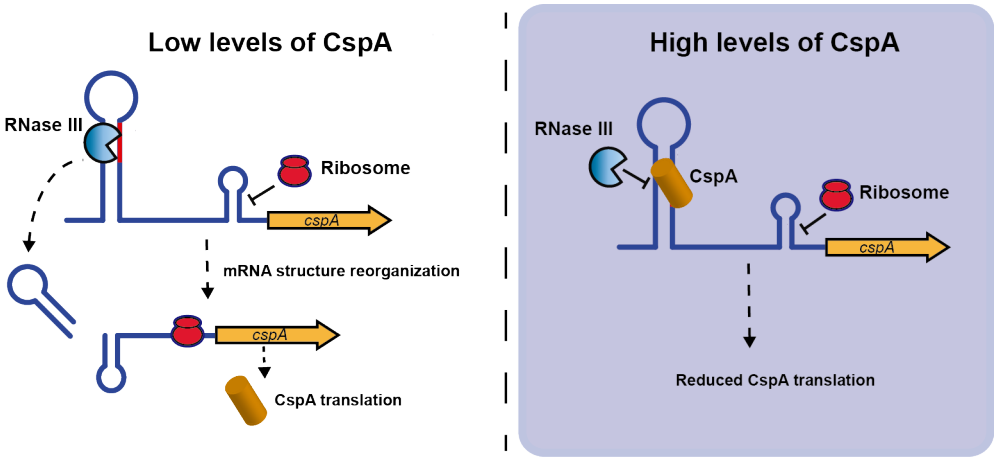

Figure 6. Putative CspA auto-regulatory mechanism. When bacteria senses low levels of CspA protein, RNase III binds the *cspA* 5'UTR mRNA and processes its hairpin. The processed *cspA* mRNA changes its conformation, liberating the RBS and promoting translation (left panel). However, if the levels of CspA are sufficient, CspA can bind to its own 5'UTR repressing RNase III processing and ultimately, implying a reduction in CspA translation.

4. RNA thermoregulators

When bacteria face low temperatures, the expression of some CSPs have been found to be activated at the post-transcriptional level by RNA thermosensitive elements located in the *csp* 5'UTRs (Giuliodori *et al.*, 2010; Zhang *et al.*, 2018; Ignatov *et al.*, 2020). However, these RNA thermosensors significantly differ from the typical RNA thermometers (RNATs) that induce expression when environmental temperature increased. In this section, we discuss the different types and mode of actions of the RNA thermosensors described so far in bacteria (Table 1).

Table 1. Summary of different types of RNA regulatory elements in bacteria

Type	Mechanism	Signal	Examples	References
Heat shock	Secondary structure in the 5'UTR controls translation	Heat shock	*prfA* gene of *L. monocytogenes*	Johansson *et al.*, 2002
ROSE element	Presence of a G opposite the SD	Heat shock	*hspA* gene of *B. japonium*	Nocker *et al.*, 2001
FourU	Four Us paired with RBS	Host temperature	*lcrF* gene of *Y. pestis*	Hoe and Goguen, 1993
Cold shock	Secondary structure in the 5'UTR controls translation and mRNA stability	Cold shock	*cspA* gene of *E. coli and L. monocytogenes*	Giuliodori *et al.*, 2010 Zhang *et al.*, 2018 Ignatov *et al.*, 2020

Regular RNATs are complex structural elements usually located at the 5' untranslated region of mRNAs that modulate translation efficiency. The standard mechanism implies a change in the RNA secondary structure together with a fluctuation on protein levels of the downstream gene. Under low temperatures (<30ºC), an RNAT forms a compact secondary structure, masking the ribosomal binding site and blocking translation. However, when facing higher temperatures (>37ºC), the RNA secondary structure melts to an open conformation, liberating the RBS and making it accessible for the ribosome to bind and initiate translation (Kortmann and Narberhaus, 2012; Loh *et al.*, 2018). RNATs that behave under this mechanism are named RNA zippers (Figure 7A). However, RNAT zippers are clearly not compatible for responding to cold shock stress, where expression of certain genes is activated under low temperature conditions. In these cases, protein expression is controlled through alternative exclusive RNA secondary structures, called RNA switches, which alternates from ON to OFF conformations in function of the environmental temperature (Kortmann and Narberhaus, 2012) (Figure 7B). The conformation formed at low temperatures is better translated and less susceptible to degradation than the conformation formed at 37ºC. In the "cold" structure (ON conformation), the RBS is unpaired and accessible for the ribosome. However, in the alternative structure formed at higher temperatures (OFF conformation), the RBS is occluded in a stable secondary configuration (Figure 7B) (Kortmann and Narberhaus, 2012).

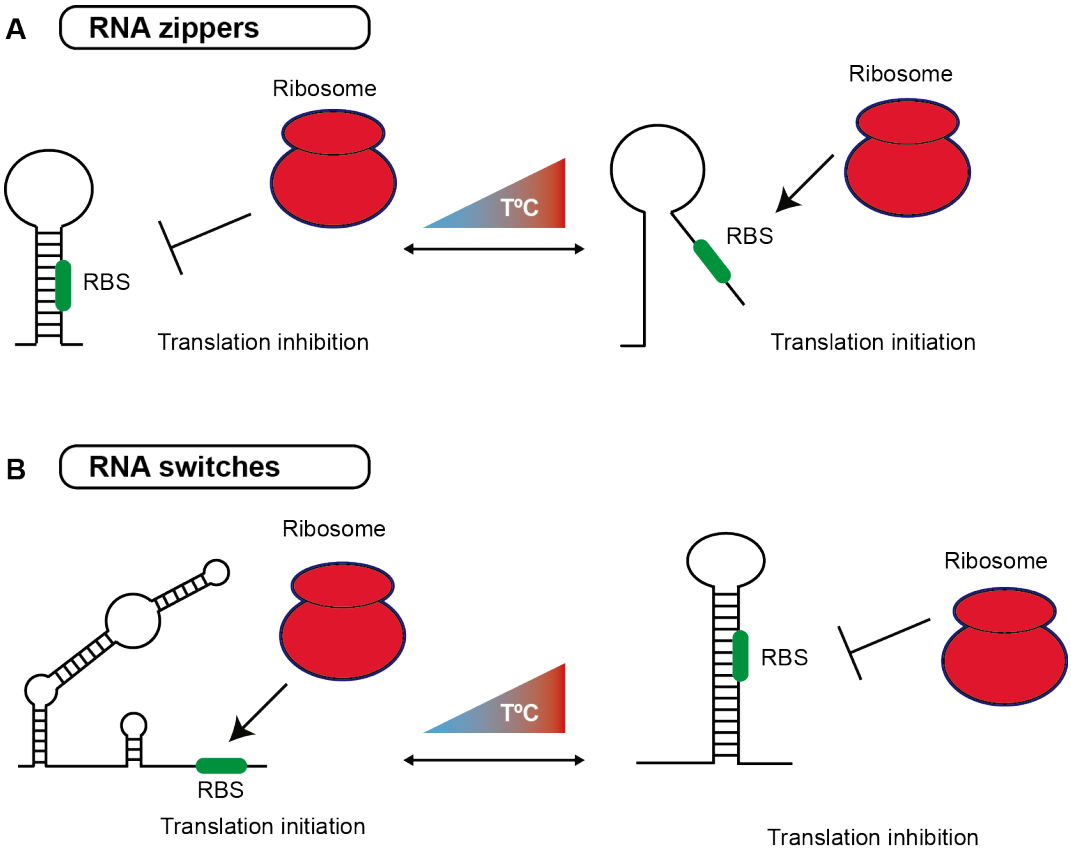

Figure 7. Schematic representation of RNA zippers and RNA switches. (**A**) A zipper like thermosensor is in equilibrium between OFF and ON conformations. At high temperatures, the secondary structure melts, liberating the RBS and promoting mRNA translation. (**B**) A RNA switch consists of two alternative structures that are formed regarding ambient temperature.

4.1. RNA-zipper thermometers

RNA zippers have been discovered in studies related to the heat shock response (Loh *et al.*, 2018). Increasing temperatures melt the RNA secondary structure located at the 5'UTRs enhancing ribosome entry and mRNA translation initiation (Nagai *et al.*, 1991; Morita *et al.*, 1999; Narberhaus *et al.*, 2006). Although some RNATs control the expression of heat shock proteins, such as the heat shock σ-factor σ^{32} (*rpoH*) (Morita *et al.*, 1999), most of the RNATs found so far activate virulence when a pathogen enters into the human host. In the Gram-positive bacteria *L. monocytogenes*, the expression of the main virulence transcriptional regulator PrfA is controlled by an RNAT located at the *prfA* 5'UTR (Johansson *et al.*, 2002). PrfA controls the expression of essential proteins required for human infection including invasion proteins (InlA and InlB), hemolysin (listeriolysin O) or phospholipases (PlcA and PlcB). The 5'UTR of *prfA* mRNA forms a stable secondary structure (OFF structure) at 30ºC where translation of PrfA is inhibited. This structure melts when *Listeria* enters to the human body activating PrfA expression and subsequently virulence genes. Mutations that destabilize the OFF structure induced expression of PrfA at 30ºC and, consequently, virulence could be also activated (Johansson *et al.*, 2002). Similar temperature-sensitive rearrangements that activate gene regulators of virulence were also observed in other pathogens including *Vibrio choleare*, *Yersinia*

pseudotuberculosis, Neisseria meningitidis and *Pseudomonas aeroginosa* (Weber *et al.*, 2014; Böhme *et al.*, 2012).

4.2. ROSE elements

ROSE (repression of heat-shock gene expression) elements are known to control translation efficiency of small heat shock genes by forming an extended secondary structure in their 5'UTRs. The length of this RNA elements ranges between 60 to 100 nucleotides folded into 2-4 stem loops (Narberhaus, 2010). Although this RNA element was initially discovered in *Rhizobia*, specifically in *Bradyryhizobiun japonicum*, it was also found to be conserved in α- and γ-proteobacteria like *E. coli*, *Salmonella* or *Vibrio*. LacZ reporter experiments showed that the expression of *B. japonicum* HspA was very low at 30ºC. However, HspA expression increased drastically when part of their 5'UTR sequence was deleted (Narberhaus *et al.*, 1996; Nocker *et al.*, 2001; Narberhaus, 2010). Computational predictions revealed a structure where the SD sequence and AUG start codon were occluded. The regulatory structure was validated by introducing mutations in the paired regions of the stem-loop IV. This mutation resulted in an unstable loop that increased expression of translational *lacZ* fusions. In addition, compensatory mutations that restored repression, and mutations in unpaired nucleotides that had no effect on protein expression, confirmed the RNA structure and not the RNA sequence as the relevant factor for thermosensing (Nocker *et al.*, 2001; Chowdhury *et al.*, 2003; Narberhaus *et*

al., 2006; Chowdhury *et al.*, 2006). Sequence conservation of ROSE elements is narrow but shares one characteristic, the presence of a G opposite the SD. This G is essential for the ROSE function as its deletion made the thermosensor unresponsive to high temperatures (Nocker *et al.*, 2001). It has not been elucidated yet whether the entire ROSE RNA melts as the temperature increases, or perturbations around the ribosome-binding site are sufficient to initiate translation.

4.3 FourU element

Another type of RNAT is the FourU element that depends on a stretch of four uridines that pairs with the SD sequence. In contrast to ROSE, FourU thermosensors not only control heat shock genes but also virulence (Narberhaus, 2010). The first FourU was identified in early 1993 at the 5'UTR of *lcrF* mRNA of *Yersinia pestis* which encodes a transcription activator responsible for inducing several virulence proteins in response to host temperature (Hoe and Goguen, 1993). Later on, several FourU elements have been discovered in Gram-negative bacteria controlling the expression of the *agsA* gene in *Salmonella* (Waldminghaus, Gaubig, *et al.*, 2007), *toxT* in *V. cholerae* (Weber *et al.*, 2014), *lcrF* in *Y. pseudotuberculosis* (Böhme *et al.*, 2012), *lpxT* in *P. aeruginosa* (Delvillani *et al.*, 2014), *shuA* of *Shigella dysenteriae* (Kouse *et al.*, 2013) or *htrA* of *Salmonella enterica* (Klinkert *et al.*, 2012; Choi *et al.*, 2017). Experiments suggested that mutations in the FourU element prevented repression at

30ºC. A mismatch in the FourU is sufficient for destabilization of the hairpin (Waldminghaus, Gaubig, *et al.*, 2007; Narberhaus, 2010).

Based on this simple mechanism, in which the RBS is sequestered by a structured 5'UTR, the presence of putative FourU or ROSE elements located in the 5'UTRs of genes from 62 different bacterial genomes could be predicted. This information was compiled into the searchable database RNA-SUBIRA (structures of untranslated regions in bacteria) (Waldminghaus, Heidrich, *et al.*, 2007; Marchfelder and Hess, 2012). Interestingly, the heat shock genes *groES* and *dnaJ* of *S. aureus* were predicted as potential candidates carrying the typical FourU sequence in their 5'UTRs. Nevertheless, the FourU–mediated regulation of these genes has not been experimentally validated yet.

4.4 Cold shock thermometers

Whereas the regulatory pathways controlling the heat shock response are well studied, the cold shock adaptation processes remain poorly understood. The first post-transcriptional mechanism that modulated protein expression through thermosensitive alternative structures was described by Altuvia and co-workers (Altuvia *et al.*, 1989). They found that the expression of the *cIII* gene of the *E. coli* bacteriophage λ, requires a sequence located upstream the CDS. The *cIII* gene is responsible of regulating the lytic and lysogenic cycle of the phage. The *cIII* 5'UTR could fold into two alternative structures that existed in equilibrium. The structure A comprised a stem loop

that occluded the RBS while, in the structure B, this stem-loop is reorganized in two smaller hairpins allowing ribosome binding (Figure 8). When temperature increases, the structural equilibrium is shifted towards the structure A where the RBS sequence is occluded. In contrast, lower temperatures favor the folding of the structure B, inducing *cIII* translation. Point mutations included in the *cIII* 5'UTR or in the initial codons could lock the *cIII* mRNA in one or the other structure affecting translation of the downstream gene (Altuvia *et al.*, 1989).

Several years later, Giuliodori and co-workers demonstrated that the induction of CspA expression in *E. coli* also relies in a temperature-sensitive re-structuration of the mRNA secondary structures (Giuliodori *et al.*, 2010). Authors revealed that at low temperatures, the *cspA* mRNA adopts a more efficient translated conformation, which in addition, is less prone to degradation. At host-related temperatures, *cspA* mRNA forms a secondary structure where both the AUG start codon and the RBS are paired, inhibiting ribosome binding and translation initiation (Giuliodori *et al.*, 2010; Zhang *et al.*, 2018). Recently, the presence of an orthologous RNA thermoswitch at the *cspA* 5'UTR of the Gram-positive *L. monocytogenes* has been demonstrated (Ignatov *et al.*, 2020).

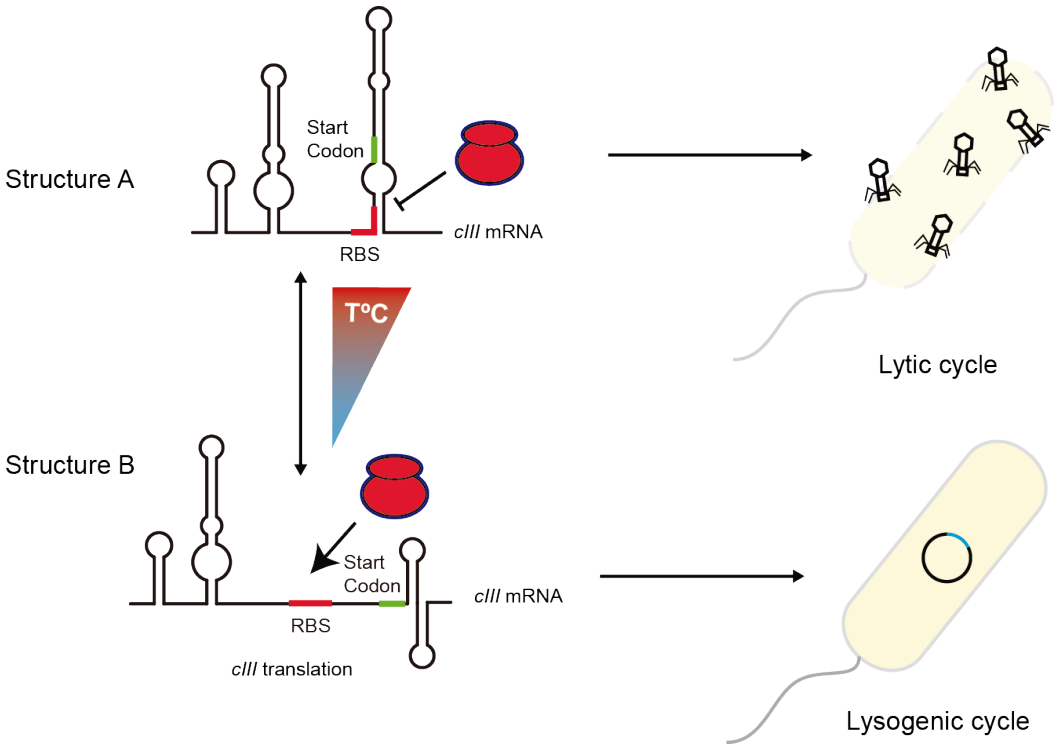

Figure 8. Model of the *cIII* thermosensor from *E. coli* bacteriophage λ. At high temperatures (45ºC) the RBS (red) and start codon (green) are paired in the structure A, which impairs ribosome binding and inhibits translation. The inhibition of *cIII* translation leads to upregulation of the lytic phase. In contrast, when bacteria face lower temperatures (37ºC), the *cIII* 5'UTR reorganizes into structure B liberating the RBS and promoting *cIII* translation. Consequently, bacteriophage λ enters into lysogenic cycle.

Although it has been reported that CSPs from several bacterial species are also induced upon cold shock, it remains to be demonstrated whether their 5'UTRs might carry thermosensitive elements (Willimsky *et al.*, 1992; Graumann *et al.*, 1997; Chapot-Chartier *et al.*, 1997; Anderson *et al.*, 2006; Duval *et al.*, 2010). Finally, a recent study reported another example of temperature-dependent 5'UTR located in the *cidA* mRNA of *S. aureus*,

which induces CidA expression when this bacterium is growing at 30ºC (Hussein *et al.*, 2019).

Altogether, these few examples highlighted the importance of cold-shock thermometers for bacterial adaptation to environmental changes. Although all of them shared a regulatory mechanism based on 5'UTRs alternative structural reorganizations, the lack of sequence conservation and/or structure homologies makes difficult the finding of additional genes that could be controlled in a similar way. Recent developed genome-wide analyses aiming at identifying *in vivo* mRNA structures will contribute to solve such issue (Zhang *et al.*, 2018; Ignatov *et al.*, 2020).

OBJECTIVES

OBJECTIVES

Understanding the regulatory mechanisms behind the most relevant biological aspects of pathogenic bacteria, such as *S. aureus*, is crucial for the development of new strategies towards the treatment and prevention of infectious diseases. Technological advancements in RNA sequencing have positioned post-transcriptional regulation as one of the most important layers of gene expression control. In addition to regulatory non-coding RNAs, RNA-binding proteins have recently attracted interest from several research groups. Among them, the cold shock proteins (CSPs) are an important protein family of RNA chaperones that participate as modulators of a wide range of bacterial biological processes, including stress adaptation and virulence. However, the molecular mechanisms involved in such regulatory pathways are poorly understood. *S. aureus* encodes three CSP paralogs that share a high protein identity. Previous works of our laboratory characterized the CspA regulon, which included more than 200 mRNA targets. We showed that CspA repressed its own expression by binding to its own 5'UTR and modifying its structural folding. Moreover, we found that the deletion of *cspA* reduced staphyloxanthin production and compromised *S. aureus* survival upon oxidative stress (Caballero, 2018; Caballero *et al.*, 2018). The staphyloxanthin phenotype could not be restored by the CspB or CspC paralogs, suggesting a possible functional specificity towards CspA. In addition, we realized that the expression of CspB and CspC was

post-transcriptionally regulated, however, the molecular mechanisms were unknown (Caballero, 2018). Although the work performed so far meant a significant advance in the knowledge of CSP functions in *S. aureus*, several questions remained unanswered. For example, what are the protein motifs responsible for the putative functional specificity of CspA? How CspB and CspC are expressed in relation to CspA? What are the regulatory elements involved in the post-transcriptional control of CspB and CspC? What are the biological functions of CspB and CspC? In order to answer these and other relevant questions we defined the following objectives:

1. Determine the protein motifs responsible for providing functional specificity in *S. aureus* CspA.
2. Study the expression patterns of CspB and CspC and characterize the molecular mechanisms responsible for their post-transcriptional control.
3. Investigate the biological importance of CspB and CspC in *S. aureus*.

MATERIALS AND METHODS

MATERIALS AND METHODS

Strains, plasmids, oligonucleotides and growth conditions

The bacterial strains, plasmids and oligonucleotides used in this study are listed in Annex 1, Annex 2 and Annex 3, respectively. *Staphylococcus aureus* strains were grown in Mueller Hinton Broth (MH) (Sigma-Aldrich) or Tryptic Soy Broth (Pronadisa) supplemented with 0.25% of glucose whereas *Escherichia coli* was grown in LB broth (Pronadisa). To prepare *S. aureus* and *E. coli* competent cells B2 and SuperBroth media were used, respectively. When selective bacterial growth was required, media were supplemented with the appropriate antibiotics at the following concentrations: Erythromycin (Erm), 1.5 µg/ ml or 10 µg/ml; Ampicillin (Amp), 100 µg/ml. In addition, 1.0 µM of cadmium was added whenever activation of the P*cad* promoter was required.

Plasmid construction

The plasmids used in this study (Annex 2) were engineered as follows: PCR fragments were amplified from chromosomic or plasmidic DNA with the DreamTaq DNA polymerase (Thermo Scientific) using appropriate oligonucleotides listed in Annex 3. PCR products were purified from agarose gels using the Macherey-Nagel NucleoSpin Gel and PCR Clean-up kit

(Thermo Scientific). Purified products were then ligated into the cloning vector pJET 1.2 (Thermo Scientific) and transformed into *E. coli* cells XL1-blue or IM01B cells. DNA fragments were excised using the corresponding FastDigest restriction enzymes (Thermo Scientific) and ligated into the final vector with the Rapid DNA ligation kit (Thermo Scientific). All constructs were verified by Sanger sequencing and transformed into the corresponding competent cells by electroportation (Lee, 1995).

The pMAD plasmids (pMAD_Δ*cspB*, pMAD_Δ*cspC*, pMAD_*cspB*^{3xF}, pMAD_*cspC*^{3xF}, pMAD_Δ24*cspB*, pMAD_Δ24*cspC*, pMAD_Δ24*cspB*^{3xF}, pMAD_Δ24*cspC*^{3xF}) (Annex 2), were used for chromosomal mutations, either to insert the 3xFLAG tag or delete the first 24 nucleotides from *cspB* and *cspC* mRNAs, respectively. Briefly, the flanking regions (AB and CD) from the target genes were amplified using specific oligos A/B and C/D (Annex 3). The flanking regions were amplified by an overlapping PCR using primers A and D and ligated into pJET plasmid. The resulting vectors were digested and the fragments corresponding to the flanking regions inserted into a previous excised pMAD vector.

The pmA_CspA_L3_C^{3xF} and pmA_CspA_β4_C^{3xF} plasmids were generated by overlapping PCR using the oligonucleotides listed in Annex 3**.** Specifically, the pmA_CspA_L3_C^{3xF} and pmA_CspA_β4_C^{3xF} plasmids (Annex 2) were generated by overlapping PCR using pCspA^{3xF} as a template and oligonucleotides CspA +1 BamHI and CspA_L3_C_izq or CspA_β4_C_izq to generate the first PCR fragment and CspA ter EcoRI

and CspA_L3_C_dcha or CspA_β4_C_dcha to generate the second PCR fragment. These fragments were fused in a second PCR using the corresponding external primers and cloned into pCN51 using BamHI and EcoRI restriction sites. The pmA_CspA_β5_C^{3xF} plasmid (Annex 2) was constructed by digesting pCspA^{3xF} with BamHI and SacII and pmA_CspC^{3xF} with SacII and EcoRI. The digested fragments were ligated into a previously BamHI and EcoRI processed pCN51 plasmid. Analogously, pmA_CspC_L3β4_A^{3XF} (Annex 2) was generated by digesting pmA_CspCA^{3xF} with BamHI and SacII and pmA_CspC^{3xF} with SacII and EcoRI. The resulting DNA fragments were cloned into a previously BamHI and EcoRI processed pCN51. The pmA_CspC_β5_A^{3xF} plasmid (Annex 2) resulted from digesting pmA_CspC^{3xF} with BamHI and SacII and pCspA^{3xF} with SacII and EcoRI. Both fragments were then ligated into a BamHI and EcoRI digested pCN51. The pmA_CspA^{3xF} _P58E and pmA_CspC^{3xF} _E58P plasmids (Annex 2) were generated by digesting the pmA_CspA_β5_C^{3xF} and pmA_CspC_β5_A^{3xF} with BamHI, AclI and EcoRI restriction enzymes and combining the resulting DNA fragments accordingly to ligate them into a EcoRI and BamHI processed pCN51. The pmA_CspB^{3xF} _D58P plasmid was constructed by PCR amplification using oligonucleotides CspA_+1_BamHI and CspB_D58P (Annex 3). The resulting PCR fragment was cloned into pJET, digested by BamHI and AclI restriction enzymes and subcloned into pmA_CspB^{3xF}, which was digested with the same enzymes.

The pHRG plasmid that expressed the *gfp* gene under the control of the phyper promoter, whose sequence was adapted from the promoter that drives transcription of early genes in the SP01 *Bacillus subtilis* bacteriophage (G Lee *et al.*, 1980) to include an EcoRI site upstream of the native transcriptional start site. This plasmid was constructed by PCR amplification using the plasmidic DNA of pCN57 (Charpentier *et al.*, 2004) as a template and oligonucleotides phyper-RBSicaR-GFP and GFPend-AscI oligonucleotides (Annex 3). The amplified product was ligated into pJET. The resulting vector was digested using SphI and AscI and the fragments of interest inserted into the pCN47 plasmid (Charpentier *et al.*, 2004). Plasmids p5'UTR^{cspB}-gfp and p5'UTR^{cspC}-gfp were generated by amplifying the 5'UTR sequences from the pCspB^{3xF} and pCspC^{3xF} plasmids (Annex 2) with oligonucleotides pairs 5UTR_CspB_FW_EcoRI/5UTR_CspB_RV_SpeI or 5'UTR_cspC_FW_EcoRI/5'UTR_CspC_RV_SpeI (Annex 3), respectively. The amplified PCR products were then digested and ligated into pHRG using the EcoRI and SpeI enzymes. Similarly, plasmids for mutating 5'UTRs were constructed by PCR amplification from p5'UTR^{cspB}-gfp or p5'UTR^{cspC}-gfp using the corresponding 5'UTR mutated forward oligonucleotides (Annex 3) and 5UTR_CspB_RV_SpeI or 5'UTR_CspC_RV_SpeI (Annex 3). The amplified fragments were then digested with EcoRI/SpeI and ligated into the pHRG plasmid. The resulting vectors were named p5'UTR^{cspB}Δ24-gfp, p5'UTR^{cspC}Δ24-gfp, p5'UTR^{cspB}UAU47AA-gfp, p5'UTR^{cspB}C50G-gfp,

p5'UTR^{cspB}UU55AA-gfp, p5'UTR^{cspB}UU55AA+UU26AA-gfp, p5'UTR^{cspC}UU48A-gfp plasmids (Annex 2). Lastly, the pEW-5'UTR^{cspB}-gfp was generating by digesting p5'UTR^{cspB}-gfp and pEW (Menendez-Gil, Caballero, Catalan-Moreno, *et al.*, 2020) with EcoRI and SpeI.

Generation of csp mutants by homologous recombination

The *csp* mutant strains were obtained by marker-less homologous recombination, using the pMAD plasmid system (Arnaud *et al.*, 2004). Briefly, the Δ*cspB*, Δ*cspC, cspB*^{3xF}, *cspC*^{3xF}, Δ*cspBC*, Δ*24cspB*, Δ*24cspC*, Δ24*cspB*^{3xF} and Δ24*cspC*^{3XF} strains were generated by a two-step procedure that replaces a gene of interest by a mutant allele contained within the pMAD plasmid (Valle *et al.*, 2003). The resulting mutant strains were confirmed by PCR using the corresponding oligonucleotides, E and F (Annex 3)**.** In addition, the resulting PCR fragments were verified by Sanger sequencing.

Bacterial cultures for total protein extractions

Bacterial cultures for Staphyloxanthin assays were grown in 250 ml-Erlenmeyer flasks containing 50 ml of MH supplemented with 1 μM $CdCl_2$ and 10 μg/ml erythromycin. Media were inoculated (1:250) with normalized bacterial aliquots, which were previously grown overnight. Bacterial cultures were incubated at 37ºC and 200 rpm for approx. 15 h. Each culture was divided into two aliquots, one of 2-ml for total protein extraction and another

of the remaining volume for staphyloxanthin extraction. Eppendorf tubes containing 2-ml of cultures were centrifuged for 10 min at 21,000 g and 4ºC and the other aliquots in falcon tubes for 10 min at 4,400 g and 4ºC. The resulting pellets were incubated at 4ºC if protein extraction was performed immediately or frozen in liquid nitrogen and stored at -80ºC until required.

For thermoregulation experiments, bacterial cultures were grown in Erlenmeyer flasks containing MH or LB supplemented with 10 µg/ml erythromycin or 100 µg/ml ampicillin for *S. aureus* or *E. coli* cells, respectively. Media were inoculated (1:250) with normalized bacterial aliquots, which were previously grown overnight at 37ºC and 200 rpm. Bacterial cultures were incubated at different temperatures (22, 28 and 37ºC) and 200 rpm until cells reached an early exponential phase (OD_{600} 0.4). Cultures were harvested by centrifugation for 10 min at 4,400 g and 4ºC. Bacterial pellets were stored at -80ºC until required.

Total protein extraction and Western blotting

Pellets were washed once with PBS 1X and centrifuged for 10 min at 21,000 g and 4ºC. The resuspended bacteria were placed in Lysing Matrix B tubes containing acid-washed 100 µm glass beads (Sigma) and lysed for 45 s and speed 6 using a FastPrep-24 instrument (MP Biomedicals). This step was repeated and lysed bacteria were centrifuged for 10 min at 21,000 g and 4ºC. The supernatants containing total protein extracts were transferred to 1.5-ml Eppendorf tubes. Total proteins were quantified using a Bradford

protein assay (Bio-Rad) and samples prepared at the desired concentration in Laemmli buffer. Samples were stored at -20ºC until needed.

Total protein sample stocks were prepared at the same concentration, loaded into 12% SDS-polyacrylamide gels that were prepared using the SureCast™ Handcast Station (Invitrogen, ThermoFisher Scientific), and run in Mini Gel Tanks (Life technologies). Resolved proteins were stained with Coomassie brilliant blue R250 (Sigma) to control sample preparation. Next, diluted sample aliquots were run into 12% SDS-polyacrylamide gels and transferred to nitrocellulose membranes (Amersham Biosciences). The wild type and 3xFLAG tagged CSPs were developed with anti-FLAG antibodies (Sigma) as previously described (Caballero *et al.*, 2018). Asp23 protein was developed using polyclonal rabbit anti-Asp23 antibodies and and the GFP samples were incubated with monoclonal anti-GFP antibodies 1:5,000 (Living colors, Clontecht) and peroxidase-conjugated goat anti-mouse immunoglobulin G and M antibodies 1:2,500 (Pierce-Thermo Scientific). Membranes were developed in a ChemiDoc Imaging system using the SuperSignal West Pico Chemiluminiscent Subtrate kit (Thermo Scientific). Protein levels of three independent replicates were quantified by measuring band intensity with ImageJ (https://imagej.nih.gov/ij/).

Staphyloxanthin extraction and quantification

Staphyloxanthin (STX) extraction and quantification was performed as previously described, with slight modifications (Caballero *et al.*, 2018). Pre-

weighted 50 ml-Falcons containing the bacterial cultures were centrifuged for 10 min at 4,400 g. Bacterial pellets were washed with 50 ml of PBS, centrifuged again, and weighted after discarding the supernatant. The pellets were resuspended in a variable volume of PBS, proportional to their weight. Next, 700 µl of bacterial suspensions were transferred to Eppendorf tubes and centrifuged. Pellets were resuspended in 700 µl of ethanol 96% (Merck), incubated at 45ºC for 1 h and centrifuged for 10 min at 21,000 g. Finally, the STX concentration of the supernatants was determined by measuring their optical density at 460 nm. The STX extractions were repeated at least three times from biological replicates.

Generation of CSP structure models

The 3D models of CspA and CspC were generated via templates and *ab initio*-based processes through the Phyre2 server (Kelley *et al.*, 2015) using *S. aureus* CspA and CspC amino acid sequences. Ribbon representations of CspA and CspC models were generated with Pymol (Schrodinger, LLC., 2015).

PIA-PNAG detection

PIA-PNAG production was quantified as previously described with slight modifications (Toledo-Arana *et al.*, 2005). Two millilitres of overnight cultures in TSB supplemented with 0.25% of glucose were centrifuged. In order to obtain similar bacterial density, the pellets were weighted and resuspended in a proportional quantity of 0.5 M EDTA (pH 8.0).

Subsequently, 50 μl of the bacterial suspensions were boiled for 5 min and centrifuged. Supernatants (40 μl) were incubated with 10 μl of proteinase K (20 mg/ml; Sigma) for 30 min at 37°C. Next, 10 μl of Tris-buffered saline (20 mM Tris-HCl, 150 mM NaCl [pH 7.4]) containing 0.01% bromophenol blue were added to each tube. Serial dilutions were performed and spotted on a nitrocellulose membrane using a Bio-Dot microfiltration apparatus (Bio-Rad). Membranes were blocked overnight with 5% skim milk in PBS 0.1% Tween 20. After three washes of 15 minutes with the same buffer, membranes were incubated for 2 hours with an anti-PNAG antibody (1: 25,000). After incubation, membranes were washed three times with PBS 0.1% Tween 20 and incubated with a peroxidase-conjugated goat anti-rabbit immunoglobulin G antibody (1: 5,000). Finally, membranes were developed using the Amersham ECL Western blotting kit and a Chemi-Doc apparatus (Bio-Rad).

RNA extraction and Northern Blotting

Bacteria were culture as mentioned in the protein extraction section. Cultures were centrifuged for 3 min at 4,400 g and 4ºC. Pellets were then frozen in liquid nitrogen and stored at -80ºC until needed. RNA extractions were performed as previously described (Toledo-Arana *et al.*, 2009). An appropriate amount of RNA was mixed with formaldehyde loading dye (Ambion), denatured for 15 min at 65ºC and run in 1.25 % agarose gels with Midori Green (Teknovas). Gels were checked for RNA integrity and correct

loading under UV light exposure. RNAs were then transferred to 0.2 μm pore size Nitran N membranes (GE Healthcare Life Sciences) by capillarity, using the NorthernMax Transfer Buffer (Ambion), for 1.5 h at RT. The transferred RNAs were crosslinked to the membranes by exposing them to UV light with a UV Stralinker 1800 (Stratagene). Membranes were then prehybridized using ULTRAHyb solution (Ambion) for at least 30 min at 40ºC in a rotating oven. After the prehybridaztion step, the appropriate oligonucleotide probes (anti_3xFLAG_probe or anti-GFP probe) (Annex 3) were radioactively labelled with [γ^{32}-P]-ATP (Perkin Elmer) following the manufacturer's recommendation. Probes were then purified with Illustra MicroSpin G-50 columns (GE Healthcare) and incubated with prehybridazed membranes ON at 40ºC. Membranes were then washed three times for 5 min with preheated solution 1(2X SCC, 0.1% SDS) at 40ºC followed by at least two washing steps of solution 2 (0.1X SCC, 0.1% SDS) at RT until the background signal was non-detectable. Membranes were developed by autoradiography for different time periods. The mRNA levels from three independent replicates were measured by densitometry of Northern blot autoradiographies using ImageJ (https://imagej.nih.gov/ij/).

FAM-quencher assay

The FAM-quencher assay was performed as previously described by (Menendez-Gil, Caballero, Solano, *et al.*, 2020) with the following modifications. Briefly, the *cspB* and *cspC* ssDNA oligonucleotides (Annex

3) labelled with the 6-FAM and the quencher Iowa Black FQ (IBkFQ) molecules at the 5' and 3' ends, respectively, were purchased from Integrated DNA Technologies. The *cspA* ssDNA oligonucleotide (Caballero *et al.*, 2018) was used as a control. 2 pmol of ssDNA oligonucleotides were mixed with 2.5 μl of 10X reaction buffer (100mM Tris-Hcl pH 7.5, 300 mM KCl, 200 mM NH4Cl, 15 mM DTT, 50 mM MgCl2) and miliQ water up to a final volume of 25 μl. The FAM fluorescence was then measured using the BioRad CFX96 Touch Real-Time PCR Detection system and the following incubation periods: 13ºC, 10 min; 18 cycles of 5 min each starting at 16ºC and with a 3ºC increase per cycle; 5 min at 65ºC; and 18 cycles of 5 min each with a 3ºC decrease per cycle. FAM emission was registered throughout the incubation steps. Three independent replicates were performed.

In vitro transcription

PCR fragments containing the T7 promoter were amplified using oligonucleotides listed in (Annex 3). *In vitro* transcription was performed at 37ºC ON using the Megascript T7 transcription kit (Ambion) following the manufacturer's recommendation. RNAs were loaded to a 6% polyacrylamide gel and visualized with UV-light after Midori green (Teknovas) staining. Bands of the appropriate size were cut and the RNA was extracted using 0.5 M ammonium acetate pH 5.5 at 15ºC for 2 h. Next, 1 volume of acid phenol pH 4.5 was added and samples incubated at 15ºC

ON. After centrifugation for 5 min at 21,000 g and 4ºC, RNAs were purified using phenol-chloroform and precipitated by adding 3 volumes of 96% ethanol and 1/10 volume of 3M sodium acetate pH 5.5. The mixture was incubated at -80ºC for at least 1 h. Samples were then centrifuged for 30 min at 21,000 g and 4ºC. Pellets were washed with 70% ethanol, air dried and resuspended in DEPC water (Ambion). RNA integrity was checked by agarose gel and quantified by Nanodrop system (Agilent Technologies).

5'-end labelling of RNA

Before labelling, RNAs were dephosphorylated using the FastAP enzyme (Thermo Scientific) at 37ºC for 15 min followed by a phenol-chloroform extraction. Inactivation of the enzyme was performed by an ethanol/chloroform extraction followed by ethanol precipitation supplemented with 1 μl of glycoblue (Thermo Scientific). Pellets were finally resuspended in 20 μl DEPC water. Dephosphorylated nucleic acids were incubated with [γ^{32}-P]-ATP (Perkin Elmer) and 0.4 U of PNK (Thermo Scientific) for 1 h. Labelled RNAs for enzymatic probing were purified by electrophoresis on a 6% polyacrylamide denaturing gel (8 M urea). The bands of interest were cut from the gel and the RNAs eluted with 400 μl of elution buffer (500 mM AcNH4, 1 mM EDTA and 0.1% SDS) at 4ºC, ON. RNAs were then precipitated as previously described, and resuspended in 80 μl DEPC water.

Enzymatic probing

The enzymatic probing experiments with RNase T1 and S1 (Thermo Scientific) were performed to determine *in vitro cspB* and *cspC* 5'UTR structures. Labelled RNAs were first denatured (1 min at 90ºC followed by 1 min in ice) and then renatured at 22 or 37ºC for 15 min. 2 pmol of labelled RNA was incubated in RNA structure buffer or S1 buffer (Thermo Scientific) supplemented with 20 μg yeast tRNA in the presence of different enzymes concentrations (T1: $1x10^{-3}$ U/μl, $2x10^{-2}$ U/μl and $5x10^{-2}$ U/μl and S1: $5x10^{-5}$ U/μl, $2x10^{-5}$ U/μl and $1x10^{-5}$ U/μl) for 5 min at 22 or 37ºC. In parallel, alkaline hydrolysis and T1 controls were performed to assign the gel bands. Alkaline hydrolysis was accomplished by mixing 2 pmol of labelled RNA with 20 μg of yeast tRNA and 1X Alkaline hydrolysis buffer (Thermo scientific). The mix was then incubated at 95ºC for 10 min. For the denaturing T1 reaction, 2 pmol of labelled RNA were preheated with 20 μg yeast tRNA and 1X RNA structure buffer for 3 min at 65ºC. Samples were then incubated with $2.5x10^{-2}$ U/μl U of RNase T1 for 1 min 10 sec. All reactions were stopped by addition of 40 μl of the Stop Mix solution (0.6M NAOAc, 4mM EDTA, 0.1 mg/mL yeast tRNA and 1 μg glycoblue) and ethanol precipitated. The pellets were washed twice with 70% ethanol, air dryed, and resuspended in 12 μl of loading buffer II (Thermo Scientific). Samples were loaded into a 12% polyacrylamide denaturing gel.

Bacterial growth in TSA plates

For the phenotypic growth experiments in TSA plates, bacteria were grown in 5 ml MH ON at 37ºC and 200 rpm. The bacterial preinocula were then normalized to OD_{600} 1. Serial dilutions were plated on TSA plates and incubated at 37ºC 24 h or at 22ºC for 72 h.

Survival experiment in nasal media SNM3

The Synthetic Nasal Media (SNM3) was prepared as previously described (Krismer *et al.*, 2014) and used for the survival experiments of different *S. aureus* strains. Bacteria were grown in 5 mL of MH at 37ºC and 200 rpm ON. 1 mL of preinocula was centrifuged, washed with 1X PBS and resuspended in 1 mL of SNM3. Bacteria were then diluted 1:250 in 10 mL of SNM3 and grown at 32ºC and 200 rpm for 2 days. Next, bacteria were inoculated in fresh SNM3 and grown at 22ºC without shaking. Samples were taken at different time points and serial dilutions were plated in TSA plates. CFU were counted from three independent biological replicates.

CHAPTER I:

One evolutionary-selected amino acid variation is sufficient to provide functional specificity in the cold shock protein paralogs of Staphylococcus aureus

CHAPTER I:

One evolutionary-selected amino acid variation is sufficient to provide functional specificity in the cold shock protein paralogs of *Staphylococcus aureus*

S. aureus CspA specificity is restricted to the β5-strand

S. aureus CSP paralogs (CspA, CspB and CspC) show a high degree of identity between them. When comparing the protein sequence of CspA with those of CspB and CspC, 20 and 13 out of 66 amino acid (aa) differences are found, respectively (Figure 9). CspA is required for the activation of the stress-associated sigma factor B (SigB), which in turn induced the biosynthesis of staphyloxanthin (STX) (Katzif *et al.*, 2005). Since deletion of the *cspA* gene abolished STX production and STX levels are easily measured by spectrophotometry after pigment extraction (Liu *et al.*, 2008), we chose STX production as an *in vivo* reporter to evaluate if *S. aureus* CSP paralogs play redundant roles. In previous works of our laboratory, we demonstrated that CspB and CspC proteins could not restore the CspA phenotype when the *cspB* and *cspC* mRNAs were expressed under the control of the P*cad* constitutive promoter in the Δ*cspA* mutant.

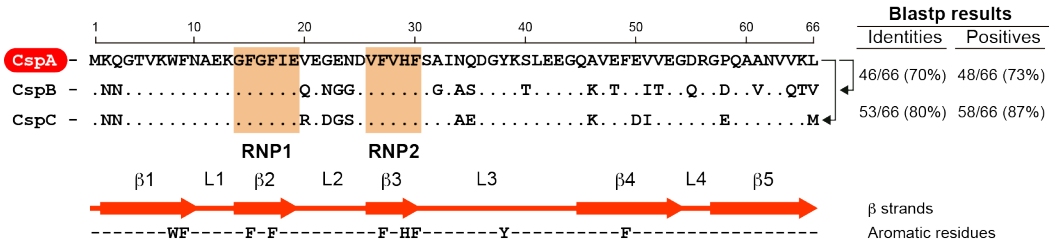

Figure 9. *S. aureus* CSP paralogs share a high sequence identity. Comparison of CSPs (CspA, CspB and CspC) amino acid sequence. Identical amino acids are shown as dots. The RNP1 and RNP2 motifs are indicated. The secondary structure layout is shown along with the aromatic residues across CSP paralogs. Adapted from Caballero C.J., 2018.

However, Western blot analyses revealed that the expression of the *csp* mRNAs from the P*cad* promoter led to much lower CspB^{3xF} and CspC^{3xF} protein yields than those of CspA^{3xF} (Caballero, 2018). This indicated that different post-transcriptional events may modulate the expression of CSPs in *S. aureus*. Therefore, in order to minimize the effect of such post-transcriptional control, the *cspA* mRNA was engineered by including the fewest nucleotide changes that made it encode CspB^{3xF} or CspC^{3xF} instead of CspA^{3xF} (Annex 4). Western blot analyses confirmed that the new chimeric mRNAs expressed similar levels of CspA^{3xF}, CspB^{3xF} and CspC^{3xF}. However, CspA^{3xF} remained as the only CSP able to restore STX in a Δ*cspA* strain (Caballero, 2018). These data demonstrated that CspA specifically modulates STX biosynthesis and suggested the existence of specific roles for CSPs in *S. aureus*. Preliminary data suggested that the few amino acid differences in the C-half of the *S. aureus* CSPs may be responsible for CSP specificity *in vivo* (Caballero, 2018). Specifically, amino acids located at loop 3 and β5-strand (Figure 9), might be important for RNA interaction by

increasing the protein surface that makes contact with nucleic acids in addition to RNP1 and RNP2 motifs (Max *et al.*, 2006; Max *et al.*, 2007; Sachs, Max, Heinemann, and Balbach, 2012). Therefore, in this Thesis, to evaluate the functional consequence of amino acid variations located at the C-terminal half of the protein, we focused on the differences between CspA and CspC since the identity between their protein sequences was the highest (Figure 9). When comparing the C-terminal half of CspA and CspC, only seven aa differences made one distinguishable from the other. Specifically, there were two aa variations between CspA and CspC in loop 3 (N34A; Q35E), three in β4-strand (A46K, E50D, V51I) and two in β5-strand (P58E; L66M), respectively (Figure 9). Following the codon substitution criteria showed in Annex 4, we constructed plasmids that expressed chimeras CspA_L3_C^{3xF} (N34A; Q35E), CspA_β4_C^{3xF} (A46K; E50D; V51I) and CspA_β5_C^{3xF} (P58E; L66M) (Figure 10A). We used these constructs to complement the *cspA* mutant and their expression was checked by Western blot (Figure 10B). Next, we measured STX production and found that the strains expressing the CspA_L3_C^{3xF} and CspA_β4_C^{3xF} chimeras produced pigment levels similar or slightly higher than those of the WT strain (Figure 10C). In contrast, complementation of the *cspA* mutant with CspA_β5_C^{3xF} did not restore the STX synthesis, suggesting that CspA functional specificity might be comprised in β5-strand (Figure 10C).

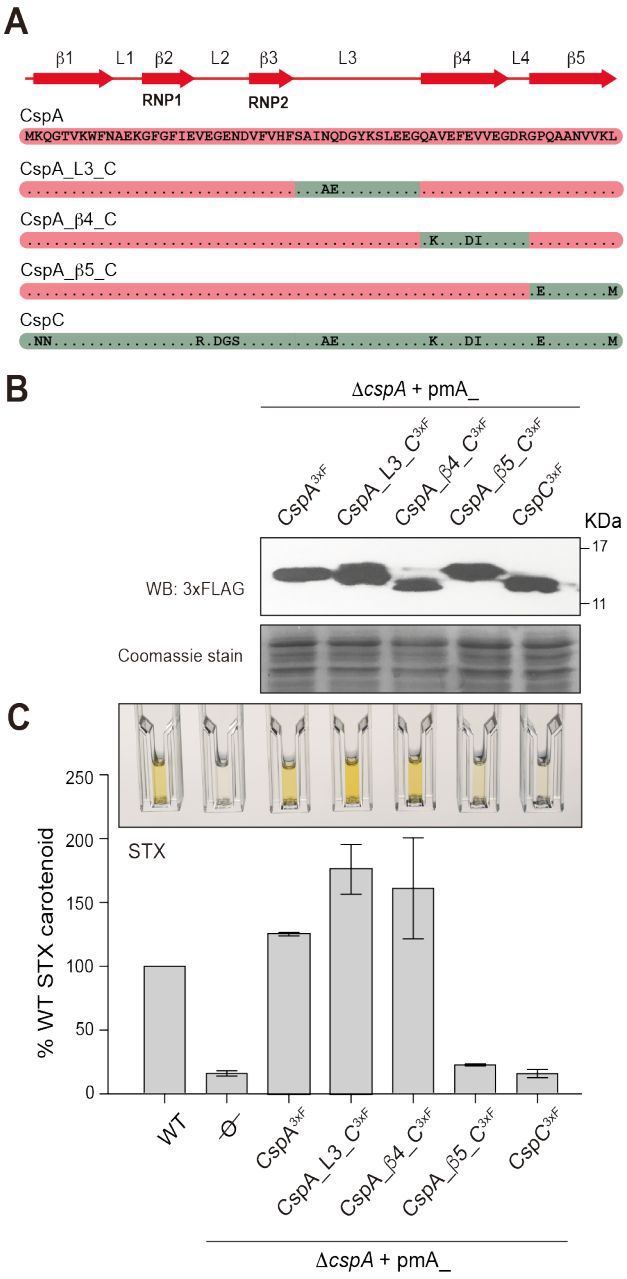

Figure 10. CspA functional specificity might be comprised in the β5 strand. (**A**). Schema showing the amino acid substitutions performed to create the different chimeric 3xFLAG proteins. (**B**) Western blot showing the expression of the 3xFLAG CSPs and their corresponding chimeras in a *ΔcspA* strain. Total protein samples were run in 12% PAGE, transferred to Nitrocellulose membranes and developed using peroxidase-conjugated anti-FLAG antibodies. Coomassie stained gel portions show sample preparation controls (**C**) Quantification of STX production in the *ΔcspA* strains complemented with the plasmids expressing the constructs shown in (A). The WT and *ΔcspA* strains harbouring the pCN51 plasmid were used as positive and negative controls, respectively. The STX pigment was quantified by measuring the absorbance from the ethanol solutions at 460 nm. The production level of STX for each strain is expressed in %, considering the WT STX levels as 100%. Column and error bars represent the mean and standard deviation from three independent biological replicates.

To study this in detail, we created two different plasmids that expressed CspC_L3β4_A^{3XF} (carrying loop 3 and β4-strand of CspA) and CspC_β5_A^{3xF} (carrying the E58P and M66L substitutions in β5-strand) (Figure 11A). The expression levels of these chimeric proteins were again found to be similar to those of CspA^{3xF} (Figure 11B). Interestingly, the strain expressing the chimeric CspC^{3xF} protein that carried CspA β5-strand produced STX while the strain expressing CspC_L3β4_A^{3XF} showed an absence of pigment production (Figure 11C). These results restricted the putative CspA functional specificity to only two amino acid variations within β5-strand (positions 58 and 66, Figure 9).

One amino acid at the C-terminal end of CspA drives the specific control of STX production

Previous structural and *in vitro* binding experiments with *B. subtilis* CspB and an hexa-nucleotide RNA suggested that position 58 could participate in target binding (Sachs, Max, Heinemann, and Balbach, 2012a). To explore this idea, we expressed a new chimeric CspA^{3xF} protein carrying the orthologous P58E substitution naturally present in CspC (Figure 12A). After verifying by Western blot that protein levels were similar (Figure 12B), we measured STX production and observed that the STX levels in the Δ*cspA* strain expressing the CspA^{3xF}_P58E protein were below those in the WT strain (Figure 12C).

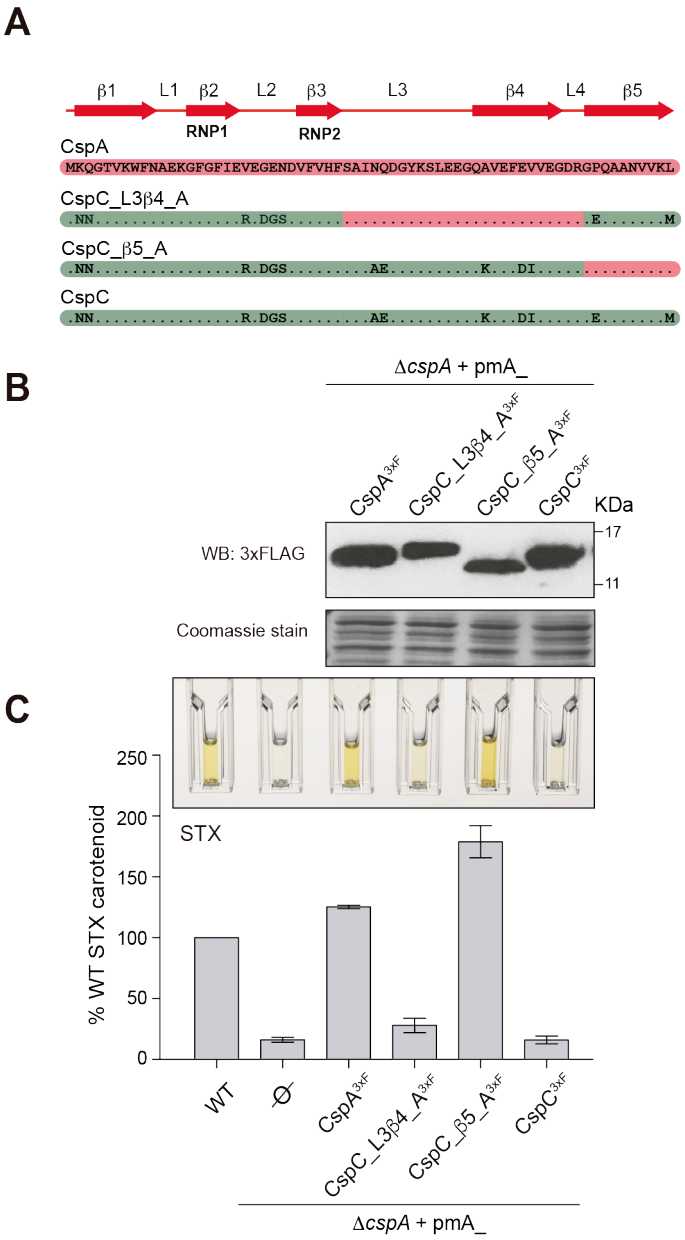

Figure 11. The β5 strand of CspA is sufficient to confer CspC the ability to restore STX WT levels in a *ΔcspA* strain. (**A**) Schematic representations of the amino acid substitutions performed to create the different chimeric 3xFLAG-tagged protein variants. (**B**) Western blot showing the expression of the 3xFLAG-tagged CspA and CspC proteins and their corresponding chimeric variants in a *ΔcspA* strain. Proteins were run, transferred and developed as described in Figure 10 (**C**) Quantification of STX production in the *ΔcspA* strains complemented with the plasmids expressing the constructs shown in (A). The WT and *ΔcspA* strains harbouring the pCN51 plasmid were used as positive and negative controls, respectively. The STX pigment was extracted and quantified as indicated in Figure 10 The production level of STX for each strain is expressed in %, considering the WT STX levels as 100%. Column and error bars represent the mean and standard deviation from three independent biological replicates.

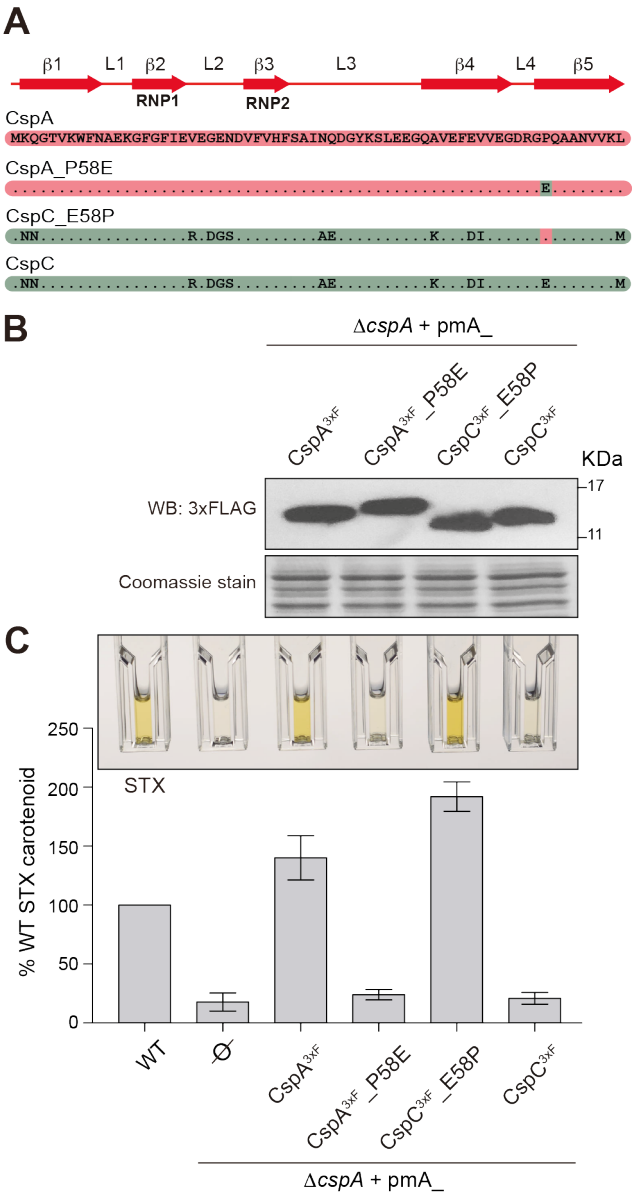

Figure 12. Proline 58 confers CspA specificity to control STX production. (**A**) Schematic representation of the amino acid substitutions that were performed to create the chimeric 3xFLAG tagged CspA and CspC proteins harbouring the P58E and E58P changes, respectively. (**B**) Western blot showing the expression of the protein constructions depicted in (A) in a *ΔcspA* strain. Proteins were run, transferred and developed as described in Figure 10 (**C**) Quantification of STX production in the *ΔcspA* strains complemented with the constructs shown in (A). The WT and *ΔcspA* strains containing the empty pCN51 vector were used as positive and negative controls, respectively. The STX pigment was extracted and quantified as indicated in Figure 10. The production level of STX for each strain is expressed in %, considering the WT STX levels as 100%. Column and error bars represent the mean and the standard deviation from three independent biological replicates.

Notably, when doing the opposite, that is substituting CspC Glu58 by CspA Pro58 in CspC (chimeric CspC^{3xF}_E58P) (Figure 12A), STX production was restored to WT levels in a Δ*cspA* strain (Figure 12C). This gain of function in the chimeric CspC^{3xF}_E58P protein confirmed that Proline 58 is critical for modulating STX biosynthesis.

We also analysed the consequences of substituting CspB Asp58 by CspA Pro58. When the chimeric CspB^{3xF}_D58P was expressed in a Δ*cspA* strain, STX production was not complemented, suggesting that additional amino acids might participate in target discrimination (Figure 13). From these experiments, we concluded that just one amino acid was enough to create functional divergence between two CSPs (e.g. CspA and CspC).

To evaluate how amino-acid changes in position 58 impact CSP functionality, we performed structural CSP modelling (Figure 14A). Superposition of CspA and CspC models (alpha-carbonsuperposition, root mean squared XYZ displacement: 0.340 Å) showed that there were no major differences between their RNP motifs (Figure 14B). Specifically, position 58 in CspA is occupied by a proline that is oriented to potentially enable a stronger interaction with the RNA target. Following this line of reasoning, the solvent exposed side chain of Glu58 in CspC would determine an alternative binding target with a different affinity. This might explain the specificity of CspA towards controlling STX production (Figure 14C).

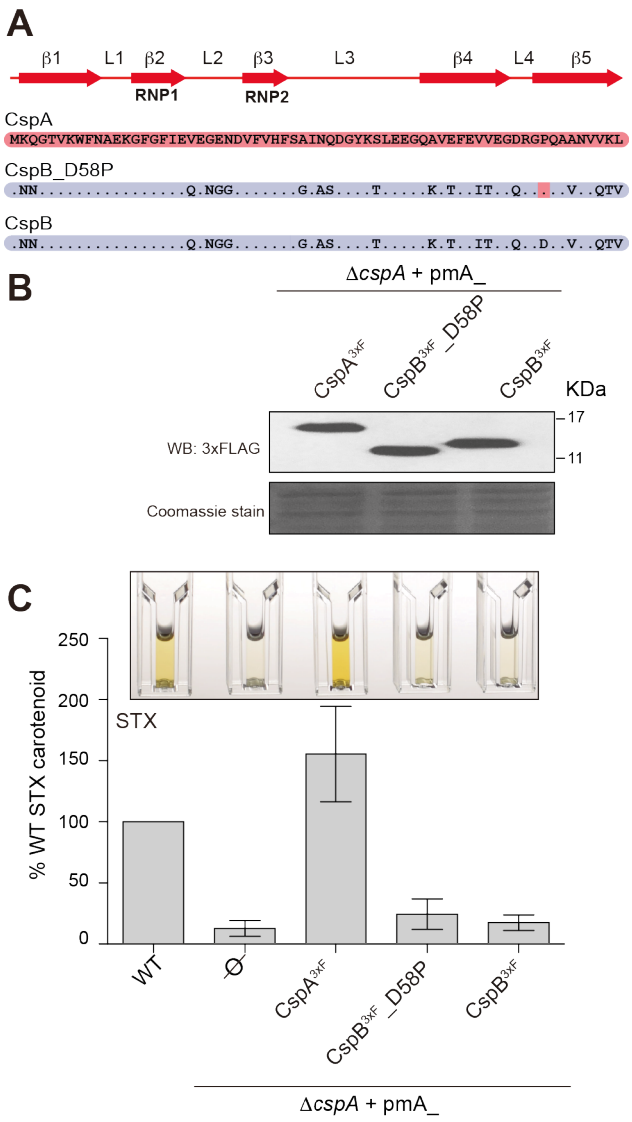

Figure 13. Substitution of the orthologous amino acid 58 from CspA to CspB did not complement STX production. (**A**) Schematic representation of the substitution of CspB Asp58 by CspA Pro 58 in CspB. (**B**) Western blot showing the expression of the 3xFLAG-tagged CSPs (see A) in a Δ*cspA* mutant strain. Total protein extracts were processed as described in Figure 10. (**C**) Quantification of STX production in the Δ*cspA* strains complemented with the plasmids expressing the 3xFLAG-tagged CSPs (see A). Positive and negative controls are also included. The STX pigment was extracted and quantified as indicated in Figure 10. The production level of STX for each strain is expressed in %, considering the WT STX levels as a 100%. Column and error bars represent the mean and the standard deviation from three independent biological replicates.

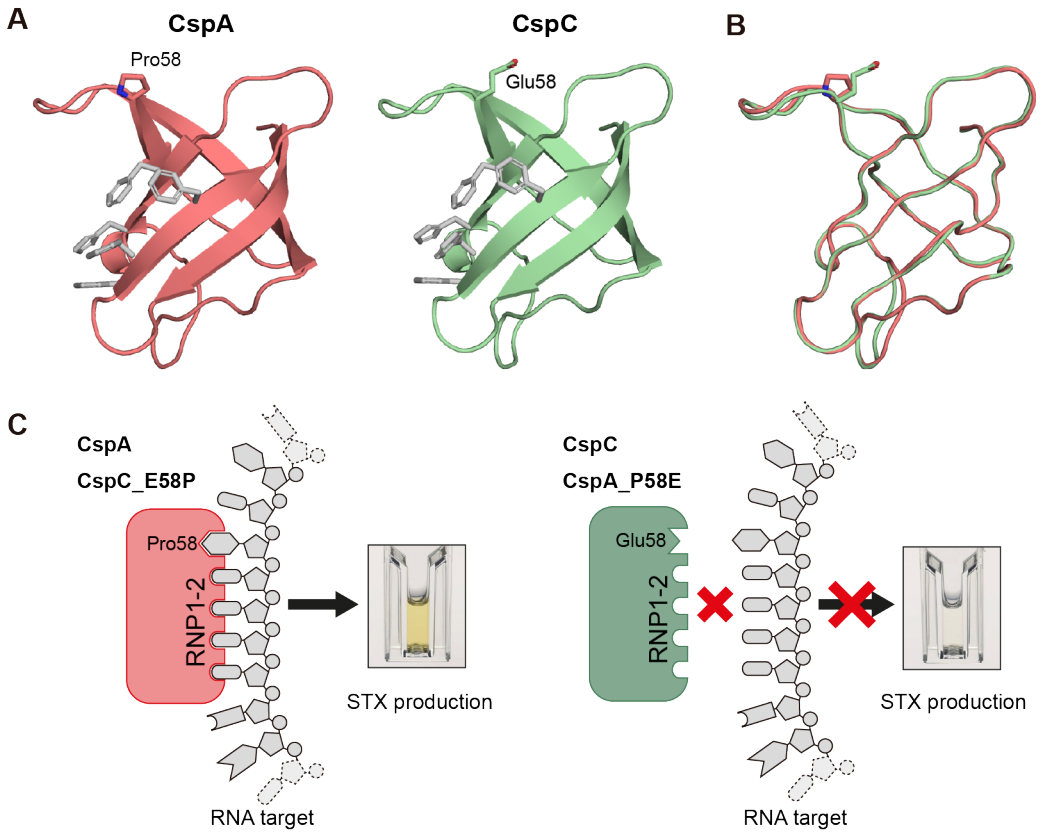

Figure 14. Structural models of CspA and CspC proteins. (**A**) Comparison of CspA and CspC protein structures modelled by Phyre2 (Kelley *et al.*, 2015). Aromatic residues from the RNP motifs and the amino acid in position 58 are indicated. (**B**) Superposition of CspA and CspC 3D models. (**C**) Schematic representation of the interaction between CspA and its putative RNA target required to control STX production. A similar interaction might occur in the CspC_E58P mutant. In contrast, the side chains or charge of glutamate in position 58 of CspC and the CspA_P58E mutant protein might allosterically interfere with the recognition of the specific target needed to promote STX synthesis.

Proline 58 leads to CspA specific control of σ^B activity

STX production is carried out by the proteins encoded in the *crtOPQMN* operon, which depends on the alternative sigma B factor (σ^B) for its transcription. Analogously, the activity of σ^B is modulated by CspA (Katzif *et al.*, 2005; Caballero *et al.*, 2018; Donegan *et al.*, 2019). We previously showed that CspA directly interacts with the *rsbV-rsbW-sigB* operon, resulting in an improved σ^B activity (Caballero *et al.*, 2018). To confirm that the CspA-mediated specific control of STX production by Pro58 occurs through the modulation of σ^B activity, we analysed additional σ^B-associated phenotypes in *cspA* mutants complemented with CspA^{3xF}, CspC^{3xF}, CspA^{3xF}_P58E and CspC^{3xF}_E58P. First, we used the alkaline shock protein Asp23 as a natural reporter for testing σ^B activity, since it was previously described to be exclusively activated by σ^B (Gertz *et al.*, 1999; Giachino *et al.*, 2001). Western blot analyses using specific anti-Asp23 antibodies showed that Asp23 expression levels could be restored in Δ*cspA* strains expressing CspA^{3xF} and CspC^{3xF}_E58P. In contrast, Δ*cspA* strains expressing CspC^{3xF} and CspA^{3xF}_P58E presented similar Asp23 levels to those of the *cspA* mutant (Figure 15A). Second, since the production of the poly-N-acetylglucosamine exopolysaccharide (PIA/PNAG) and biofilm formation in *S. aureus* are inhibited by CspA and σ^B (Caballero *et al.*, 2018; Valle *et al.*, 2019), we analysed both phenotypes and found that they could only be restored when CspA^{3xF} or CspC^{3xF}_E58P proteins were expressed

in the Δ*cspA* strains (Figure 15B and C). Altogether, these results indicated that Pro58 in CspA is required to specifically control σ^B activity and subsequently modulate σ^B-associated phenotypes such as Asp23 expression, STX biosynthesis, PIA/PNAG production and biofilm formation in *S. aureus*.

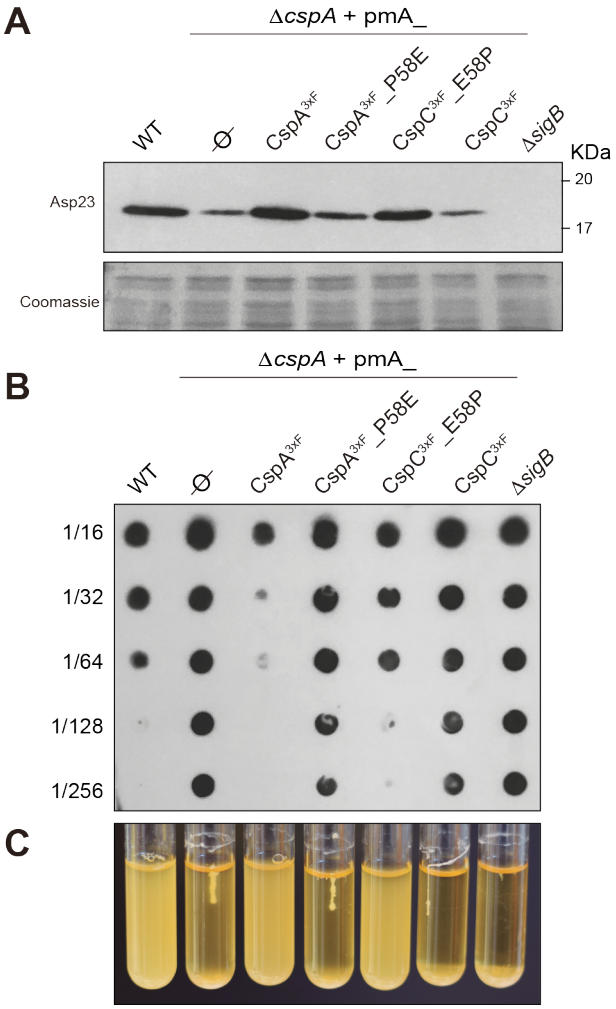

Figure 15. Proline 58 leads to specific control of σ^B-associated phenotypes. (**A**) Western blot showing the expression of the Asp23 protein in *ΔcspA* strains expressing chimeric CSPs. The WT, *ΔcspA* and *ΔsigB* strains were included as controls. Total protein extracts were transferred to Nitrocellulose membranes and incubated with rabbit anti-Asp23 antibodies. A Coomassie stained gel portion is shown as loading control. (**B**) Dot-blot assays showing the PIA-PNAG production. Membranes were incubated with anti-PNAG antibodies. Western and dot blot membranes were developed using peroxidase-conjugated goat anti-rabbit antibodies and bioluminescence kit. (**C**) Bacterial aggregation phenotypes after incubation for 24 h at 250 rpm and 37°C in 5 ml of TSBglu.

Proline 58 is evolutionarily conserved among CspA orthologs in *Staphylococcus* species

Previous analysis of the consensus sequence of thousands of proteins carrying the CSD (both in eukaryotic and bacterial species) revealed several highly-conserved amino acids, which resulted critical for the molecular function of CSPs regardless of their evolutionary origin (Amir *et al.*, 2018). In this study, position 58 appears as not conserved among the superfamily of CSPs. In *S. aureus* CspB and CspC, position 58 is represented by Asp and Glu, respectively (Figure 9). We hypothesized that if Pro58 plays a relevant role in CspA specificity, it should be conserved among its orthologs. To test this idea, we analysed 98 CSP sequences from 44 *Staphylococcus* species. On the one hand, we performed multiple CSP sequence alignments using Clustal Omega (Madeira *et al.*, 2019), which produced phylogenetic CSP trees (Annex 5). On the other hand, we classified the CSP sequences according to their PATRIC-assigned protein family group (Wattam *et al.*, 2017). This classification was based on sequence similarity over the entire protein length and the conserved genomic context (Wattam *et al.*, 2017). A total of three protein family groups: PLF_1279_00007112 (red), PLF_1279_00001953 (blue) and PLF_1279_00007034 (green) were assigned. Most of the CSPs that fell into the red category were clustered in the same tree branches, which could be associated to CspA orthologs.

Interestingly, 52 out of 53 CspA orthologs carried a proline in position 58 (Annex 5). In contrast, when analyzing CspB and CspC orthologs, which are included in the blue and green groups, respectively, several other amino acids were found in position 58 (Annex 5). Note that the number of CSPs for a given staphylococcal species is between 1 and 4, with 2 being the most common number (Figure 16). CspA is present in all species and in at least five of them it is duplicated. Interestingly, when CspA was accompanied by a CspC ortholog, the latter usually included a glutamate, aspartate or alanine in position 58, depending on the species. In the few cases in which the CspB variant coexisted with CspA, an aspartic acid was found in such position (Figure 16 and Annex 5). The fact that Pro58 is highly-conserved among CspA orthologs highlighted the relevance of this particular amino acid in CspA specificity. At the same time, the substitutions in position 58 among CSP paralogs suggested functional divergence among them.

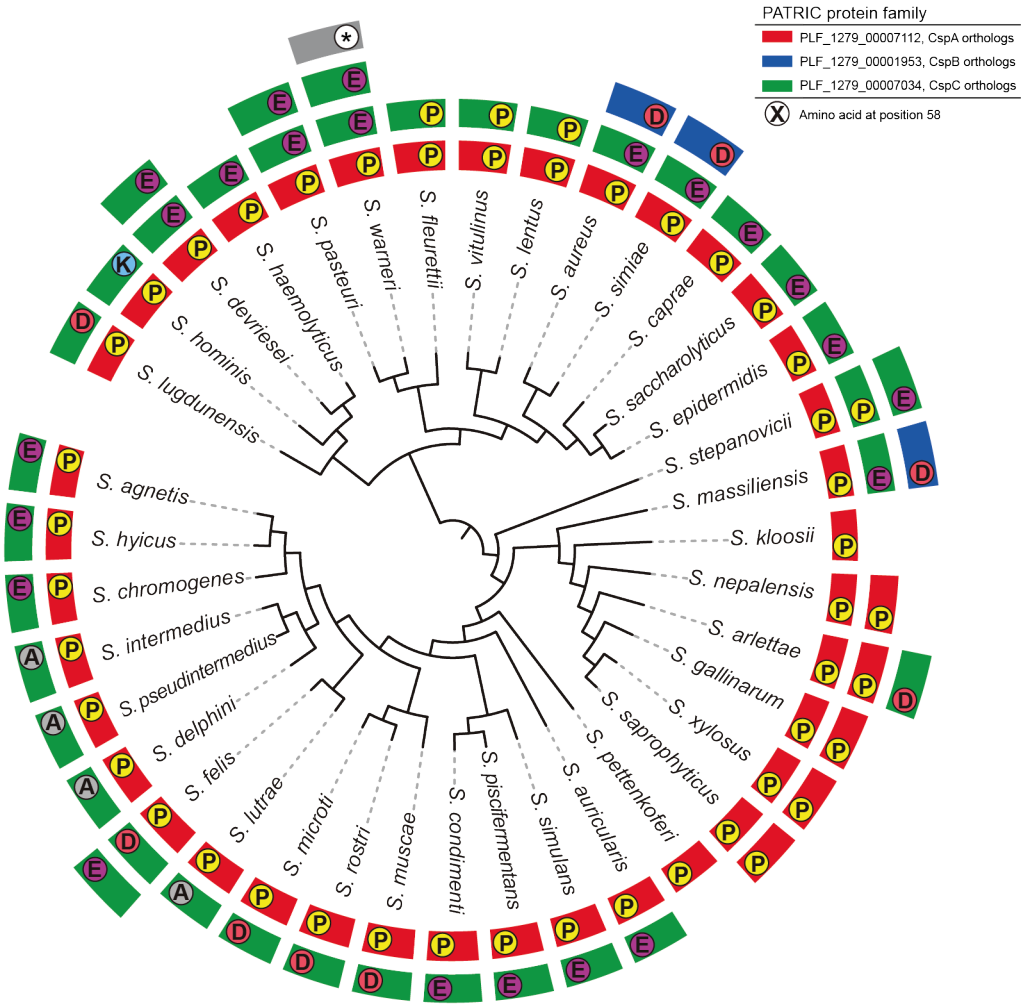

Figure 16. Comparison of the number and type of CSP paralogs among staphylococcal species. Representation of *Staphylococcus* phylogenetic tree using the TimeTree application (http://www.timet ree.org/) (Kumar *et al.*, 2017) that includes the number of CSPs encoded by each staphylococcal species and their PATRIC (https ://www.patri cbrc.org/) protein family group (Wattam *et al.*, 2017). The circled letters indicate the amino acid present in position 58 (see Annex 5). The asterisk indicates that one of the four *S. warneri* CSPs is truncated.

CHAPTER II:

Thermoregulation of CspB and CspC proteins is required for Staphylococcus aureus growth at ambient temperatures

CHAPTER II:

Thermoregulation of CspB and CspC proteins is required for *Staphylococcus aureus* growth at ambient temperatures

S. aureus CspB and CspC proteins are differentially expressed in function of the environmental temperature.

In order to monitor the expression patterns of CSPs when bacteria grow at different temperatures, we chromosomally tagged the *S. aureus csp* genes by fusing the 3xFLAG epitope to the C-terminal end. We then incubated the tagged strains in MH medium at 37ºC, which is the host-related temperature, and at 22ºC and 28ºC, two different environment temperatures that *S. aureus* may face upon leaving the host. Once the bacterial cultures reached the exponential phase (OD_{600nm} = 0.4), we extracted the total RNA and protein pools to determine the mRNA and protein levels *of cspA, cspB* and *cspC* genes. Northern blot analyses revealed that the mRNA concentration of the three *csp* genes was not significantly affected when bacteria were grown at different temperatures (Figure 17A). In agreement with this, the Western blot results confirmed that the $CspA^{3xF}$ protein levels were also invariable between the tested conditions (Figure 17B). In contrast, $CspB^{3xF}$ and $CspC^{3xF}$ were poorly expressed at 37ºC when compared to $CspA^{3xF}$ and their levels were significantly higher when bacteria were grown at 22º and 28ºC. Note that the highest $CspB^{3xF}$ and $CspC^{3xF}$ protein levels were found at 22ºC (Figure 17B). These results indicated that the

expression of CspB and CspC was regulated by changes in the environmental temperature, suggesting a potential role of these proteins in the adaptation of *S. aureus* outside the host.

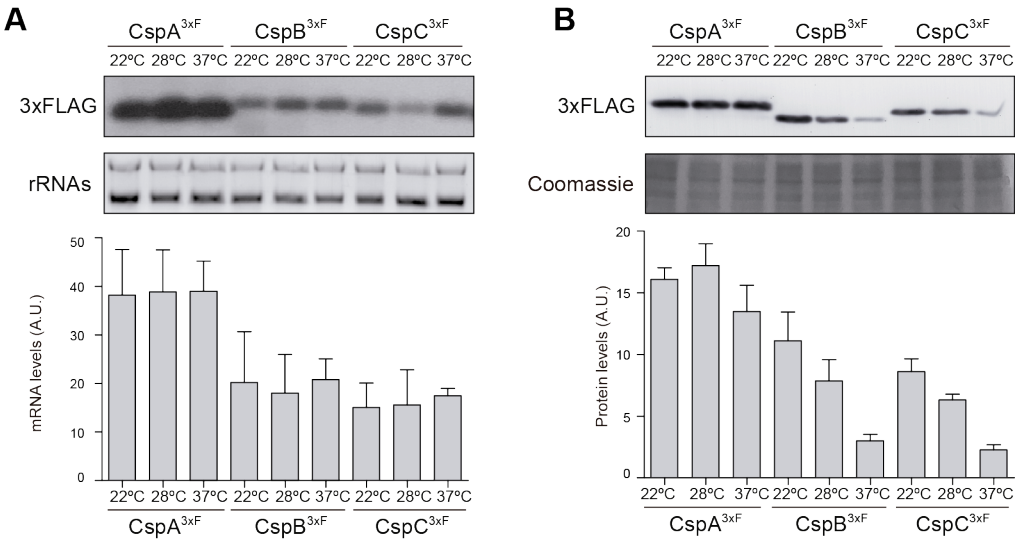

Figure 17. The CspB and CspC protein levels are differentially regulated in response to environmental temperatures. (**A**) Northern Blot showing *csp* mRNA levels, which were detected using a radiolabelled antisense 3xFLAG oligonucleotide probe. Midori Green-stained ribosomal RNAs are included as loading controls. (**B**) Western blot showing the levels of chromosomally 3xFLAG tagged CSPs, which were developed using peroxidase conjugated anti-FLAG antibodies and a bioluminescence kit. A Coomassie stained protein gel portion is included as loading control. Strains were grown until exponential phase (OD_{600} 0.4) in MH broth at environmental (22 and 28ºC) and host-related (37ºC) temperatures. Bar plots represent the mean and standard deviation of the mRNA and protein levels from three independent biological replicates, which were determined by densitometry of mRNA and protein bands using ImageJ (https://imagej.nih.gov/ij/). Representative images from the triplicates are shown.

Thermoregulation of the CspB and CspC expression is conducted through their 5'UTRs

The lack of correlation between the protein and mRNA levels of CspB and CspC when exposed to lower temperatures (22 and 28ºC), indicated that their expression might be controlled at the post-transcriptional level. This hypothesis was in agreement with previous results from our research group that showed how *S. aureus* CSPs were differentially produced when expressed from the same heterologous promoter (Caballero, 2018). Similar *S. aureus* CSPs levels were only achieved when the CDSs of these proteins were flanked by the same UTRs, indicating that such UTRs probably constituted, or at least harboured, post-transcriptional regulatory elements (Caballero, 2018). Interestingly, our transcriptomic maps showed that the *cspB* and *cspC* mRNAs carried long 5'UTRs of 112 and 113 nucleotides, respectively (Lasa *et al.*, 2011; Caballero, 2018). Since, it had already been proven that 5'UTRs were required to modulate CSPs expression in response to temperature changes in other bacterial models (Willimsky *et al.*, 1992; Graumann *et al.*, 1997; Giuliodori *et al.*, 2010; Zhang *et al.*, 2018; Ignatov *et al.*, 2020), it seemed reasonable for *cspB* and *cspC* 5'UTRs to play a role in the thermoregulation of CspB and CspC in *S. aureus*. To evaluate this hypothesis, we fused the whole 5'UTR plus the first five codons of *cspB* and *cspC* mRNAs to the ATG-less *gfp* gene of the pHRG construct, generating reporter plasmids p5'UTR^{cspB}-gfp and p5'UTR^{cspC}-gfp, respectively. Note that both reporter gene fusions were under the control of

the constitutive promoter Phyper, whose sequence was adapted to include an EcoRI site upstream of the native transcriptional start site. We used these plasmids to transform the *S. aureus* wild type strain and monitored the chimeric mRNA and GFP expression by Northern and Western blots, respectively. Figure 18A shows that the reporter plasmids expressed similar levels of the chimeric *5'UTR*^{cspB}*-gfp* and *5'UTR*^{cspC}*-gfp* mRNAs. In contrast, higher GFP levels were found when bacteria were grown at 22 and 28ºC than at 37ºC (Figure 18B). Interestingly, these results confirmed that the expression of both CspB and CspC proteins was significantly affected by the environmental temperature and that their thermoregulation was highly dependent on the 5'UTRs of their mRNAs.

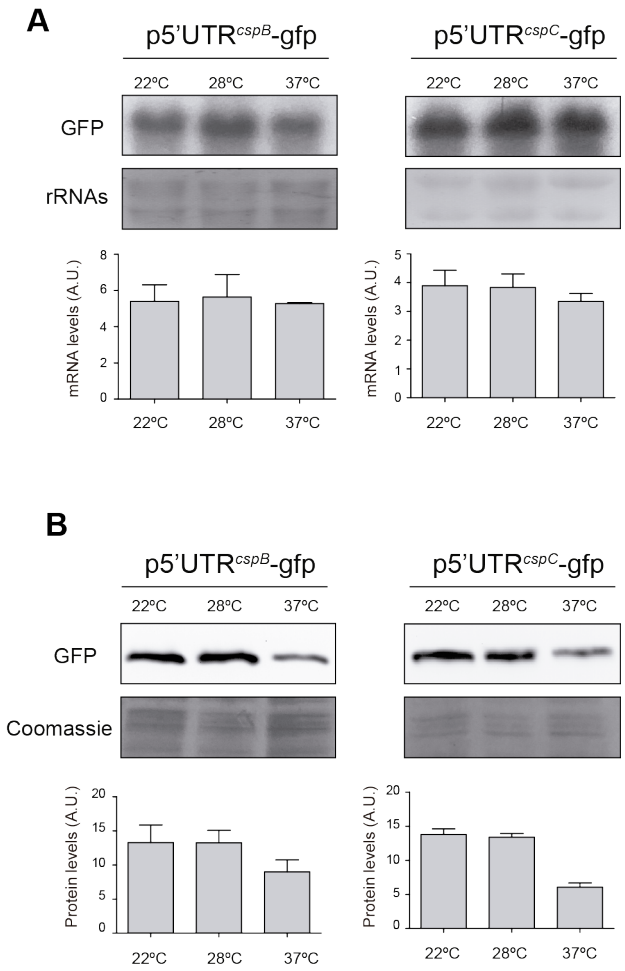

Figure 18. Thermoregulation is restricted to *cspB* and *cspC* 5'UTRs. (**A**) Northern blots showing the 5'UTR-gfp chimeric mRNA levels expressed from the corresponding reporter strains. Bacteria were grown in MH supplemented with appropriate antibiotic and incubated at 22, 28 and 37ºC until exponential phase was reached. Midori Green-stained ribosomal RNAs are included as loading controls. (**B**) Western blots showing the GFP protein levels in the strains expressing the *cspB* and *cspC* 5'UTR-GFP reporter fusions. GFP was developed using monoclonal anti-GFP and peroxidase-conjugated goat anti-mouse antibodies. Coomassie stain gel portions are included as loading controls. Bar plots represent the mean and standard deviation of mRNA and protein levels from three independent biological replicates, which were determined by densitometry of mRNA and protein bands using ImageJ (https://imagej.nih.gov/ij/). Representative images from the triplicates are shown.

The *cspB* and *cspC* 5'UTRs adopt alternatives RNA structures that work as RNA thermoswitches

The *cspA* 5'UTRs of *E. coli* and *L. monocytogenes* contain thermo-responsive secondary structure elements, which act as thermosensors that promote CspA expression at low temperatures (Giuliodori *et al.*, 2010; Zhang *et al.*, 2018; Ignatov *et al.*, 2020). To analyse whether *S. aureus cspB* and *cspC* 5'UTRs could also experiment temperature-dependent conformational changes that affected their translation, the first 130 nucleotides from the *cspB* and *cspC* mRNAs secondary structures were modelled using the *mfold* web server (Zuker, 2003). Interestingly, the RNA folding predictions revealed that each 5'UTR was able to adopt two alternative secondary structures. Despite some minor nucleotide differences between *cspB* and *cspC* 5'UTRs sequences, both 5'UTRs adopted homologous structures (Figure 19). One of the 5'UTR structures included a long and imperfect hairpin that comprised nucleotides ~3 to 76 while leaving the RBS exposed. Therefore, we defined this folding as "open" (O) conformation. In contrast, the alternative predicted configuration formed a double stranded structure through base pairing of nucleotides ~25 to 54 with nucleotides ~100 to 129 (nucleotide stretch that includes the RBS region). This nucleotide interaction masked the RBS, making it inaccessible to the ribosomes. For this reason, we named this structure "locked" (L) conformation (Figure 19).

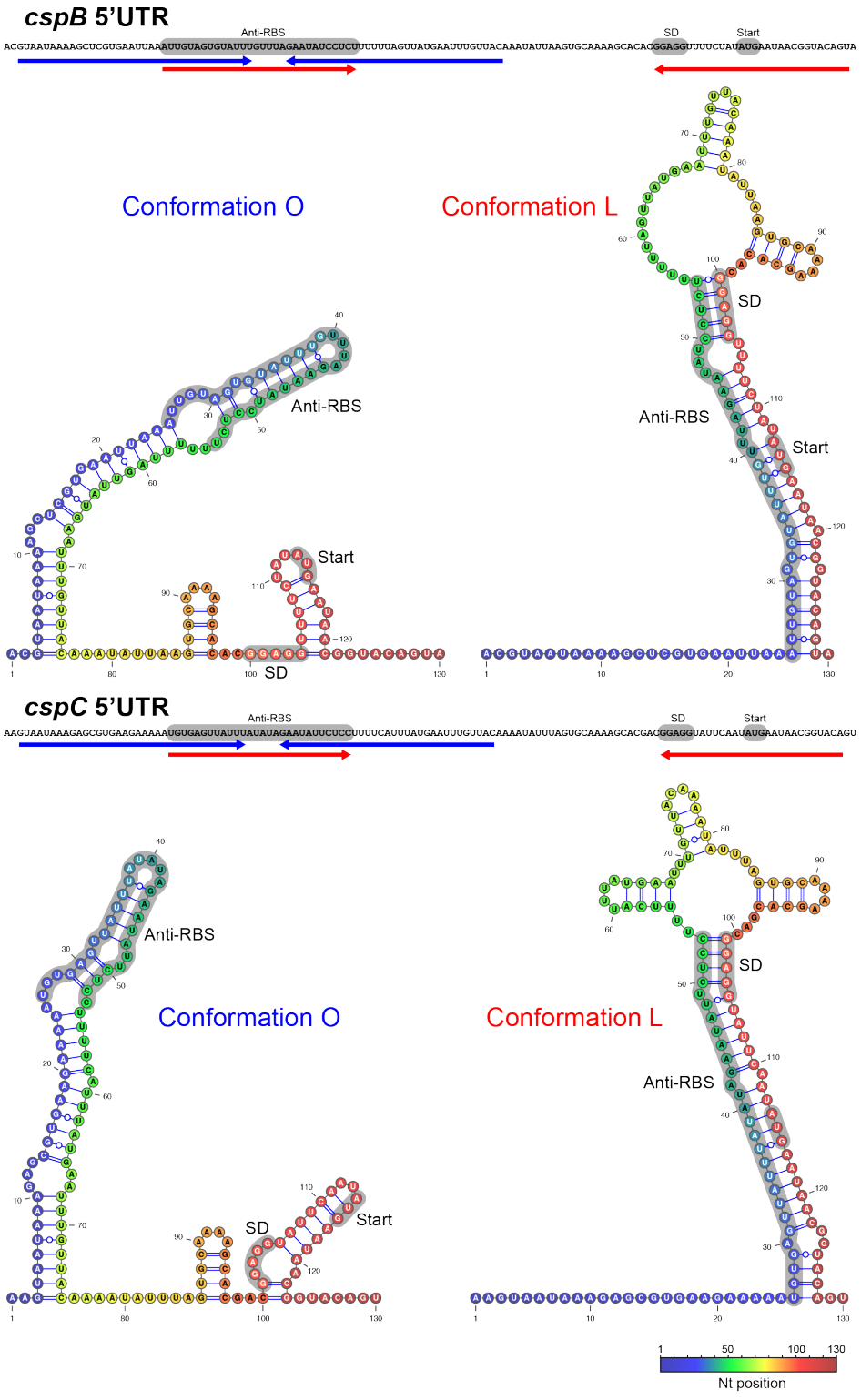

Figure 19. Putative alternative structures adopted by the *cspB* and *cspC* 5'UTRs. RNA structures were predicted using the mfold web server tool (Zuker, 2003) and visualized and drawn using the VARNA software. Colours represent nucleotide position within the RNA. Arrows below the 5'UTR sequences indicate the interacting nucleotide regions. Blue arrows, conformation O; Red arrows, conformation L. The Shine-Dalgarno (SD), the start codon and the anti-RBS region appear as grey shaded areas.

Both alternative conformations for the *cspB* and *cspC* mRNAs were orthologous to ones described for the 5'UTR of *L. monocytogenes cspA*, despite the lack of sequence similarity between the 5'UTRs of both species (Ignatov *et al.*, 2020).

Considering that the 5'UTRs of *cspB* and *cspC* seemed affected by the environmental temperature (Figure 18), we reasoned that such effect might be explained by shifts between the two alternative conformations (O and L) upon temperature changes, as previously described (Zhang *et al.*, 2018; Ignatov *et al.*, 2020). Hypothetically, conformation O would be favoured at lower temperatures, promoting CspB and CspC translation, while conformation L would be more dominant during *S. aureus* growth at 37ºC. To validate this idea, we performed *in vitro* enzymatic structural probing of the *cspB* and *cspC* 5'UTRs at 22 and 37ºC using RNases T1 and S1, which cleave unpaired bases G and A>U>C, respectively. The enzymatic cleavage patterns of the *cspC* 5'UTR illustrated the differences between both structures more clearly than those of the *cspB* 5'UTR (Figure 20).

Figure 20. Enzymatic probing at different temperatures of the alternatives structures found in the *cspB* and *cspC* 5'UTRs. Electrophoretic migration of the radiolabelled *cspB* 5'UTR (**A**) and *cspC* 5'UTR (**B**) after RNase T1 (T1) and RNAse S1 (S1) cleavage at 22 and 37ºC. Samples were subjected to denaturation at 90ºC and renaturation at 22 or 37ºC for 15 min. Lane C: incubation control in the absence of RNase T1/S1. Cleavage reactions were performed in the presence of increasing concentrations of T1: $1x10^{-3}$ U/µl, $2x10^{-2}$ U/µl and $5x10^{-2}$ U/µl or S1:$5x10^{-5}$ U/µl, $2x10^{-5}$ U/µl and $1x10^{-5}$ U/µl. Lanes RNA: RNA control; HA: alkaline hydrolysis ladder and T1: RNAse T1 control.

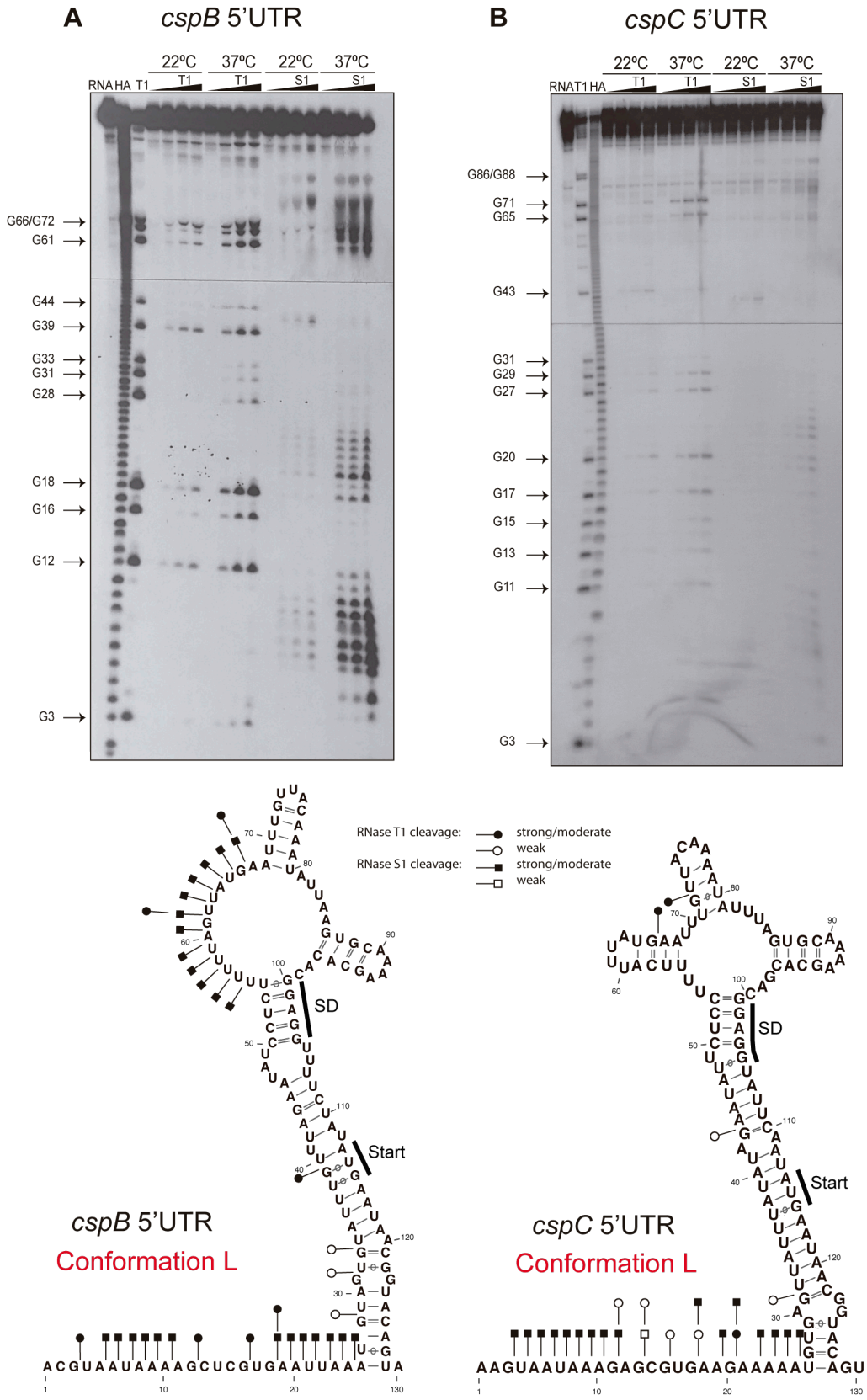

The *cspC* 5'UTR showed an increased sensitivity to RNase S1 and T1 reactivities between nucleotides 7-11, 19-24, 65 and 72 at 37ºC (Figure 20) while only few RNase cleavages (~42-43) could be observed at 22ºC, indicating that the region comprising the first ~60-70 nucleotides adopts a double-stranded configuration at such temperature. Regarding the *cspB* 5'UTR probing, RNAse S1 cleavage patterns were similar to those found in *cspC*, suggesting that both 5'UTRs might be analogously reorganized in function of temperature changes (Figure 20). Note that although several of the RNase T1 processing correlated with the expected structure at the corresponding temperature, there were some minor cleavages that suggested that both structures might coexist at some point.

The existence of two alternative structures in each of the 5'UTRs of *cspB* and *cspC* mRNAs indicated that they could also work as thermo-sensitive RNA elements to control protein expression.

Conformation O contains a thermo-responsive RNA hairpin that favours RBS accessibility

The long hairpin found in conformation O appeared to be critical for the reorganization of the *cspB* and *cspC* 5'UTRs structures. Since the anti-RBS region was sequestered within this structure (Figure 19), one could reason it worked as an anti-anti-RBS element. This would imply that the hairpin must be unfolded for the anti-RBS region to pair the RBS and impair CspB/CspC translation. Since such mechanism would apparently respond

to temperature changes, it seemed possible that the hairpin itself acted as a thermosensor. To explore this idea, we used a molecular beacon (MB) system, as previously described (Caballero *et al.*, 2018; Menendez-Gil, Caballero, Solano, *et al.*, 2020). The MB consisted of ~75-mer ssDNA oligonucleotides that were designed to mimic the long hairpin found in conformation O of the *cspB* and *cspC* 5'UTRs (Figure 19). Additionally, the 5'- and 3'-end of the oligonucleotides carried the carboxyfluorescein fluorescent dye (FAM) and the Iowa Black FQ quencher (IBkFQ), respectively (Figure 21A and Figure 21B). Should the MB fold as expected, both molecules would fall in close proximity to each other, preventing fluorescence emission (Menendez-Gil, Caballero, Solano, *et al.*, 2020). We began by incubating the *cspB* and *cspC* MBs at 16ºC for 5 min and then increased the temperature in intervals of 3ºC every 5 min until 65ºC were reached. After incubating them for 5 min at 65ºC, the temperature was gradually decreased using the same intervals. Fluorescent emission was monitored for the duration of the process. We also included the MB that mimicked the *cspA* 5'UTR hairpin as a control (Caballero *et al.*, 2018). Note that CspA expression was not dependent on temperature changes (Figure 17B). The results showed that fluorescence emission could be registered for the *cspB* and *cspC* MBs when reaching temperatures above ~31ºC, with a maximum signal peak at ~43ºC (Figure 21C). Correspondingly, when the temperature was gradually decreased, a drop in the fluorescent emission was observed. There was no detectable signal below 30ºC, indicating that

the hairpin structure had been restored (Figure 21C). All in all, these results indicated that the *cspB* and *cspC* hairpins started to unfold at host-related temperatures, which range from 30-33ºC (human nose temperature) to 37-43ºC (human infection temperature) (Lindemann *et al.*, 2002; Tong *et al.*, 2015). In contrast, the *cspB* and *cspC* MBs were completely folded (no fluorescence emission was detected) when exposed to ambient temperatures (below 30ºC). The *cspA* MB melts emitting fluorescence when incubated above 43ºC, which are not correlated with conditions that permits the optimal *S. aureus* growth. Altogether, these data indicated that *cspB* and *cspC* 5'UTR structural reorganizations might be critical to modulate the expression of both CSPs according the environmental temperatures that *S. aureus* faced when moving from the host to the environment.

Figure 21. *cspB* and *cspC* hairpins from conformation O could work as thermo-responsive RNA elements. Schematic representation of the molecular beacon (MB) design that mimics the stem loop of conformation O from the *cspB* (**A**) and *cspC* (**B**) 5'UTRs. The 5'-end and 3'-end harbour the fluorescein (FAM) and the Iowa Black FQ (IBkFQ) molecules, respectively. (**C**) Detection of FAM fluorescence emission of MB-CspB (red), MB-CspC (green) and MB-CspA (blue) in function of the temperature. MBs were equilibrated at 13ºC for 10 min and then the temperature was increased 3ºC every 5 min. After 5 min of incubation at 65ºC, the temperature was gradually decreased following the inverse pattern. Fluorescence was registered for the duration of the experiment. Mean and standard deviations from three independent biological replicates are plotted.

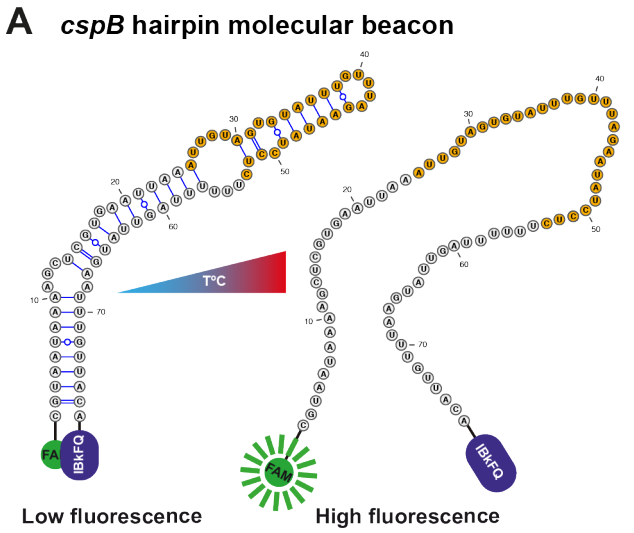

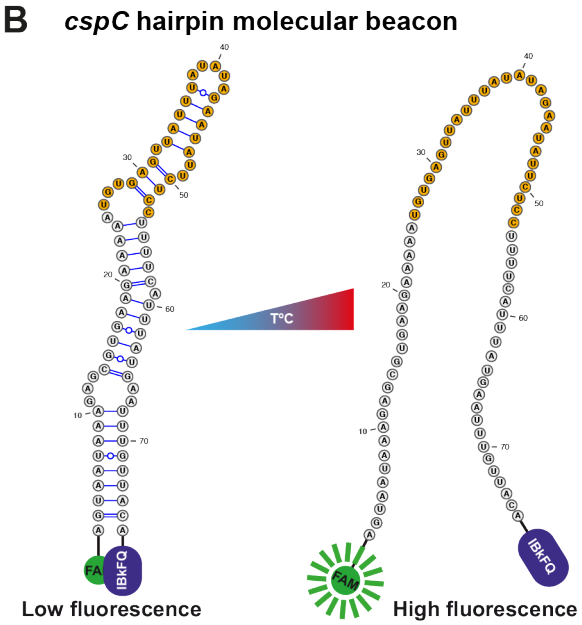

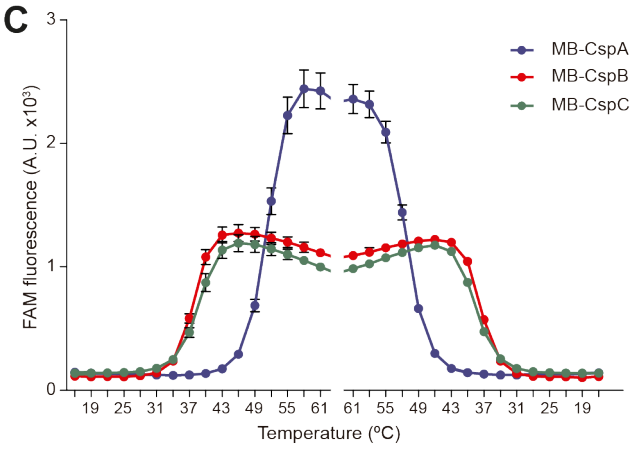

Mutations in the 5'UTR of the *cspB* and *cspC* genes confirm that their expression is thermoregulated *in vivo*.

To further validate the predicted alternative 5'UTR structures *in vivo*, we constructed variations of the p5'UTR^{cspB}-gfp and p5'UTR^{cspC}-gfp plasmids that included several mutations in the 5'UTR of the *cspB* and *cspC* mRNAs (Annex 6). We began by generating the 5'UTR$^{cspB}\Delta$24-gfp and 5'UTR$^{cspC}\Delta$24-gfp plasmids, which carried a deletion of the first 24 nucleotides of both 5'UTRs (Annex 6). These nucleotides would be essential to form the long thermo-responsive element that sequesters the anti-RBS in the O conformation (Figure 19). At the same time, these 24 nucleotides would be unpaired when conformation L is adopted, making them irrelevant for the formation of the structure that blocks the RBS (anti-RBS). The expected outcome from this deletion was to find a dominant L conformation (Figure 19 and Annex 6). In agreement with this, Western blot analyses revealed that the GFP expression was drastically reduced in strains expressing the 5'UTR$^{cspB}\Delta$24-gfp and 5'UTR$^{cspC}\Delta$24-gfp mRNAs (Figure 22). We then performed site-directed mutagenesis in the *cspB* 5'UTR of the p5'UTR^{cspB}-gfp plasmid, by replacing nucleotides 47-UAU-49 with AA. Since nucleotides 47-UAU-49 would base pair with nucleotides 33-GUA-35 to form the anti-anti-RBS structure in conformation O, such substitution would cause a destabilisation and, hence, favour alternative conformation L (Annex 6 and Figure 19).

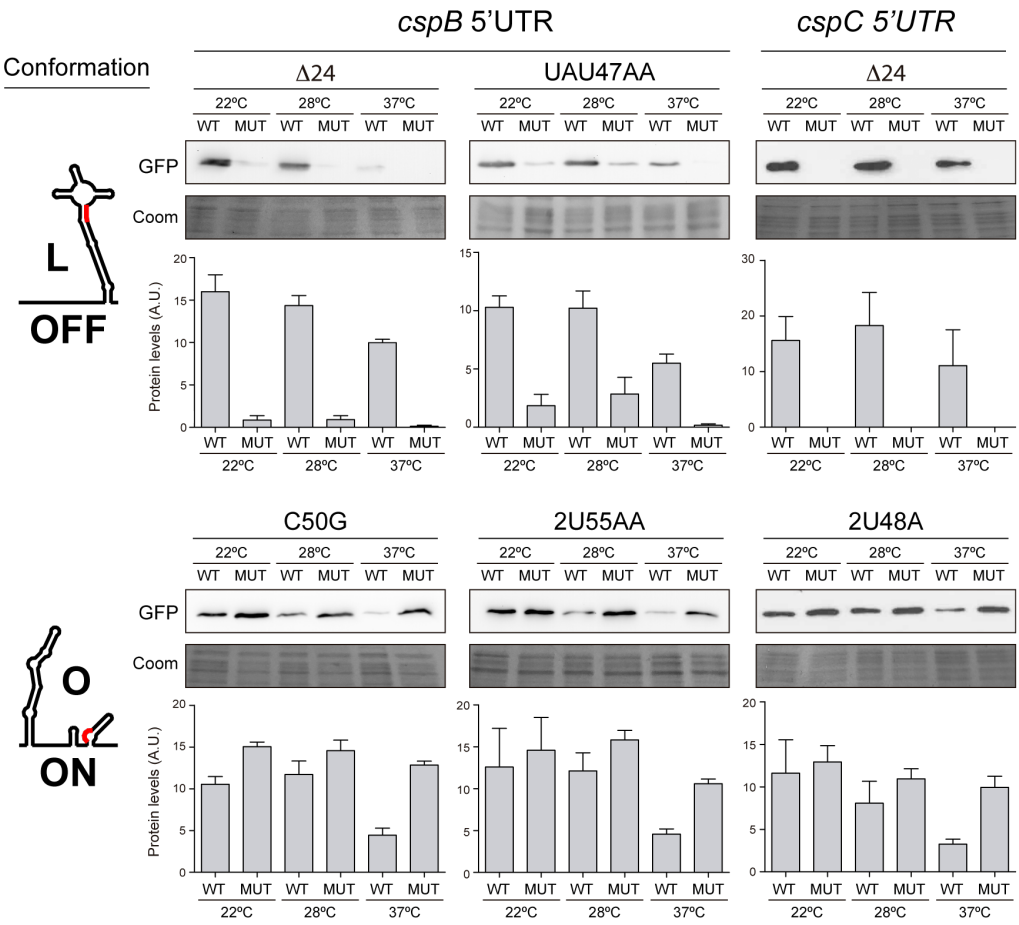

Figure 22. CspB and CspC expression is controlled by their alternative 5'UTR structures *in vivo*. Western blots showing the effect on the GFP levels of different mutations in the 5'UTR of the p5'UTR^{cspB}-gfp and p5'UTR^{cspC}-gfp plasmids. Such mutations favoured one of the two 5'UTR alternative conformations. The expected conformation for each mutation, O (translation ON) or L (translation OFF), is indicated on the left-hand side of the figure. Coomassie stained gel portions (Coom) were included as loading controls. Bar plots represent the mean and standard deviation of protein levels from three independent biological replicates, which were determined by densitometry of protein bands using ImageJ (https://imagej.nih.gov/ij/). Representative images from the triplicates are shown.

As anticipated, Western blot results showed lower GFP levels for the strains carrying the mutated plasmids regardless of the temperature (Figure 22). This indicated that the 5'UTR was probably adopting the L conformation, for which translation of *cspB* is reduced. Finally, we substituted 50-C for G and 55-UU-56 for AA in the *cspB* 5'UTR of p5'UTR^{cspB}-gfp and 48-UU-49 by A in the *cspC* 5'UTR of p5'UTR^{cspC}-gfp (Annex 6). These mutations would stabilize the anti-anti-RBS hairpin within the *cspB* and *cspC* 5'UTRs, respectively, favouring conformation O over conformation L (Figure 19 and Annex 6). We analysed the GFP levels for these *cspB* and *cspC* 5'UTR substitutions at different temperatures by Western blot and found that they were similar to the ones found for p5'UTR^{cspB}-gfp and p5'UTR^{cspC}-gfp at 22ºC (Figure 22). This indicated that such nucleotide substitutions made the 5'UTRs unresponsive to temperature changes. These results showed that the expression of CspB and CspC may be controlled by alternative 5'UTR structures *in vivo* that block or facilitate RBS recognition by the ribosome depending on the environmental temperature.

CspA is required for the thermoregulation of CspB and CspC in *S. aureus*

Thermosensors are self-functional structures located at the 5'UTRs that suffer rearrangements upon shifts in the temperature. This usually affects RBS accessibility and, hence, translation initiation (Narberhaus *et al.*, 2006; Klinkert and Narberhaus, 2009; Loh *et al.*, 2018). To evaluate if the alternative structures of the *S. aureus cspB* 5'UTRs relied entirely on temperature, we decided to transfer the 5'UTR GFP-reporter plasmid to a different bacterial system. This strategy was built around the idea that if no additional factors were needed, the 5'UTR would still respond to temperature changes once decontextualized. First, we inserted the 5'UTR^{cspB}-gfp module into a vector harbouring the *pblaZ* promoter. As a result, the pEW-5'UTR^{cspB}-gfp plasmid was generated. Next, we transformed the *E. coli* XL1B strain with the new construct. Finally, we performed Western blots and showed that the GFP levels were similar at all the tested temperatures (Figure 23). This suggested that the *cspB* thermoregulatory mechanism might require additional host-specific factors.

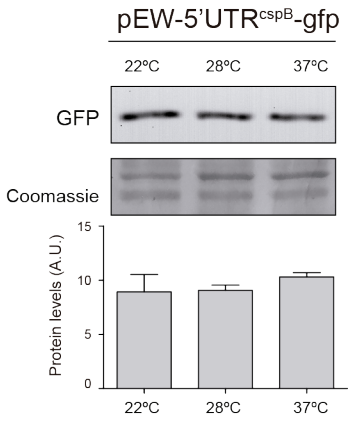

Figure 23. Thermoregulation of CspB does not occur in *E. coli*. Western Blot showing GFP expression from *E. coli* cells harbouring pEW-5'UTR^{cspB}-gfp plasmid. Bacteria were grown at 22, 28 or 37ºC in LB until exponential phase (OD_{600} 0.4). GFP was developed as described in Figure 18. Bar plots show the mean and standard deviation of GFP protein levels from three independent biological replicates, which were determined by densitometry of protein bands using ImageJ (https://imagej.nih.gov/ij/). Representative images from the triplicates are shown.

This was in agreement with previous results that showed that the *E. coli cspA* and *cspB* thermosensors required the action of CSPs to modulate their 5'UTR structures (Zhang *et al.*, 2018). Zhang *et al* reported that the structural rearrangements did not occur in a Δ*cspABEG strain*, which lacked the *csp* ORFs while retaining their 5'UTRs. In fact, they showed that CspA regulated its own expression by binding to its own mRNA and avoiding the formation of a double stranded *cspA* 5'UTR structure (Zhang *et al.*, 2018). To test whether CspB or CspC could be the host factors participating in the structural reorganization, the reporter plasmids p5'UTR^{cspB}-gfp and p5'UTR^{cspC}-gfp were electroporated into the *S. aureus* Δ*cspB* and Δ*cspC*

strains, respectively. The Western blot results showed a similar behaviour in terms of GFP expression between the WT and the mutant strains for all the tested temperatures (Figure 24). This indicated that the expression of both proteins was not auto-regulated, at least in the tested conditions.

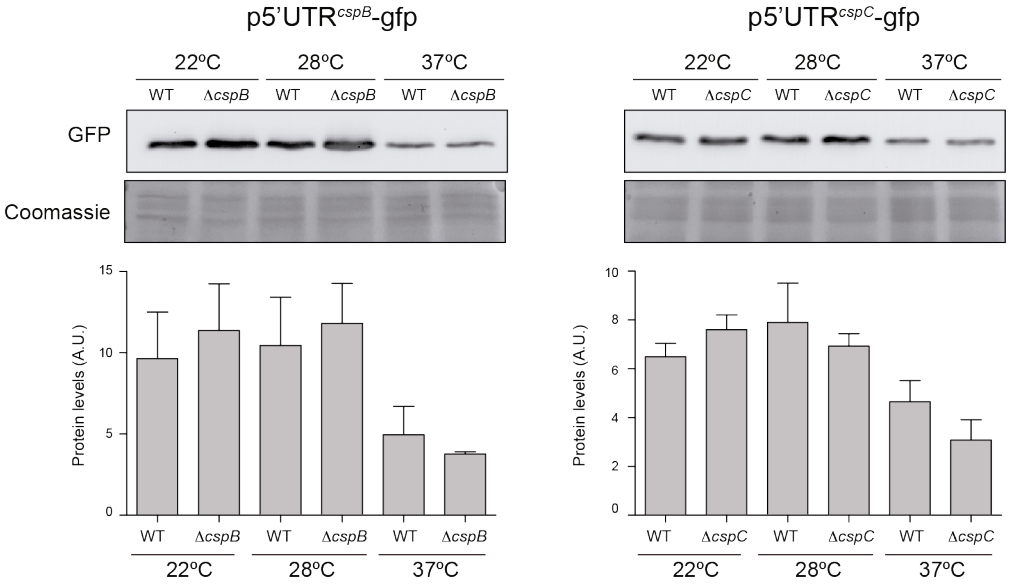

Figure 24. The CspB and CspC protein expression is not auto-regulated in *S. aureus*. Western blot analyses of GFP levels expressed from the *S. aureus* WT, Δ*cspB* and Δ*cspC* strains carrying *cspB* and *cspC* 5'UTR-GFP reporters, which were grown in MH at 22, 28 and 37ºC. GFP was developed as described in Figure 18. Bar plots show the mean and standard deviation of the GFP protein levels from three independent biological replicates, which were determined by densitometry of protein bands using ImageJ (https://imagej.nih.gov/ij/). Representative images from the triplicates are shown.

Previous studies of our group showed that CspA was able to bind to the *cspB* and *cspC* mRNAs in *S. aureus*. Deletion of *cspA* increased CspC expression indicating that CSPs regulation is interconnected (Caballero *et al.*, 2018). We wondered whether CspA could be the additional factor participating in the thermoregulation of CspB and CspC expression in *S. aureus*. Therefore, reporter plasmids p5'UTR^{cspB}-gfp and p5'UTR^{cspC}-gfp were introduced in the Δ*cspA* mutant and Western blot experiments were carried out. The GFP levels in the Δ*cspA* mutant were higher than those of the WT strain when grown at 37ºC, confirming that CspA repressed CspB and CspC expression through their 5'UTRs (Figure 25A). When strains were grown at 22 and 28ºC no differences on their GFP levels were found between the WT and Δ*cspA* strains. To confirm these results, we chromosomally deleted the *cspA* gene from the strains expressing the tagged CspB^{3xF} and CspC^{3xF} proteins and performed Western blots. Figure 25B shows that deletion of the *cspA* gene increased the CspB^{3xF} and CspC^{3xF} protein levels at 37ºC, confirming that CspA repressed the expression of both CSPs and suggesting its involvement in their thermoregulation.

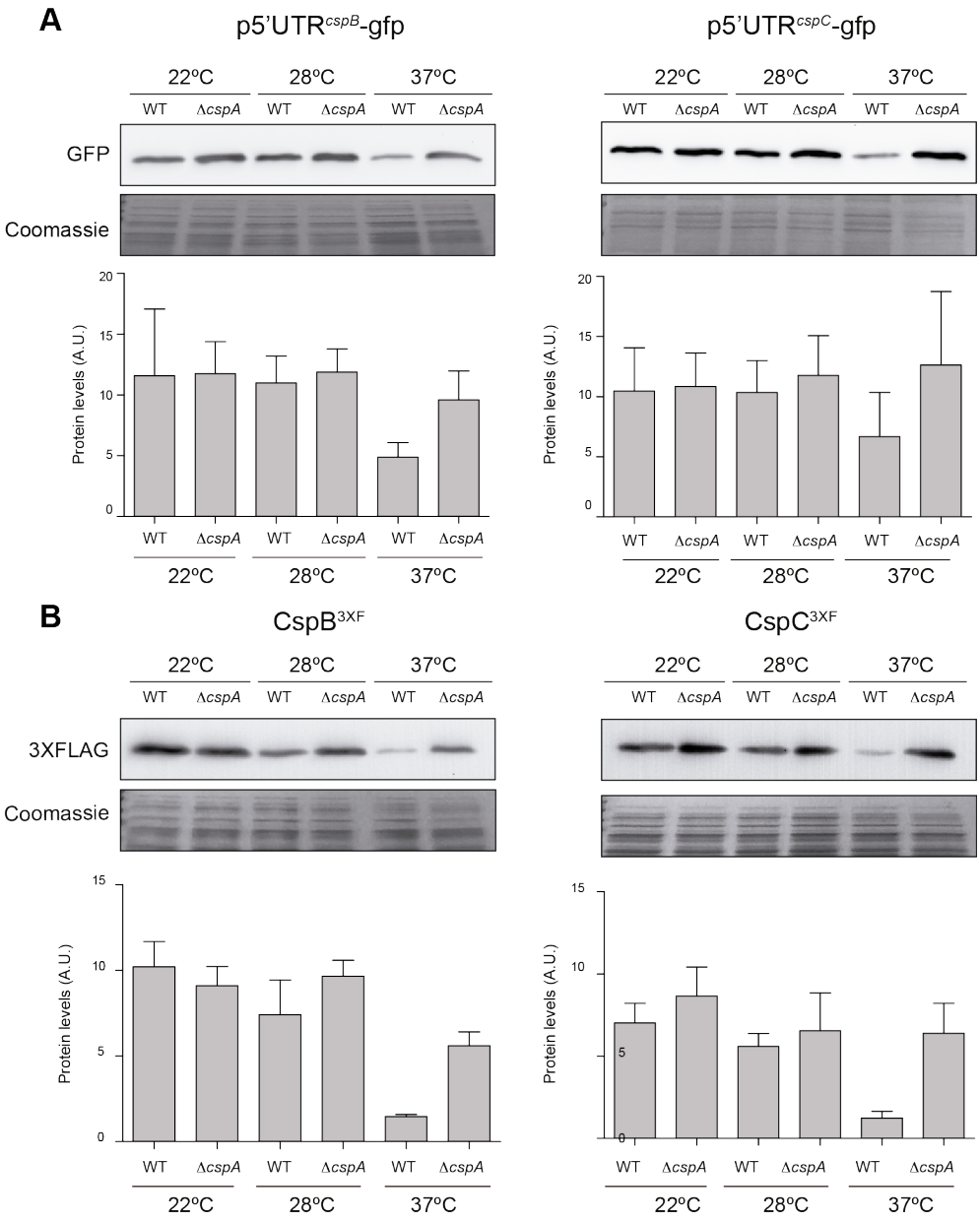

Figure 25. CspA is required for CspB and CspC thermoregulation. (**A**) Western blot results of the GFP levels expressed from the *S. aureus* WT and Δ*cspA* strains, carrying the *cspB* and *cspC* 5'UTR-GFP reporter plasmids and grown in MH at 22, 28 and 37ºC. GFP was developed as described in Figure 18. (**B**) Western blot showing the chromosomal expression of $CspB^{3XF}$ and $CspC^{3XF}$ from the WT and Δ*cspA* strains grown in MH at 22, 28 and 37ºC and developed as described in Figure 17. Coomassie stain gel portions are included as loading controls. Bar plots represent the mean and standard deviation of protein levels from three independent biological replicates, which were determined by densitometry of protein bands using ImageJ (https://imagej.nih.gov/ij/). Representative images from the triplicates are shown.

CspA represses CspB and CspC expression by favouring conformation L at 37ºC

In order to explain how CspA might repress CspB and CspC at 37ºC, we considered two hypotheses as the most plausible. On the one hand, CspA could directly bind to the RBS region and block protein translation. On the other hand, CspA could interact with the 5'UTRs to favor conformation L, which is the one that represses translation through an anti-RBS structure. To prove either of both hypothesis, we transformed the Δ*cspA* mutant with the reporter plasmids carrying some of the above mentioned 5'UTR mutations. We then compared by Western blot the GFP levels of the Δ*cspA* reporter strains grown at 37ºC with their WT counterparts (Figure 26). If CspA bound to the RBS, a higher expression of GFP would be expected in the 5'UTR mutants that favor the folding of conformation O (C50G and UU55AA in *cspB* 5'UTR and UU48A in *cspC* 5'UTR) in the Δ*cspA* strain. However, Figure 26 shows no differences between the GFP expression of the WT and Δ*cspA* strains. This result supported the second hypothesis, meaning that CspA might favors conformation L at 37ºC. Moreover, no differences were found when comparing the GFP levels between the WT and Δ*cspA* strains carrying the reporter plasmids with mutations Δ24 for the *cspB* 5'UTR and Δ24 for the *cspC* 5'UTR (which favour conformation L) (Annex 6 and Figure 26). This suggested that CspA was not required for repression when enforcing conformation L.

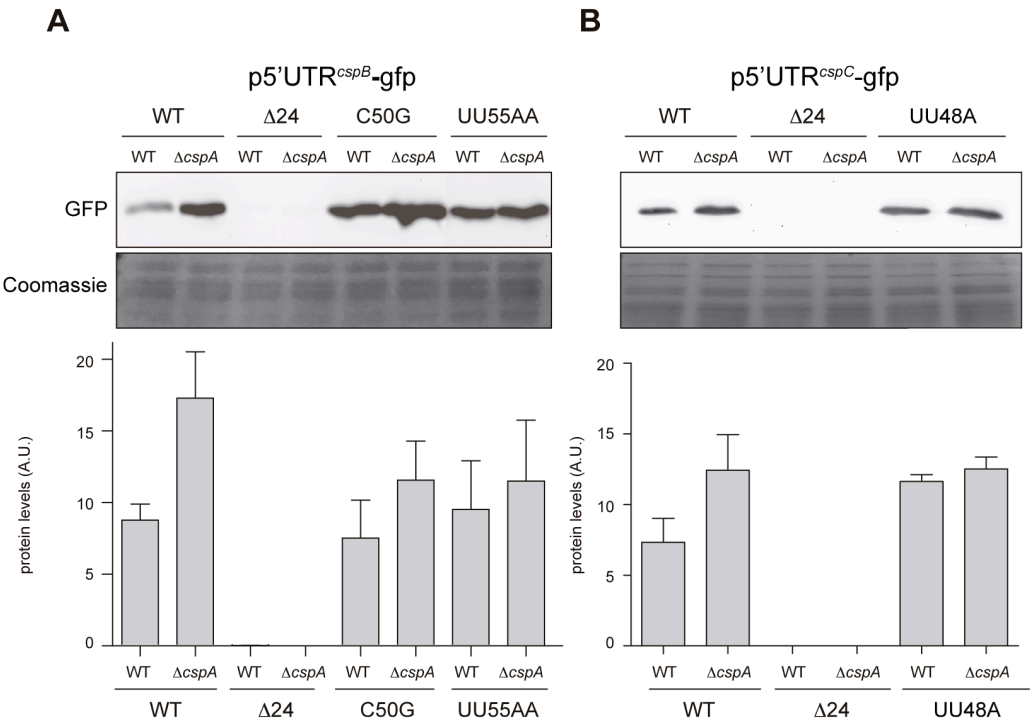

Figure 26. CspA is essential for CspB and CspC repression by promoting conformation L at 37ºC. Western blots showing GFP levels from the WT and Δ*cspA* strains expressing the *cspB* (**A**) or *cspC* and (**B**) 5'UTR-GFP reporter plasmids, including the mutations used in Figure 22. Total protein extracts were processed as described in Figure 18. Coomassie gel portions were included as loading controls. Bar plots represent the mean and standard deviation of GFP levels from three independent biological replicates, which were determined by densitometry of protein bands using ImageJ (https://imagej.nih.gov/ij/). Representative images from the triplicates are shown.

However, we were aware of the possibility of CspA might be sensitive to 5'UTR mutations that lead to changes in nucleotide-pairing affinity. It has been proposed that CSP proteins bind to RNA weakly and in a non-specific way, however, in some occasions certain RNA motifs could contribute to CSPs functionality (Jiang *et al.*, 1997; Phadtare and Inouye, 1999; Sachs, Max, Heinemann, and Balbach, 2012b; Caballero *et al.*, 2018). For example, we showed that the auto-regulation of CspA in *S. aureus* requires an U-rich motif located in the *cspA* 5'UTR (Caballero *et al.*, 2018). The *cspB* 5'UTR carries two U-rich regions (36-UUUGUUU-43 and 54-UUUUUU-59) located at the hairpin of conformation O (Figure 19). It is possible that CspA could be targeting these regions to avoid hairpin folding at 37ºC. Note that making 5'UTR mutants to discriminate these potential CspA binding sites without affecting the folding of both alternative conformations is extremely difficult. Among the two U-rich regions, the second motif presented more unpaired bases in both conformations than the first one. In fact, this was a reason to make the mutant UU55AA in *cspB* 5'UTR. To analyse if the increased reporter expression observed with this mutant was due to the change of folding affinities or the inability of CspA to bind to the motif, we generated another 5'UTR mutant that compensated the UU55AA mutation. By introducing the UU26AA mutation in the p5'UTR^{cspB}UU55AA-gfp reporter plasmid we reconstituted the original hairpin bubble while eliminating U-rich stretch (Figure 27A).

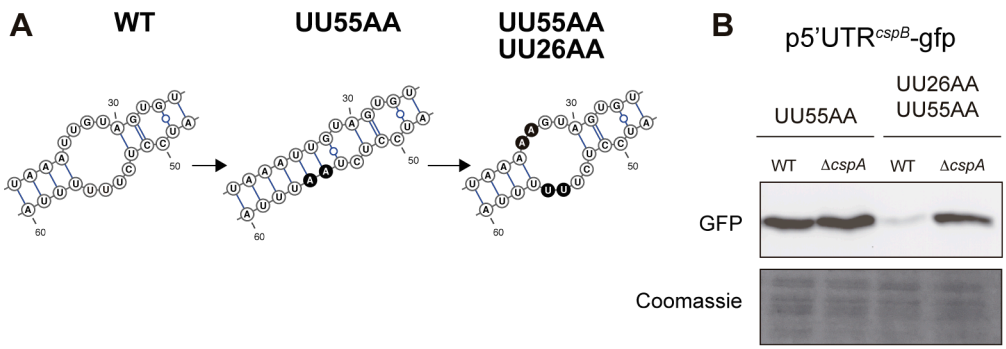

Figure 27. CspA is essential for CspB and CspC repression by promoting conformation L at 37ºC. (A) Schematic representation of the *cspB* 5'UTR mutation UU55AA UU26AA. (**B**) Western blots showing GFP levels from the WT and Δ*cspA* strains expressing the *cspB* 5'UTR-GFP reporter plasmids, including the mutations indicated in A. Total protein extracts were processed as described in Figure 18. Coomassie gel portions were included as loading controls. A representative image from the triplicates is shown.

Western blot experiments showed that CspA could still repress the GFP reporter translation in this compensated mutant, suggesting that motif 54-UUUUUU-59 was not required for CspA to exert its repression (Figure 27B). Although we cannot exclude that other mutations could affect potential CspA binding sites, the mutations were initially thought to favour one or the other conformation in the 5'UTR. Therefore, changes in these nucleotide-pairing affinities could be also affected by the role of CspA. Although the *cspB* and *cspC* 5'UTR regions targeted by CspA remain elusive, these results confirmed that CspA is essential for the repression of CspB and CspC expression by promoting the folding of conformation L at 37ºC.

Thermoregulation of CSPs is required for suitable growth of *S. aureus* at ambient temperatures.

Besides its pathogenicity, the ability to colonize different niches as well as its capacity to spread rapidly by direct contact and/or throughout contaminated surfaces makes *S. aureus* a life threating pathogen (Tong *et al.*, 2015). The higher expression rate of CspB and CspC proteins when *S. aureus* grows at ambient temperatures suggested that these proteins should contribute to the adaptation of *S. aureus* when it leaves the host. To further investigate this, we plated serial dilutions of overnight cultures of the WT and isogenic Δ*cspB* and Δ*cspC* mutant strains in TSA plates and incubated at 22 and 37ºC. Figure 28A shows no growth differences between the WT and *csp* mutants at the tested temperatures. Since both CSPs were induced at ambient temperatures (Figure 17), it seemed possible that these proteins were playing redundant roles, as previously described in *E. coli* (Xia *et al.*, 2001; Michaux *et al.*, 2017). To address this issue, we generated a double mutant strain (Δ*cspBC*) and analysed its growth capacity at different temperatures. Interestingly, the growth of the Δ*cspBC* strain was decreased at 22ºC when compared with the WT strain (Figure 28A). This result suggested redundant roles for both CspB and CspC proteins in *S. aureus* adaptation to the environment when outside the host.

In order to evaluate the biological relevance of the thermoregulation controlling CspB and CspC expression, we constructed chromosomal

mutants that modified the structural organization of the 5'UTR to prevent *cspB* and *cspC* mRNA translation. Out of the different mutations shown in Annex 6, we chose to delete the first 24 nucleotides from both *cspB* and *cspC* mRNAs since it produced a stronger repression of the GFP reporter (Figure 22). First, to control that these mutations produced the same effect in the chromosome as seen for the reporter plasmids, the corresponding 24 nt were deleted from the tagged *cspB*^{3xF} and *cspC*^{3xF} strains. Western blot analyses confirmed that the chromosomal Δ24B^{3xF} and Δ24C^{3xF} mutant strains were unable to express CspB^{3xF} and CspC^{3xF} (Figure 28B).

Next, the same mutations were performed in the wild type strain to produce the single-mutants Δ24B and Δ24C and the double-mutant Δ24B-Δ24C. Overnight cultures of these strains were diluted and plated on TSA plates. Figure 28C shows that the Δ24B-Δ24C strain presented a growth defect comparable to the Δ*cspBC* mutant when incubated at 22ºC (Figure 28C). This result confirmed that the structures located at the *cspB* and *cspC* 5'UTRs are essential for the thermoregulation of the CspB and CspC proteins and, in return, critical *S. aureus* growth at ambient temperatures.

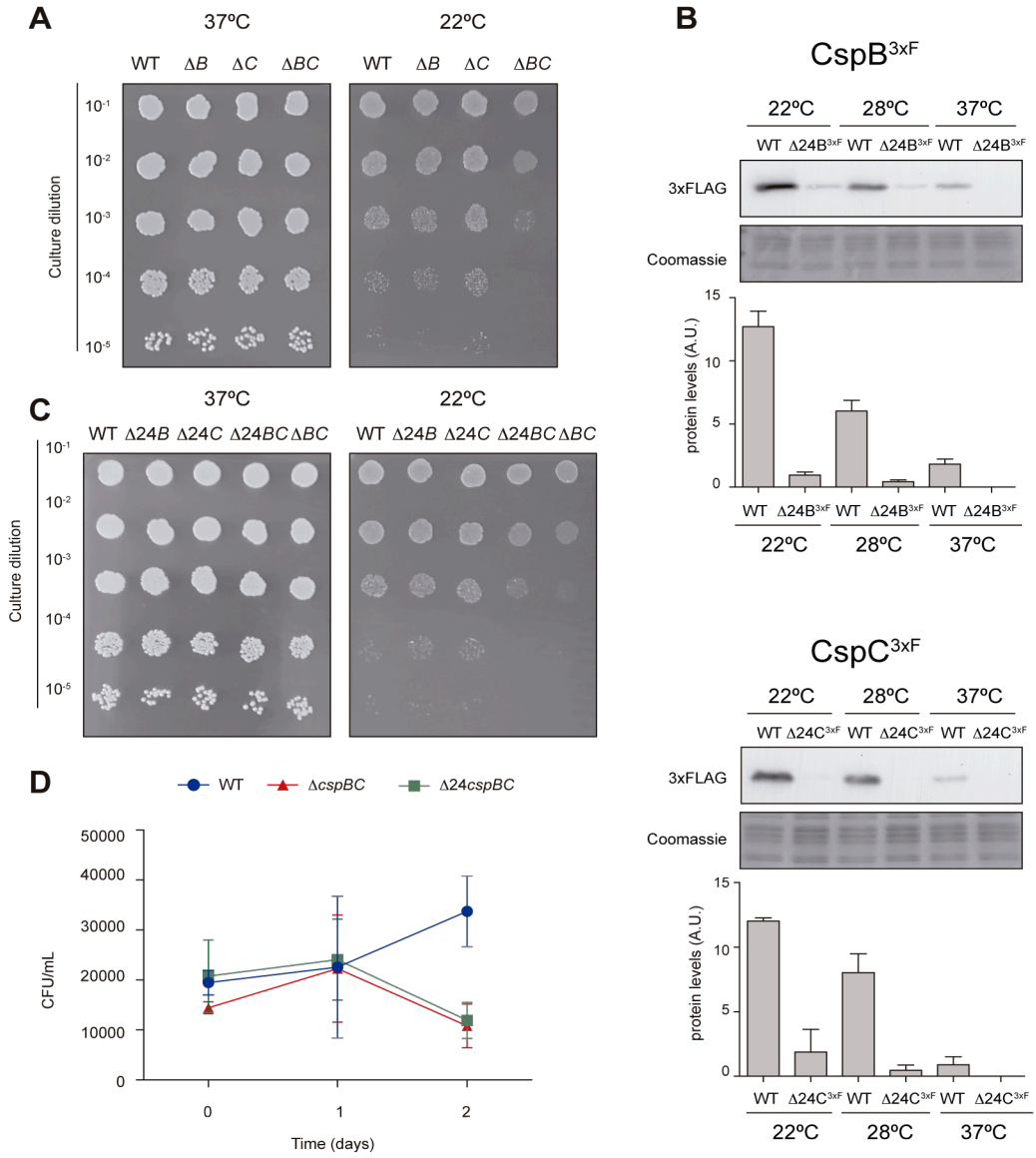

Figure 28. Thermoregulation is essential for *S. aureus* growth at ambient temperatures. (**A**) and (**C**) Growth assays at 37ºC and 22ºC of the different CSP mutants. Bacteria were grown overnight at 37ºC and 200 rpm and diluted to OD_{600} 1. Ten-fold dilutions were plated in TSA plates an incubated at 37ºC and 22ºC for 24 and 72 h. (**B**) Western blot showing the expression of the $CspB^{3xF}$ and $CspC^{3xF}$ proteins from the Δ24B and Δ24C mutants, which were grown at the indicated temperatures. Protein extraction and Western blots were performed as previously described in Figure 17. Coomassie gel portions were included as loading controls. Bar plots show the mean and standard deviation of protein levels from three independent biological replicates, which were determined by densitometry of protein bands using ImageJ (https://imagej.nih.gov/ij/). Representative images from the triplicates are shown. (**D**) Assay mimicking the conditions that *S. aureus* might face when leaving the host. A preinoculum was grown ON in TSB at 37ºC and 200 rpm. Bacteria were then washed, diluted 1:250 and re-grown at 32ºC and 200 rpm for 2 days in SNM3, resembling the nasal state. To imitate fomite contamination, bacteria were transferred to fresh SNM3 and incubated at 22ºC. Colony forming units (CFUs) were counted 0, 1 and 2 days after incubation at 22ºC. The plot represents the results from at least three independent replicates.

Considering that one of the major reservoirs of *S. aureus* in the human body is the nose and that *S. aureus* is often disseminated through human nasal secretions that contaminate diverse fomites (Wertheim *et al.*, 2005), we decided to evaluate the possible impact of thermoregulation in such conditions. For this purpose, we recreated such scenario by growing the WT, Δ24B-Δ24C and Δ*cspBC* strains in Erlenmeyer flasks containing synthetic nasal medium (SNM3) for 2 days at 32ºC and 220 rpm. The SNM3 reproduces the composition of nasal secretions (Krismer *et al.*, 2014), 32ºC is the temperature found in the nose (Lindemann *et al.*, 2002) and agitation (220 rpm) favours aeration. Once the incubation period had elapsed, we normalized the bacterial samples and transferred them to new flasks containing fresh SNM3. The WT and mutant strains were incubated for 48 h at 22ºC without shaking to mimic the transition between the nasal and the fomite state. The number of viable *S. aureus* cells was then estimated by counting the colony-forming units per millilitre (CFU/ml) on TSA plates. Figure 28D showed that, whereas the WT strain replicated in SNM3 at 22ºC, the Δ24B-Δ24C and Δ*cspBC* mutant strains suffered a significant drop of CFUs after 2 days of incubation. Altogether, these data demonstrated that thermoregulation of both CspB and CspC proteins is essential for the adaptation of *S. aureus* to survive at ambient conditions, when it leaves its natural host.

Post-transcriptional thermoregulation of CSPs is widely distributed in bacteria.

In order to analyse whether the thermoswitch mechanism that we found for the *cspB/cspC* 5'UTR was conserved among other bacterial species, we performed blastn analysis using the first 127 nucleotides of the *cspB* mRNA as a query in the Microbes NCBI web site (https://blast.ncbi.nlm.nih.gov/Blast.cgi). The results showed that more than 50 *csp* genes from 43 different *Staphylococcus* species carried an orthologous *cspB* 5'UTR (Annex 7). The sequences were highly conserved, with an identity higher than 74% (Annex 7). The number of CSPs among the analysed staphylococcal species was variable, ranging from 1 to 3 (Figure 16). In most of the *Staphylococcus* genomes containing 3 *csp* genes, 2 of them harboured 5'UTRs similar to *S. aureus cspB/C* 5'UTRs. However, among the genomes with 2 *csp* genes, only one of them carried a putative thermoswitch (Annex 7). In the case of *Staphylococcus pettenkoferi* and *Staphylococcus kloosii*, whose genomes contained just one *csp* gene, the 5'UTR sequence was significantly different from the *S. aureus cspB* 5'UTR. This might be explained by the fact that their CSP showed a high degree of identity with *S. aureus* CspA protein (Annex 5).

Multiple sequence alignments revealed that the nucleotides required for adopting the alternative conformations were highly conserved among staphylococcal species (Annex 8 and Figure 29). Although the *cspB/C*

5'UTR sequence conservation was not extended beyond the *Staphylococcus* genus, the fact that orthologous thermoswitch mechanisms had also been found in *E. coli* and *L. monocytogenes* (Giuliodori *et al.*, 2010; Zhang *et al.*, 2018; Ignatov *et al.*, 2020) indicated that thermoregulation of CSPs based on mutually exclusive alternative 5'UTR conformations could be a common regulatory mechanism in bacteria.

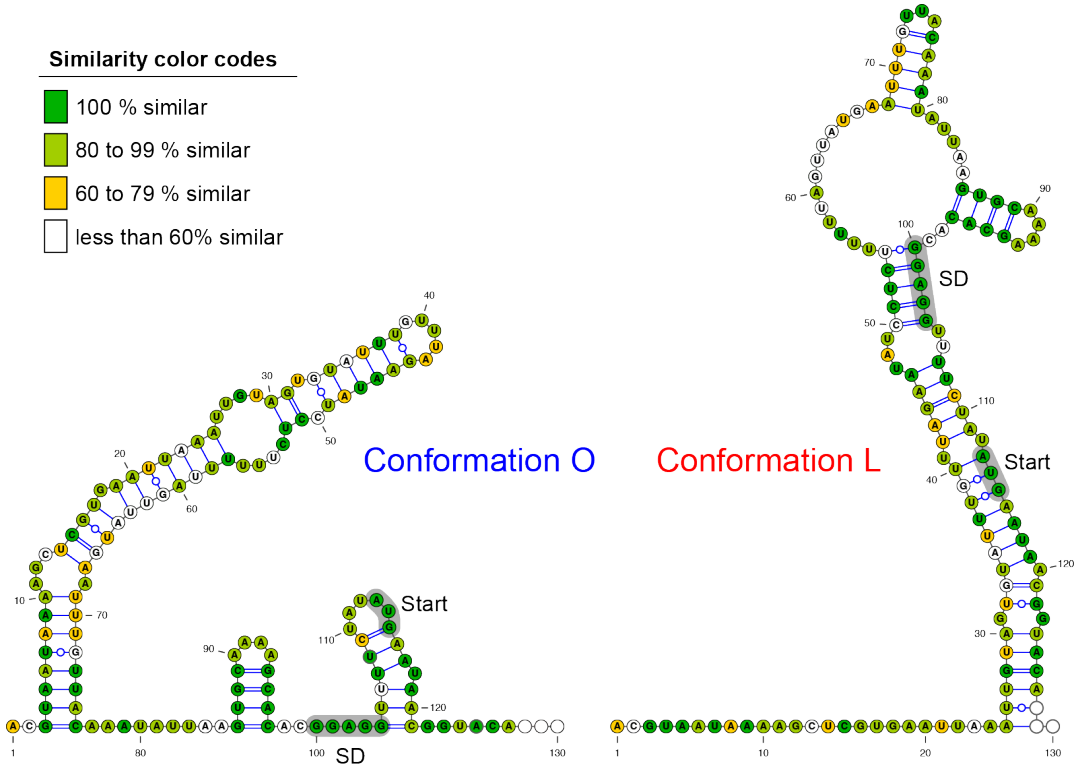

Figure 29. The nucleotides required for adopting the alternative conformations are highly conserved. RNA structures were predicted by the mfold web server (Zuker, 2003) and visualized and drawn using the VARNA software. Nucleotides were coloured according to the similarity percentage. The Shine-Dalgarno (SD) and the start codon are grey shaded.

Since bacterial genomes often encode several CSP paralogs with a high protein identity, it might be difficult to predict which CSPs might be involved in cold adaptation without further experimentation. Although the *csp* 5'UTRs did not share a high sequence identity with the RNA thermoswitches described so far, the presence of alternative structures in their 5'UTRs could be an indicator of such function. To validate this idea, we looked for putative alternative conformations in the 5'UTRs of all the *csp* genes from representative bacteria such as *Enterococcus faecalis*, *Bacillus subtilis*, *Clostridium perfringens*, *Salmonella enterica* sv Typhimurium and *Pseudomonas aeruginosa* (Annex 9). Since the already identified thermoswitches were located at 5'UTRs with lengths ranging from 110 to 160 nt, query sequences including at least 120 nt upstream of the start codon of each CSP were used to predict putative secondary structures using the mfold web server (Zuker, 2003). According to preliminary predictions, query sequences were enlarged or shortened to look for alternative folding options. Thus, we identified several putative *csp* 5'UTRs that displayed alternative structures resembling the ones previously described (Annex 9 and Figure 30). On the one hand, these results suggested that alternative conformations of *csp* 5'UTRs may be a conserved regulatory feature in bacteria despite lacking significant sequence similarity. On the other hand, prediction of these structures could help identifying the CSPs whose expression might be controlled by post-transcriptional thermoswitches.

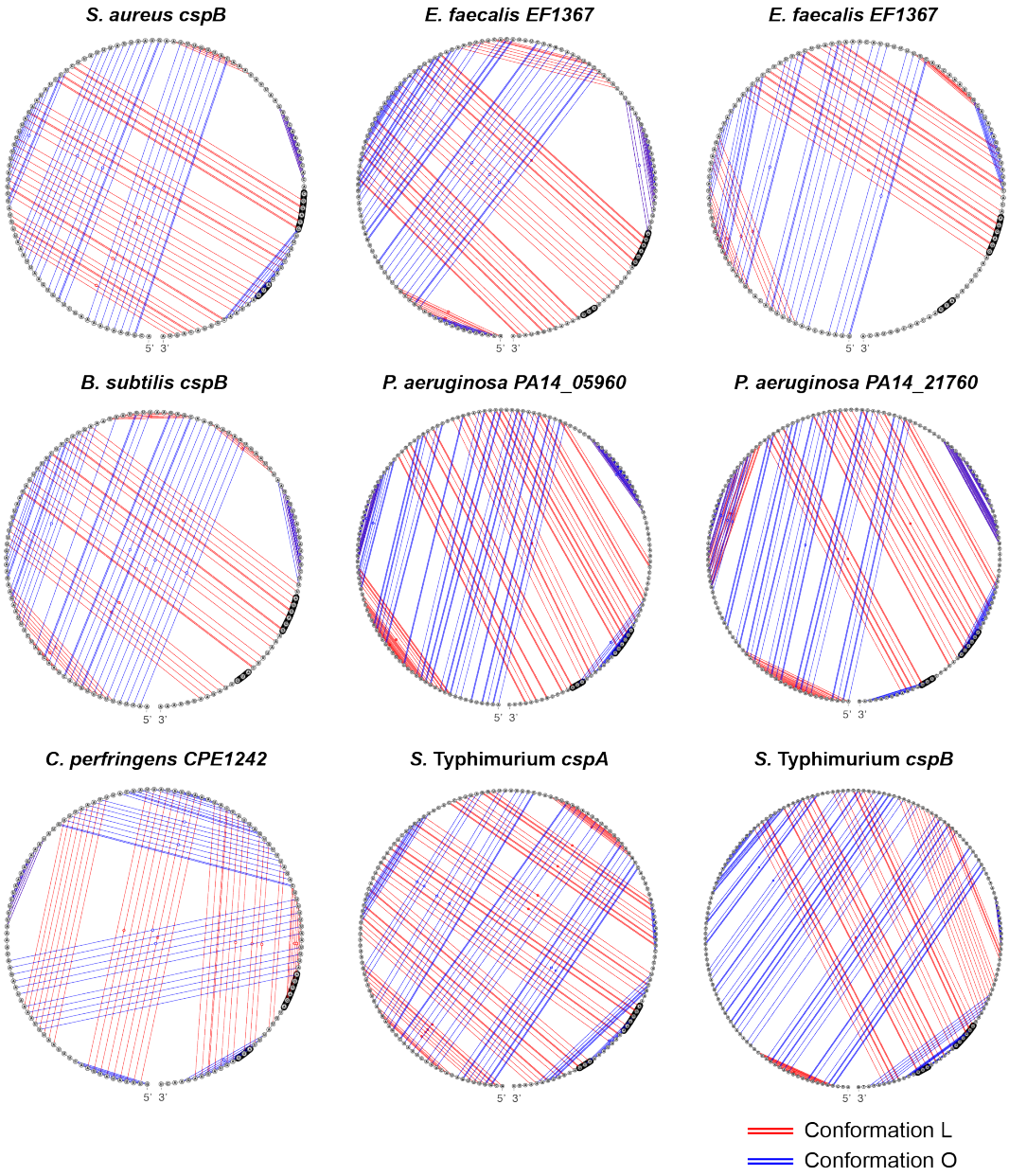

Figure 30. Comparative analyses of the 5'UTRs of *csp* genes from representative bacteria. Circular structural representation of RNA secondary structures from the first 120 nt of *csp* mRNAs from *Enterococcus faecalis*, *Bacillus subtilis*, *Clostridium perfringens*, *Salmonella enterica* sv Typhimurium and *Pseudomonas aeruginosa.* The 5'UTR secondary structure of *cspB* from *S. aureus* was included as a control. Blue and red lines represent the bindings between nucleotides in conformation O and L, respectively. Circular structures were visualized and drawn using the VARNA software.

DISCUSSION

DISCUSSION

CSPs might have functional divergence

The identification, annotation and classification of paralogs in a genome is currently determined by comparative genomics, based on sequence similarity and conserved genomic contexts across closely related genomes (Zallot *et al.*, 2016). On average, protein paralogs represent approximately 24% of bacterial proteomes (Gevers *et al.*, 2004). When looking at a specific paralogous family, like CSPs, all members share the same molecular function, e.g. the capacity to bind nucleic acids. However, it is almost impossible to infer from protein sequences (unless they share 100% of identity) if two paralogs play the same biological function, e.g. control of σ^B activity or the growth at low temperature. Likewise, it is not easy to address what amino acid differences between paralogs correspond to silent changes, not having an influence on the biological function, and what amino acids might provide, if any, a specific role. Since protein specificity resides at the level of molecular interaction with their corresponding target, such discrimination *in vivo* is difficult without having a robust phenotype or reporter system. In the Chapter I, we used the staphyloxanthin production as a natural *in vivo* reporter to demonstrate that interchanging just one orthologous amino acid is sufficient to transfer CspA functionality to its paralog CspC in *S. aureus*. Specifically, when Pro58 of CspA was

substituted by Glu58 of CspC, CspA lost the capacity to modulate σ^B activity and its associated phenotypes. On the contrary, a chimeric CspC protein carrying a Pro instead of a Glu in position 58 gained the ability to promote σ^B activation (Figure 12 and Figure 15).

Despite the CspA specificity controlling STX production, we also found a putative redundancy between CspB and CspC proteins when *S. aureus* grows at low temperatures. Similar functional redundancy was found among CSPs of *E. coli*, *Salmonella* and *B. subtilis* (Graumann *et al.*, 1997; Xia *et al.*, 2001; Shenhar *et al.*, 2012; Michaux *et al.*, 2017). However, it remains to be elucidated if these proteins are functionally redundant in a mechanistic way. Are the CSPs proteins recognizing the same RNA motifs? Are CSPs binding different mRNA targets but with redundant functions? Amino acids occupying the same position 58 in the CspB and CspC were different (note that all *S. aureus* CSPs are 66 aa long). It is possible that, despite their similarities, *S. aureus* CSPs have different preferences when it comes to sequence affinities as previously shown for *E. coli* and *Salmonella* CSPs (Phadtare *et al.*, 1999; Michaux *et al.*, 2017). Determination of RNA targetomes would help elucidating how CspB and CspC participate on gene expression when *S. aureus* grows at low temperatures.

Pro58 drives functional specificity in CspA

It was clear that in the case of the STX phenotype, only CspA was responsible for their activation. According to the protein structural models (Figure 14), Pro58 is located on the CspA surface, close to the RNA-binding motifs, suggesting that this amino acid might directly interact with the RNA to provide a specific target selection. This idea is in agreement with a previous work that showed how *B. subtilis* CspB establishes *in vitro* water-mediated contacts between the backbone carbonyl group of Pro58 and the O4 of the third uracil of an hexa-nucleotide RNA (Sachs, Max, Heinemann, and Balbach, 2012a). Thus, different amino acid substitutions in position 58 throughout evolution would contribute to the selection and/or allosteric exclusion of specific targets. The structural models also showed that Pro58 is in *trans* configuration (Figure 14A). In spite of this, it might be possible that Pro58 alternates between *cis*/*trans* isomerization *in vivo*. Proline isomerization by peptidyl-prolyl *cis-trans* isomerases (PPIases) has been proven relevant for virulence and antibiotic resistance in previous studies (Ünal and Steinert, 2014; Wiemels *et al.*, 2017). Regardless of the possibility of PPIases targeting CSPs, a putative Pro58 isomerization from *trans* to *cis* configuration might rearrange the protein structure by causing a reorientation of loop 4 (Figure 14A). The *cis* configuration in CspA Pro58 could impact the binding interface with the target and add versatility for target recognition in comparison to other amino acids in such position. This

also opens the door to two different target profiles being recognized by the same protein depending on its Pro58 isomerization state. Addressing whether just one or both of the CspA configurations exist *in vivo* and what PPIases would be responsible for such proline isomerization requires further investigations. Conservation of Pro58 among CspA orthologs indicates that this specific amino acid position might be relevant for determining RNA target specificity (Figure 16 and Annex 5).

In agreement with our results, it has also been shown that single amino acid orthologous substitutions provide functional differences among DNA-binding proteins (Treisman *et al.*, 1989; Dabrazhynetskaya *et al.*, 2009; Hudson *et al.*, 2016; Fukuto *et al.*, 2018). For example, a substitution of a single orthologous amino acid (Asp288) in the ParB protein that recognizes *parS* to promote segregation of the plasmid DNA to daughter cells, is sufficient to change or abolish plasmid specificity (Dabrazhynetskaya *et al.*, 2009). Amino acid variations in position 215 of PhoP cause changes in the PhoP activity and probably contributed to an increased virulence in *Y. pestis* (Fukuto *et al.*, 2018).

Similarly, evolutionary substitutions of amino acids in the vicinity of the DNA-binding interface of transcription factors has been shown to provide divergent DNA specificity among paralogs (Hudson *et al.*, 2016). Our results also indicate that biological function specificity may exist outside the main RNA-binding motifs, RNP1 and RNP2. Since the efficiency of the molecular function should be preserved during evolution, it seems logical that amino

acids surrounding the active site are selected to determine target specificity among paralogs. Regardless, we have shown that this cannot be easily predicted by just analysing the protein sequence. In addition, since minor changes in the protein surface can be sufficient to discriminate or recognize a DNA/RNA target, structural models of real ribonucleoprotein complexes would be essential in order to establish their specific molecular interactions. The CspA RNA partner region participating in the control of σ^B activity has not been elucidated yet. According to previous results from our group, we would expect CspA to interact with certain regions of the *rsbV-rsbW-sigB* operon (Caballero *et al.*, 2018), providing σ^B activation and, as a consequence, controlling the σ^B-associated phenotypes (Figure 31).

Further investigations are required to determine the precise molecular interactions between Pro58 of CspA and this operon. Moreover, it cannot be excluded that different and/or additional amino acids might also be required for the interaction of CspA with this or other mRNA targets. In fact, the lack of complementation in the Δ*cspA* strain expressing the chimeric CspB^{3xF}_D58P (Figure 13) suggested that target recognition is not exclusively determined by position 58 and that other amino acid differences may contribute to it.

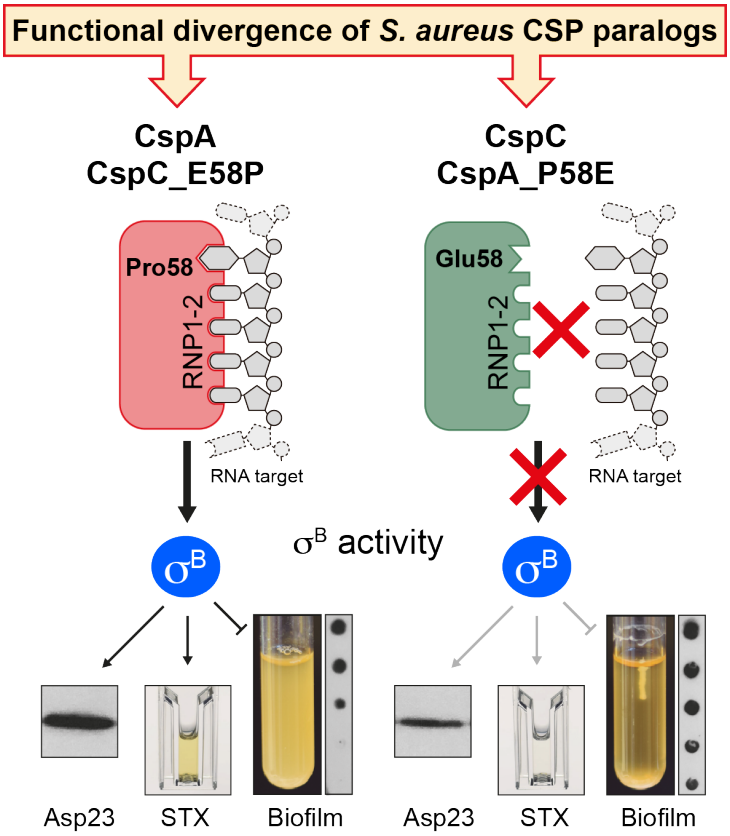

Figure 31. Model of the functional divergence of *S. aureus* CSP paralogs.
CspA is the only CSP paralog able to modulate σ^B activity and associate phenotypes (Asp23, Staphyloxanthin (STX) and biofilm). This specific control occurs through proline 58. When glutamate 58 of the CspC paralog is substituted by proline, the chimeric CSP gains the function of CspA. However, when proline 58 is changed by a glutamate the chimeric CspA could not regulate σ^B activity.

Considering that CSP sequences are highly conserved and that a tight expression control may also exist in other bacterial species, the genetic engineering strategies displayed here could be extrapolated to evaluate the putative functional divergence among CSP paralogs in bacteria. This would require the following steps: a) the identification of a functional reporter such as a phenotype or a gene target whose expression depends on one of the CSP paralogs and b) the engineering of plasmids that bypass the putative differential post-transcriptional regulation for each of the CSPs and, thus,

allow comparable protein levels. Overall, the genetic strategy presented in this thesis allowed us to unveil the key role played by one of the CspA amino acids, proline 58, in controlling σ^B activity in *S. aureus*. Therefore, it may be proposed that a single amino acid change is sufficient to produce functional divergence among CSP paralogs.

Abnormal protein migration even though CSPs share the same aa length

Different band migration patterns in the polyacrylamide gels were repeatedly observed for each of the CSPs. This could be interpreted as CSPs being affected at the post-translational level. Similar variations in band migration had previously been shown for *Salmonella* CSPs (Michaux *et al.*, 2017). A possible explanation might be protein modification but this possibility has not been found for CSPs yet (Donegan *et al.*, 2019). This also applied to several of the chimeric CSPs, which migrated differently when compared to the WT CSPs. However, protein modification events alone cannot explain this. Furthermore, the different band patterns did not correlate with the capacity to produce STX. Therefore, although post-translational modifications cannot be fully ruled out, it is very likely that the abnormal migration of CSPs in polyacrylamide gels occurs due to the additional binding of SDS molecules to specific aa stretches, a phenomenon that is accentuated in small proteins like CSPs (Shi *et al.*, 2012).

CspB and CspC expression is controlled by orthologous RNA thermoswitches

It is often assumed when performing parallel complementation experiments by expressing different proteins under the control of the same heterologous promoter, that similar protein concentrations should be reached. However, we previously showed that expressing the *csp* mRNAs from the same promoter lead to different CSP levels (Caballero, 2018). Engineered *S. aureus* strains that ensured comparable expression levels for the three CSP paralogs were achieved by generating chimeric *csp* mRNAs that shared the same UTRs (Caballero, 2018). The success of this strategy indicated that the differences found in the CSP levels should mainly be attributed to a differential post-transcriptional control. Particularly, the *csp* 5'UTRs have gained attention due to their striking refined regulatory mechanisms on allowing bacteria to rapidly sense temperature alterations (Giuliodori *et al.*, 2004; Uppal *et al.*, 2008; Zhang *et al.*, 2018; Ignatov *et al.*, 2020). In the Chapter II, we showed that the expression of CspB and CspC is regulated by temperature shifts when the pathogen moves from host-related (37ºC) to environmental temperatures (e. g. 22 and 28ºC) and vice versa. In contrast, CspA levels are unaltered under temperature variations confirming previous results (Lioliou *et al.*, 2012) (Figure 17). The CspB/C thermoregulation occurs at the post-transcriptional level through the action of two orthologous

thermo-sensitive RNA elements located at the 5'UTR of *cspB* and *cspC* mRNAs (Figure 18 and Figure 19).

RNA-mediated thermoregulation is an essential process that promotes changes in gene expression and facilitates the adaptability of pathogenic bacteria when they shift from the host to the environment and vice versa. Several RNA thermosensors have been found to induce the expression of the main regulators required for the activation of virulent genes in bacteria while infecting humans. During this process, bacteria sense an increase of the temperature by unfolding zipper-like structures located at the 5'UTRs genes required for survival inside the host. Thus, the otherwise blocked RBSs are released and become accessible to the ribosomes, which initiate translation (Johansson *et al.*, 2002; Waldminghaus, Heidrich, *et al.*, 2007; Loh *et al.*, 2013; Weber *et al.*, 2014; Righetti *et al.*, 2016; Loh *et al.*, 2018; Twittenhoff *et al.*, 2020). Conversely, a few RNA thermosensors have been identified capable of activating gene expression when bacteria leave the host, meaning that they face lower environmental temperatures (Giuliodori *et al.*, 2010; Zhang *et al.*, 2018; Ignatov *et al.*, 2020). In comparison with regular zipper-like RNA thermosensors, activation of translation when the temperatures decrease involve much more complex RNA structural reorganizations. The thermo-sensitive structural shifts found in the *S. aureus cspB* and *cspC* 5'UTRs are orthologous to the ones recently described for *E. coli* and *L. monocytogenes cspA* mRNAs (Zhang *et al.*, 2018; Ignatov *et al.*, 2020).

These type of RNA structural rearrangements, which repress translation at higher temperatures and activate it at lower temperatures, are also present in the 5'UTR of the bacteriophage *cIII* gene (Altuvia *et al.*, 1989). Recently, an RNA thermosensor that activated the expression of the holin-like protein CidA at low temperatures was also described for *S. aureus* (Hussein *et al.*, 2019). Although speculated by the authors, no alternative structures were described for the *cidA* 5'UTR. We wondered if such 5'UTR could contain regulatory elements that allowed its structural reorganization in a similar fashion to what we observed for the *csp* 5'UTRs. By using mfold, besides the closed conformation identified by Hussein and co-workers (Hussein *et al.*, 2019), we could also predict a putative alternative conformation in the *cidA* 5'UTR that makes the RBS available to the ribosome (Figure 32). This open conformation involves a long hairpin comprising nucleotides 5 to 66 of the *cidA* 5'UTR, which sequesters the anti-RBS motif (Figure 32). Additional experiments will be required to validate whether both 5'UTRs structures alternates *in vivo*.

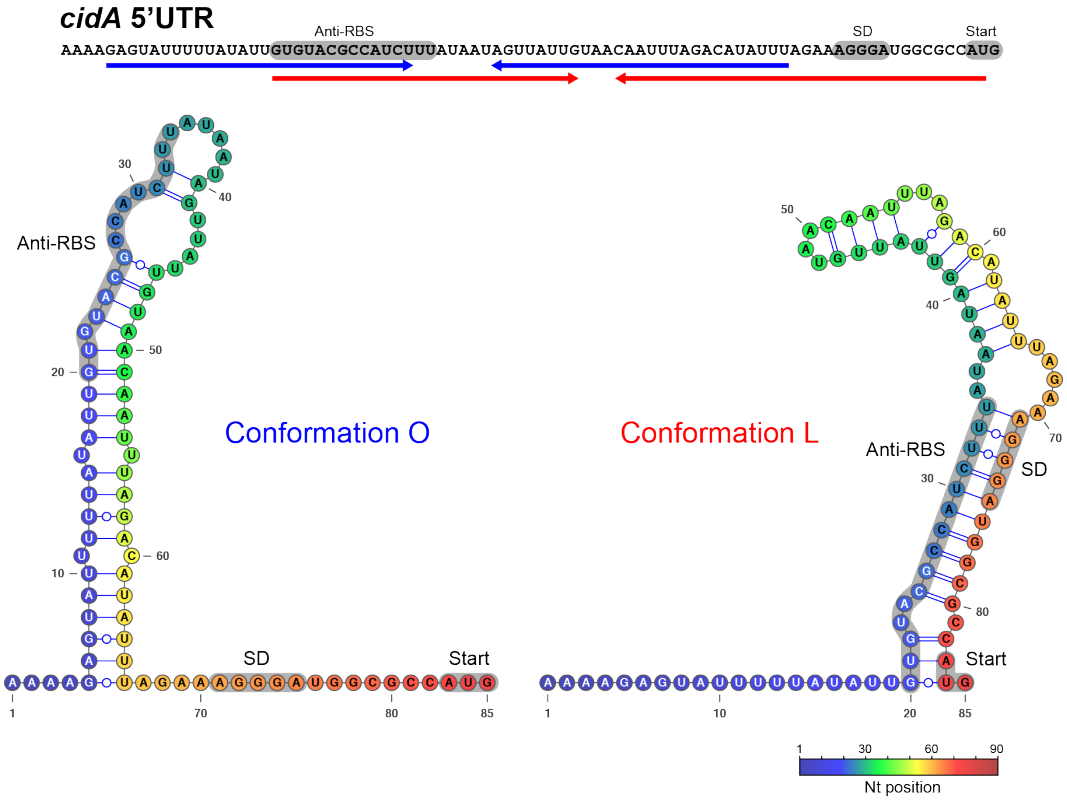

Figure 32. Putative alternative structure of *cidA* 5'UTR. RNA structures were predicted by mfold web server (Zuker, 2003) and visualized and drawn using VARNA software. Structures were coloured according the nucleotide positions as indicated in the colour scale. Arrows below 5'UTR sequence indicate the interacting nucleotide regions. Blue arrows, conformation O; Red arrows, conformation L. The Shine-Dalgarno (SD), the start codon and the anti-RBS region are indicated as a grey shadow

The RNA-mediated thermoregulatory mechanism is widely spread in bacteria

The thermoregulatory mechanism described in this work might also apply to other bacterial CSPs. Orthologous *cspB* thermosensors could be predicted in all *Staphylococcus* species, with the exceptions of *S. pettenkoferi* and *S. kloosii*, whose genomes only encoded a CspA copy (Annex 7 and Annex 8). Considering that multiple *csp* genes are included in

the core genome of most bacteria, one would expect this type of RNA thermoswitch to be widely distributed. In fact, we found that orthologous alternative structures could be also predicted in the 5'UTRs of *csp* mRNAs from several representative bacteria including *E. faecalis*, *B. subtilis*, *C. perfringens*, *S.* Typhimurium and *P. aeruginosa* (Figure 30 and Annex 9). Although these *csp* 5'UTRs did not share a high sequence identity with the RNA thermoswitches described so far, they could adopt both open and locked conformations as described for *S. aureus cspB/C* 5'UTRs (Figure 30). Moreover, examples like the *cIII* and *cidA* thermosensors indicate that these regulatory elements may not be restricted to the *csp* gene family.

Although the *cspB* and *cspC* 5'UTRs structures significantly differ from the regular RNA thermosensors (Narberhaus *et al.*, 2006; Klinkert and Narberhaus, 2009; Loh *et al.*, 2018), the hairpin of conformation O seems to work like the already known zipper-like structures. However, the outcome of this mechanism is rather different as instead of freeing the RBS when melting, it is the anti-RBS region that is released. Therefore, in addition to masking RBSs or anti-RBSs, it could be speculated that bacterial genomes may encode alternatives thermo-sensitive hairpins that could also sequester other binding sites for ribonucleases, RNA-binding proteins and/or non-coding RNAs. Such binding sites would be available depending on the environmental temperature.

The RNA structural conformation shift requires additional factors

Thermosensors are universally described as self-sufficient elements located at the 5'UTR of mRNAs which are able to regulate target protein expression in response to temperature variations (Narberhaus *et al.*, 2006; Klinkert and Narberhaus, 2009; Loh *et al.*, 2018). However, the cold adaptation process might be largely more complex than RNA thermo-responsive elements (Zhang *et al.*, 2018). In contrast to the *L. monocytogenes cspA* thermosensor (Ignatov *et al.*, 2020), the ectopic expression of a reporter plasmid carrying the *S. aureus cspB* 5'UTRs in *E. coli* revealed that this RNA element might not be sufficient to confer thermoregulation and additional factors might be involved (Figure 23). This idea was in agreement with the work recently published by Zhang et al (Zhang *et al.*, 2018). They demonstrated that *E. coli* CspA bound its own mRNA to facilitate the structural transition and, thus auto-regulates its own expression (Zhang *et al.*, 2018). Our findings showed that *S. aureus* CspA was also a necessary player in such regulatory process (Figure 25). This was slightly different to the mechanism described in *E. coli* (Zhang *et al.*, 2018), since the *S. aureus* CspB and CspC were not auto-regulated at least in the tested conditions (Figure 24). In contrast, previous results from the group revealed that *cspB* and *cspC* mRNAs were targeted by CspA in *S. aureus* (Caballero *et al.*, 2018). Here, we showed that CspA could be the additional element favouring the conformation L over conformation O at

37ºC (Figure 25 and Figure 26). Although CspA regulates its own expression in *S. aureus* by preventing the folding of a long hairpin in the *cspA* 5'UTR (Caballero *et al.*, 2018), this hairpin was not sensitive to physiological temperatures (Figure 17). The fact that CspA levels were unaltered upon temperature changes could not explain a hypothesis in which CspA repressed translation of CspB/C on its own. It might be expected that when *cspB* and *cspC* genes are transcribed at 37ºC, 5'UTRs structures might be alternating between conformation O and L. However, we showed that CspA prevents the folding of the anti-anti-RBS hairpin of conformation O at 37ºC, allowing the RBS to be targeted by the anti-RBS and, thus, blocks translation by favouring conformation L (Figure 33). This hypothesis was in agreement with the results that showed how deleting the *cspA* gene *in vivo* increased CspB and CspC expression at 37ºC (Figure 25B). On the contrary, when testing the effect of the presence/absence of CspA on the expression of CspB and CspC at 22ºC no differences were found. In other words, there was not a temperature-dependent repression of CspB and CspC expression in the absence of CspA. This could be explained by the fact that the RNA secondary structures are more rigid at lower temperatures (Zhang *et al.*, 2018). The affinity of the RNA regions forming the hairpin of conformation O at 22ºC are probably higher than the affinity for CspA. Therefore, it seemed that CspA could not avoid the folding of such hairpin at ambient temperatures. This was further confirmed by site-directed mutations in the 5'UTRs that altered the affinities of the different

RNA regions between them (Figure 22 and Figure 26). In all cases, thermoregulation was eliminated. Although it cannot be excluded that some of these mutations could also modify the CspA binding site, we demonstrated that the thermoregulatory mechanism is based on the different affinities of the distinct elements involved. These affinities would be naturally altered by temperature shifts (Figure 33).

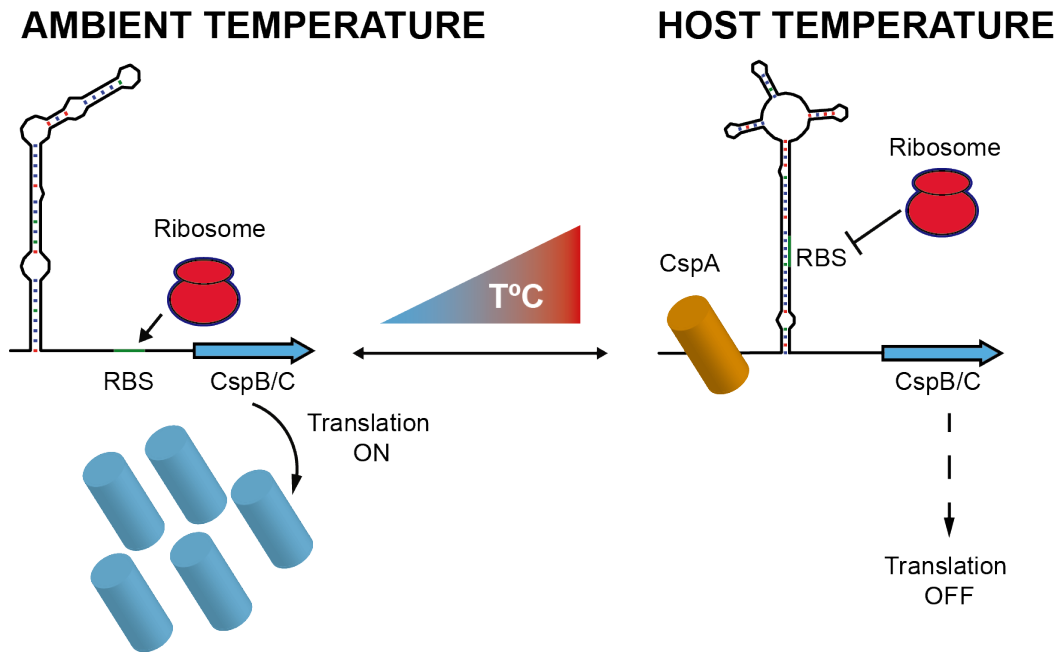

Figure 33. Model of the putative CspB and CspC thermoregulatory mechanism. At ambient temperatures de 5'UTR of *cspB* and *cspC* mRNA will fold into an open structure were the RBS is available for ribosome binding. Translation of CspB and CspC proteins will occur. In contrast, at host-related temperature, the 5'UTR structure might be altered shifting to a conformation where the RBS is occluded and protein translation inhibited. CspA will favour the conformation formed at 37ºC by binding to an unpaired region at the 5'UTR.

It remains to be elucidated if CspA bound a specific motif in the *cspB/C* 5'UTRs. We previously shown that the auto-regulatory mechanisms of CspA requires a U-rich motif located in the *cspA* 5'UTR (Caballero *et al.*, 2018). The presence of two U-rich regions (36-UUUGUUU-43 and 54-UUUUUU-59) in *cspB* 5'UTR and (32-UUAUUU-37 and 54-UUUUCAUUU-629) in *cspC* 5'UTR might represent putative sites for CspA recognition (Figure 19). We could perform only one mutation that modify one of the U-rich motifs (54-UUUUUU-59) without affecting the folding of both alternative conformations. However, the results showed that this motif was not required for CspA repression of CspB expression at 37ºC. Further experiments will be required to show how CspA bind to these 5'UTRs.

A similar mechanism might also exist in *L. monocytogenes* since the *cspA* 5'UTR also presents a U-rich motif that participates in formation of the hairpin in the O conformation. The binding would shift the structure equilibrium to the closed conformation (Ignatov *et al.*, 2020).

Moreover, analyses performed in *B. subtilis and E. coli* indicated that members of CSP family have an influence on the expression of the other members (Graumann *et al.*, 1997; Xia *et al.*, 2001), suggesting that the control of CSP expression is interconnected. Although, some authors suggest that CSPs recognition sites might be unspecific (Jiang *et al.*, 1997; Phadtare *et al.*, 1999; Sachs, Max, Heinemann, and Balbach, 2012a; Zhang *et al.*, 2018), in *E. coli* the cold-box site at the *cspA* 5'UTR has also been reported to be a binding site for the non-cold-inducible CspE, which

functions as a negative regulator of expression at 37ºC (Bae *et al.*, 1999; Phadtare *et al.*, 1999; Lim *et al.*, 2000). This cold-box region was also conserved in the cold-inducible *cspB*, *cspG* and *cspI* of *E. coli* (Jiang *et al.*, 1996) and in *csdA* mRNA, which encodes a cold-shock inducible RNA helicase that unwind double stranded mRNA and it is associated with the ribosomes (Jiang *et al.*, 1996).

Thermoregulation is essential for *S. aureus* survival outside the host

An additional observation of this study is that the structures located at the *cspB* and *cspC* 5'UTRs are essential for thermoregulation of CspB and CspC proteins (Figure 28). When forcing conformation L in the Δ24B-Δ24C mutant, the strain presented a growth defect comparable to the Δ*cspBC* mutant in both TSB and synthetic nasal media at 22ºC. In fact, mimicking the conditions that *S. aureus* would encounter when leaves the host from the nasal carriage to a fomite, we demonstrated that elimination of the thermoregulatory mechanisms significantly affected *S. aureus* survival at ambient conditions. This suggested that sensing the temperature shifts by the 5'UTR structural conformation changes is an essential step for *S. aureus* adaptation at new ambient conditions (Figure 28). *S. aureus* is a major community-based pathogen worldwide with the capacity to colonize households or community sites being part of a wide range of fomites (Knox *et al.*, 2012; Knox *et al.*, 2015). Persistence on inanimate surfaces can be a continuous source of pathogen transmission and new host colonization,

increasing the risk of outbreaks infections if no regular preventive measures are taken (Uhlemann *et al.*, 2011). Although further *in vivo* investigations are required, the preliminary results presented here may suggest a potential relevance of CSPs in the contagiousness process and could open a new field on developing innovative approaches to combat propagation of persistence pathogens on inanimate surfaces. Few recent studies on RNA regulators have suggested alternative and promising strategies by targeting post-transcriptional regulation as growth inhibitors (Mulhbacher *et al.*, 2010; Lünse *et al.*, 2011). For example, the use of a pyrimidine derivate that binds the guanine riboswitch and represses the expression of *guaA* gene, attenuates *S. aureus* infection in a mouse model (Mulhbacher *et al.*, 2010). Another example is the design of a glucosamine-6-phospate (GlcN6P) analogue (carba-GlcN6P) that activates *glmS* and destabilizes its mRNA which in term leads to transcript degradation implying a reduction of GlcN6P, a building block of bacterial peptidoglycan, and ultimately a deregulation of bacterial homeostasis (Lünse *et al.*, 2011). Therefore, the orthologous *cspB/C* 5'UTRs structures might be suitable targets for drug compounds to prevent and eradicate the spread of such a major community-based pathogen.

FUTURE PERSPECTIVES

FUTURE PERSPECTIVES

CSPs specificity and target recognition

The identification of different protein paralogs in bacterial genomes often raises the question of whether they share the same molecular and biological function or rather have different roles altogether. However, attempting to find and answer is usually challenging since no conclusions can be directly drawn by simply looking at the protein sequences. In this study, we used a measurable phenotype (STX production) to show how just one amino acid was sufficient to confer CspA functional specificity. Such functionality could be transferred to the CspC protein by introducing the E58P substitution. However, the same approach did not apply to CspB, indicating that additional amino acids might be involved in the functional specificity of CspA. As shown in Figure 9, other than the amino acid at position 58, there are several differences between the CspA and CspB protein sequences. For example, Lys2, Gln3, Val20, Gly22, Glu23, Asn23, Asn34, Gln35, Glu36, Ser46, Glu50, Val51, Asp55 or Leu66. It would be interesting to perform chimeric proteins that interchanged these amino acid differences to elucidate which are those additional residues required for target recognition. The CspA partner region that participates in the control of the σ^B activity remains unknown. As previously discussed, we would expect CspA to interact with the *rsbV-rsbW-sigB* operon. Therefore, *in vitro* binding or

immunoprecipitation studies that uncover the precise RNA region and, ideally, the CspA binding site would be of relevance.

CSPs thermoregulation

The CspB and CspC protein expression was thermoregulated by thermo-responsive elements located in the 5'UTRs of these genes. Besides, and in agreement with previous studies from our group (Caballero *et al.*, 2018), we showed that CspA had an effect on CspB and CspC by repressing their expression at 37ºC. The molecular mechanism behind it and the precise binding site of CspA at the 5'UTRs requires further investigations. To confirm that the translation initiation complex is formed at 22ºC but not at 37ºC and whether CspA is required for the structural rearrangement, *in vitro* toe-printing and translation assays could be performed. Additionally, we are currently optimizing the SHAPE-seq method for *S. aureus*. This technique unveils the *in vivo* unpaired nucleotides, which would contribute to further characterizing the *in vitro* secondary structures determined in this study. Moreover, we could compare the 5'UTR structures *in vivo* in the presence or absence of the CspA protein at different temperatures. Finally, a recently adapted *in vivo* DMS-MaPseq protocol could be also applied in *S. aureus*. This method selectively enriches the 5'UTRs and sRNAs structural modifications at different growth conditions (Ignatov *et al.*, 2020). Therefore, this methodology could contribute to validating the formation of the

alternative conformations O and L in different conditions in addition to identifying additional RNA thermosensors.

Conservation of RNA thermoregulation in bacteria

Our findings, alongside recent reports in diverse bacteria, demonstrate the involvement of *csp* 5'UTRs in cold shock response and their role in thermoregulation (Caballero *et al.*, 2018; Zhang *et al.*, 2018; Ignatov *et al.*, 2020). This indicates that the thermoregulatory mechanism might be broadly conserved in bacteria. In fact, our conservation analysis revealed that 47 different staphylococcal species carried orthologous CspB alternative structures in *csp* genes. In addition, orthologous mechanisms could be also predicated in *csp* genes from diverse bacteria. Validation of these *in silico* predictions would require further experiments. This could be carried out by constructing *5'UTR-gfp* reporter plasmids, as previously described, and analysing the GFP expression at different temperatures.

Biological importance of CspB and CspC in *S. aureus*

A relevant result from this thesis is the demonstration that CspB and CspC are essential for *S. aureus* adaptation when exposed to ambient temperatures. However, several aspects of these proteins remain to be investigated. For example, what are the genes targeted by CspB and CspC that participate in the cold shock response? Are the CspB/C proteins important for *S. aureus* environmental transmission? To answer the first

question, determining the corresponding targetome maps would be required. Regarding the second one, *in vivo* approaches in animal models would be of significance. *Caenorhabditis elegans* has been proposed as a suitable model for studying different aspects of *S. aureus* (Sifri *et al.*, 2003). It could be possible to develop a method to analyse the environmental spreading of the *S. aureus* WT and *ΔcspBC* strains in different *C. elegans* populations. Alternatively, fomite-host pathogen transmission experimental models using mice or artificial skin could be also considered.

CONCLUSIONS

CONCLUSIONS

1) The CSPs structure is formed by a β-barrel composed of five anti-parallel β-strands. *S. aureus* CSPs share a sequence identity higher than 70%. However, complementation of the *ΔcspA* strain with CspB and CspC proteins did not restore the *cspA*-associated phenotypes. Experiments with different chimeric CSPs revealed that the amino acid differences located at the β5 strand may determine the functional specificity of *S. aureus* CSPs.
2) Site-directed mutagenesis analyses of amino acid differences between CspA and CspC revealed that one amino acid (Proline 58) is enough to create functional divergence among CSP paralogs. Proline 58 of CspA is required to specifically control σ^B activity and, hence, modulate *S. aureus* σ^B-associated phenotypes such as Asp23 expression, STX biosynthesis, PIA/PNAG production and biofilm formation.
3) CspC gained the biological function of CspA when introducing the E58P substitution. However, introducing a proline in position 58 of the CspB protein did not have the same effect, suggesting that additional amino acids might be important for determining functional specificity.
4) Proline 58 is highly-conserved among CspA orthologs of the *Staphylococcus* genus, indicating that this particular amino acid position is relevant for CspA specificity. At the same time, the natural

evolutionary substitutions found in position 58 of the CSP paralogs suggested that this amino acid position could be involved in promoting functional divergence between CSPs paralogs.

5) The expression of CspB and CspC is regulated in response to temperature shifts that *S. aureus* faced when transitioning from host-related temperatures to ambient temperatures. Although, the CspB/C protein levels were increased when *S. aureus* faced ambient temperatures, their mRNA levels remained invariable. This proved the existence of a temperature-dependent post-transcriptional regulation.

6) *In silico* bioinformatic analyses, *in vitro* structural probing experiments and *in vivo* site-directed mutagenesis demonstrated that the CspB and CspC thermoregulation involves two orthologous thermo-sensitive RNA elements located at the *cspB* and *cspC* 5'UTRs. At ambient temperatures, the 5'UTRs adopt a conformation where the RBS is unpaired, thus, facilitating mRNA translation. In contrast, when *S. aureus* grows at host-related temperatures, the 5'UTRs fold into a locked conformation in which the RBS is blocked by an anti-RBS sequence that inhibits CSP translation.

7) Molecular beacon experiments showed that the long RNA hairpin, which is formed in the open conformation, might be the RNA element that responds to temperature variations. This hairpin melts at host-related temperatures and liberates the anti-RBS sequence. However, at ambient temperatures it sequesters this inhibitory motif.

8) At host-related temperatures, the 5'UTR structural conformation requires the presence of the CspA protein to inhibit CspB/C translation. CspA prevents the formation of the hairpin that sequesters the anti-RBS and favours the folding of the locked conformation, which inhibits protein translation.

9) Site-directed mutagenesis that prevented temperature-dependent 5'UTR structural rearrangements proved that CspB and CspC thermoregulation is essential for *S. aureus* survival at ambient temperatures. These results also highlight the importance of CSPs in *S. aureus* environmental adaptation and positioning them as putative candidates for drug development compounds that might contribute to the prevention of environmental contamination by *S. aureus.*

CONCLUSIONES

CONCLUSIONES

1) La estructura de las CSPs está formada por un barril β compuesto por cinco láminas β anti-paralelas. Las CSPs de *S. aureus* comparten una identidad de secuencia superior al 70%. Sin embargo, la complementación del mutante *ΔcspA* con las proteínas CspB y CspC no restauró el fenotipo asociado a este mutante. La construcción de diferentes CSPs quiméricas reveló que las diferencias de amino ácidos presentes en la lámina β5 podrían determinar la especificidad funcional de las CSPs de *S. aureus.*
2) Los análisis de mutagénesis dirigidos a las diferencias de amino ácidos entre CspB y CspC revelaron que un solo amino ácido (la prolina 58) es suficiente para crear una diferencia funcional entre los parálogos de las CSPs. La prolina 58 de CspA es necesaria para controlar específicamente la actividad de σ^B y, en consecuencia, para modular los fenotipos dependientes de σ^B, que incluyen la expresión de la proteína Asp23, la biosíntesis de la estafiloxantina, la producción del exopolisacárido PIA/PNAG y la formación de biofilm en *S. aureus*.
3) La especificidad de CspA puede ser transferida a CspC, ya que esta proteína gana la función de CspA cuando se sustituye el glutamato 58 por prolina. Sin embargo, esto no se reproduce cuando el ácido aspártico se sustituye por prolina en la proteína CspB, lo que sugiere que existen

amino ácidos adicionales que pueden participar en la discriminación de los RNAs dianas.

4) La prolina 58 está altamente conservada entre los ortólogos de CspA del género *Staphylococcus*, indicando que este amino ácido es relevante para la especificidad de CspA. Al mismo tiempo, las sustituciones evolutivas naturales que ocurren en la posición 58 de otros parálogos de CSPs sugieren que esta posición está involucrada en la creación de divergencias funcionales entre ellos.

5) La expresión de las proteínas CspB y CspC está regulada en respuesta a cambios de temperatura, que *S. aureus* encuentra cuando se mueve desde temperaturas relacionadas con el hospedador hacia temperaturas ambientales. Los niveles de las proteínas CspB y CspC se incrementan cuando *S. aureus* crece a temperaturas ambientales mientras que los niveles de mRNA permanecen prácticamente invariables, lo que muestra la presencia de una regulación post-transcripcional dependiente de temperatura.

6) Estudios bioinformáticos *in silico*, experimentos estructurales del RNA *in vitro*, y mutaciones dirigidas *in vivo* demostraron que en la termorregulación de CspB y CspC están involucrados dos elementos de RNA termosensibles localizados en las 5'UTRs de *cspB* y *cspC*. A temperaturas ambiente, las 5'UTRs adoptan un conformación donde la RBS se encuentra libre lo que facilita la traducción del mRNA. Por el contrario, cuando *S. aureus* crece a temperaturas relacionadas con el

hospedador, las 5'UTRs se estructuran en una conformación cerrada que bloquea la RBS mediante una secuencia anti-RBS que inhibe la traducción de las CSPs.

7) Los experimentos con balizas moleculares mostraron que la horquilla de RNA que se forma en la configuración abierta puede ser el elemento que detecta las variaciones en la temperatura. Esta horquilla se abre a temperaturas relacionadas con el hospedador para liberar la secuencia anti-RBS, mientras que a temperatura ambiente esta horquilla secuestra al motivo inhibidor.
8) La formación de la estructura cerrada en la 5'UTR a temperaturas relacionadas con el hospedador requiere de la proteína CspA para inhibir la traducción de CspB y CspC. CspA evita la formación de la horquilla que secuestra el motivo anti-RBS lo que favorece la conformación cerrada, inhibiendo la traducción.
9) Las mutaciones dirigidas que evitan la reorganización estructural en las 5'UTRs demuestra que la termorregulación de CspB y CspC es esencial para la supervivencia de *S. aureus* a temperatura ambiente. Estos resultados también subrayan la importancia de las CSPs en la adaptación de *S. aureus* a diferentes ambientes y muestra que las CSPs pueden ser candidatos para el desarrollo de compuestos que puedan contribuir en la prevención de la contaminación ambiental por *S. aureus.*

BIBLIOGRAPHY

BIBLIOGRAPHY

Agaras, B., Sobrero, P., and Valverde, C. (2013) A CsrA/RsmA translational regulator gene encoded in the replication region of a *Sinorhizobium meliloti* cryptic plasmid complements *Pseudomonas fluorescens rsmA/E* mutants. *Microbiology* **159**: 230–242.

Altuvia, S., Kornitzer, D., Teff, D., and Oppenheim, A.B. (1989) Alternative mRNA structures of the cIII gene of bacteriophage λ determine the rate of its translation initiation. *Journal of Molecular Biology* **210**: 265–280.

Amir, M., Kumar, V., Dohare, R., Islam, A., Ahmad, F., and Hassan, M.I. (2018) Sequence, structure and evolutionary analysis of cold shock domain proteins, a member of OB fold family. *J Evol Biol* **31**: 1903–1917.

Anderson, K.L., Roberts, C., Disz, T., Vonstein, V., Hwang, K., Overbeek, R., *et al.* (2006) Characterization of the *Staphylococcus aureus* heat shock, cold shock, stringent, and SOS responses and their effects on log-phase mRNA turnover. *J Bacteriol* **188**: 6739–6756.

Arnaud, M., Chastanet, A., and Débarbouillé, M. (2004) New vector for efficient allelic replacement in naturally nontransformable, low-GC-content, Gram-positive bacteria. *Appl Environ Microbiol* **70**: 6887–6891.

Bae, W.H., Phadtare, S., Severinov, K., and Inouye, M. (1999) Characterization of *Escherichia coli cspE*, whose product negatively regulates transcription of *cspA*, the gene for the major cold shock protein. *Mol Microbiol* **31**: 1429–1441.

Bae, W.H., Xia, B., Inouye, M., and Severinov, K. (2000) *Escherichia coli* CspA-family RNA chaperones are transcription antiterminators. *Proc Natl Acad Sci USA* **97**: 7784–7789.

Baker, C.S., Morozov, I., Suzuki, K., Romeo, T., and Babitzke, P. (2002) CsrA regulates glycogen biosynthesis by preventing translation of *glgC* in *Escherichia coli*. *Mol Microbiol* **44**: 1599–1610.

Bastet, L., Turcotte, P., Wade, J.T., and Lafontaine, D.A. (2018) Maestro of regulation: Riboswitches orchestrate gene expression at the levels of translation, transcription and mRNA decay. *RNA Biol* **15**: 679–682.

Becker, K., Ballhausen, B., Kahl, B.C., and Köck, R. (2017) The clinical impact of livestock-associated methicillin-resistant *Staphylococcus aureus* of the clonal complex 398 for humans. *Vet Microbiol* **200**: 33–38.

Bonnin, R.A., and Bouloc, P. (2015) RNA Degradation in *Staphylococcus aureus*: Diversity of ribonucleases and their Impact. *International Journal of Genomics* **2015**: 1–12.

Böhme, K., Steinmann, R., Kortmann, J., Seekircher, S., Heroven, A.K., Berger, E., *et al.* (2012) Concerted actions of a thermo-labile regulator and a unique intergenic RNA thermosensor control *Yersinia* virulence. *PLoS Pathog* **8**: e1002518.

Braun, F., Durand, S., and Condon, C. (2017) Initiating ribosomes and a 5“/3-”UTR interaction control ribonuclease action to tightly couple *B. subtilis* hbs mRNA stability with translation. *Nucleic Acids Research* **45**: 11386–11400.

Bronsard, J., Pascreau, G., Sassi, M., Mauro, T., Augagneur, Y., and Felden, B. (2017) sRNA and cis-antisense sRNA identification in *Staphylococcus aureus* highlights an unusual sRNA gene cluster with one encoding a secreted peptide. *Scientific Reports* **7**: 603–17.

Burd, C.G., and Dreyfuss, G. (1994) Conserved structures and diversity of functions of RNA-binding proteins. *Science* **265**: 615–621.

Caballero, C.J. (2018) Functional analysis of the RNA chaperone CspA in *Staphylococcus aureus*.

Caballero, C.J., Menendez-Gil, P., Catalan-Moreno, A., Vergara-Irigaray, M., García, B., Segura, V., *et al.* (2018) The regulon of the RNA chaperone CspA and its auto-regulation in S*taphylococcus aureus. Nucleic Acids Research* **46**: 1345–1361.

Chao, Y., and Vogel, J. (2016) A 3' UTR-Derived small RNA provides the regulatory noncoding arm of the inner membrane stress response. *Molecular Cell* **61**: 352–363.

Chapot-Chartier, M.P., Schouler, C., Lepeuple, A.S., Gripon, J.C., and Chopin, M.C. (1997) Characterization of *cspB*, a cold-shock-inducible gene from *Lactococcus lactis*, and evidence for a family of genes homologous to the *Escherichia coli cspA* major cold shock gene. *J Bacteriol* **179**: 5589–5593.

Charpentier, E., Anton, A.I., Barry, P., Alfonso, B., Fang, Y., and Novick, R.P. (2004) Novel cassette-based shuttle vector system for Gram-positive bacteria. *Appl Environ Microbiol* **70**: 6076–6085.

Choi, E.K., Ulanowicz, K.A., Nguyen, Y.A.H., Frandsen, J.K., and Mitton-Fry, R.M. (2017) SHAPE analysis of the *htrA* RNA thermometer from *Salmonella enterica. RNA* **23**: 1569–1581.

Chowdhury, S., Maris, C., Allain, F.H.-T., and Narberhaus, F. (2006) Molecular basis for temperature sensing by an RNA thermometer. *EMBO J* **25**: 2487–2497.

Chowdhury, S., Ragaz, C., Kreuger, E., and Narberhaus, F. (2003) Temperature-controlled structural alterations of an RNA thermometer. *J Biol Chem* **278**: 47915–47921.

Dabrazhynetskaya, A., Brendler, T., Ji, X., and Austin, S. (2009) Switching Protein-DNA recognition specificity by single-amino-acid substitutions in the P1 *par* family of plasmid partition elements. *J Bacteriol* **191**: 1126–1131.

Davis, M.F., Iverson, S.A., Baron, P., Vasse, A., Silbergeld, E.K., Lautenbach, E., and Morris, D.O. (2012) Household transmission of meticillin-resistant *Staphylococcus aureus* and other staphylococci. *Lancet Infect Dis* **12**: 703–716.

De Boer, E., Zwartkruis-Nahuis, J.T.M., Wit, B., Huijsdens, X.W., de Neeling, A.J., Bosch, T., *et al.* (2009) Prevalence of methicillin-resistant *Staphylococcus aureus* in meat. *Int J Food Microbiol* **134**: 52–56.

Delvillani, F., Sciandrone, B., Peano, C., Petiti, L., Berens, C., Georgi, C., *et al.* (2014) Tet-Trap, a genetic approach to the identification of bacterial RNA thermometers: application to *Pseudomonas aeruginosa*. *RNA* **20**: 1963–1976.

Dimastrogiovanni, D., Fröhlich, K.S., Bandyra, K.J., Bruce, H.A., Hohensee, S., Vogel, J., and Luisi, B.F. (2014) Recognition of the small regulatory RNA RydC by the bacterial Hfq protein. *Elife* **3**: 7901.

Donegan, N.P., Manna, A.C., Tseng, C.W., Liu, G.Y., and Cheung, A.L. (2019) CspA regulation of *Staphylococcus aureus* carotenoid levels and σ^B activity is controlled by YjbH and Spx. *Mol Microbiol* **188**: 6739–20.

Duval, B.D., Mathew, A., Satola, S.W., and Shafer, W.M. (2010) Altered growth, pigmentation, and antimicrobial susceptibility properties of *Staphylococcus aureus* due to loss of the major cold shock gene *cspB*. *Antimicrob Agents Chemother* **54**: 2283–2290.

Fetsch, A., and Johler, S. (2018) *Staphylococcus aureus* as a foodborne pathogen. *Curr Clin Micro Rpt* **5**: 88–96.

Figueroa-Bossi, N., Schwartz, A., Guillemardet, B., D'Heygère, F., Bossi, L., and Boudvillain, M. (2014) RNA remodeling by bacterial global regulator CsrA promotes Rho-dependent transcription termination. *Genes & Development* **28**: 1239–1251.

Flaxman, A., Diemen, P.M., Yamaguchi, Y., Allen, E., Lindemann, C., Rollier, C.S., *et al.* (2017) Development of persistent gastrointestinal *S. aureus* carriage in mice. *Scientific Reports* 1–13.

Fox, G.E. (2010) Origin and evolution of the ribosome. *Cold Spring Harb Perspect Biol* **2**: a003483.

Franze de Fernandez, M.T., Eoyang, L., and August, J.T. (1968) Factor fraction required for the synthesis of bacteriophage Qβ-RNA. *Nature* **219**: 588–590.

Fukuto, H.S., Vadyvaloo, V., McPhee, J.B., Poinar, H.N., Holmes, E.C., and Bliska, J.B. (2018) A single amino acid change in the response regulator PhoP, acquired during *Yersinia pestis* evolution, affects PhoP target gene transcription and polymyxin B susceptibility. *J Bacteriol* **200**: e00050–18–14.

Gertz, S., Engelmann, S., Schmid, R., Ohlsen, K., Hacker, J., and Hecker, M. (1999) Regulation of σB-dependent transcription of *sigB* and *asp23* in two different *Staphylococcus aureus* strains. *Mol Gen Genet* **261**: 558–566.

Gevers, D., Vandepoele, K., Simillon, C., and Van de Peer, Y. (2004) Gene duplication and biased functional retention of paralogs in bacterial genomes. *Trends in Microbiology* **12**: 148–154.

Giachino, P., Engelmann, S., and Bischoff, M. (2001) σ^B activity depends on RsbU in *Staphylococcus aureus*. *J Bacteriol* **183**: 1843–1852.

Giraud, C., Hausmann, S., Lemeille, S., Prados, J., Redder, P., and Linder, P. (2015) The C-terminal region of the RNA helicase CshA is required for the interaction with the degradosome and turnover of bulk RNA in the opportunistic pathogen *Staphylococcus aureus*. *RNA Biol* **12**: 658–674.

Giuliodori, A.M., Brandi, A., Gualerzi, C.O., and Pon, C.L. (2004) Preferential translation of cold-shock mRNAs during cold adaptation. *RNA* **10**: 265–276.

Giuliodori, A.M., Di Pietro, F., Marzi, S., Masquida, B., Wagner, R., Romby, P., *et al.* (2010) The *cspA* mRNA is a thermosensor that modulates translation of the cold-shock protein CspA. *Molecular Cell* **37**: 21–33.

Glisovic, T., Bachorik, J.L., Yong, J., and Dreyfuss, G. (2008) RNA-binding proteins and post-transcriptional gene regulation. *FEBS Letters* **582**: 1977–1986.

Graumann, P., Wendrich, T.M., Weber, M.H., Schröder, K., and Marahiel, M.A. (1997) A family of cold shock proteins in *Bacillus subtilis* is essential for cellular growth and for efficient protein synthesis at optimal and low temperatures. *Mol Microbiol* **25**: 741–756.

Graumann, P.L., and Marahiel, M.A. (1998) A superfamily of proteins that contain the cold-shock domain. *Trends in Biochemical Sciences* **23**: 286–290.

Guldimann, C., Boor, K.J., Wiedmann, M., and Guariglia-Oropeza, V. (2016) Resilience in the face of uncertainty: Sigma factor fine-tunes gene expression to support homeostasis in Gram-positive bacteria. *Appl Environ Microbiol* **82**: 4456–4469.

Hanson, K.A., Kim, S.H., and Tibbetts, R.S. (2012) RNA-binding proteins in neurodegenerative disease: TDP-43 and beyond. *Wiley Interdiscip Rev RNA* **3**: 265–285.

Hoe, N.P., and Goguen, J.D. (1993) Temperature sensing in *Yersinia pestis*: Translation of the Lcrf activator protein is thermally regulated. *J Bacteriol* **175**: 7901–7909.

Holmes, M.A., Harrison, E.M., Fisher, E.A., Graham, E.M., Parkhill, J., Foster, G., and Paterson, G.K. (2016) Genomic analysis of companion rabbit *Staphylococcus aureus*. *PLoS ONE* **11**: e0151458–9.

Holmqvist, E., and Vogel, J. (2018) RNA-binding proteins in bacteria. *Nature* **16**: 601–615.

Holmqvist, E., Wright, P.R., Li, L., Bischler, T., Barquist, L., Reinhardt, R., *et al.* (2016) Global RNA recognition patterns of post-transcriptional regulators Hfq and CsrA revealed by UV crosslinking *in vivo*. *EMBO J* **35**: 991–1011.

Holtfreter, S., Radcliff, F.J., Grumann, D., Read, H., Johnson, S., Monecke, S., *et al.* (2013) Characterization of a mouse-adapted *Staphylococcus aureus* strain. *PLoS ONE* **8**: e71142–10.

Hopkins, J.F., Panja, S., McNeil, S.A.N., and Woodson, S.A. (2009) Effect of salt and RNA structure on annealing and strand displacement by Hfq. *Nucleic Acids Research* **37**: 6205–6213.

Hör, J., Garriss, G., Di Giorgio, S., Hack, L.M., Vanselow, J.T., Förstner, K.U., *et al.* (2020) Grad-seq in a Gram-positive bacterium reveals exonucleolytic sRNA activation in competence control. *EMBO J* **46**: 9990–19.

Hudson, W.H., Kossmann, B.R., de Vera, I.M.S., Chuo, S.-W., Weikum, E.R., Eick, G.N., *et al.* (2016) Distal substitutions drive divergent DNA specificity among paralogous transcription factors through subdivision of conformational space. *Proc Natl Acad Sci USA* **113**: 326–331.

Hunger, K., Beckering, C.L., Wiegeshoff, F., Graumann, P.L., and Marahiel, M.A. (2006) Cold-induced putative DEAD box RNA helicases CshA and CshB are essential for cold adaptation and interact with cold shock protein B in *Bacillus subtilis*. *J Bacteriol* **188**: 240–248.

Hussein, H., Fris, M.E., Salem, A.H., Wiemels, R.E., Bastock, R.A., Righetti, F., *et al.* (2019) An unconventional RNA-based thermosensor within the 5' UTR of *Staphylococcus aureus cidA*. *PLoS ONE* **14**: e0214521–21.

Ignatov, D., Vaitkevicius, K., Durand, S., Cahoon, L., Sandberg, S.S., Liu, X., *et al.* (2020) An mRNA-mRNA interaction couples expression of a virulence factor and its chaperone in *Listeria monocytogenes*. *Cell Reports* **30**: 4027–4040.e7.

Jenul, C., and Horswill, A.R. (2018) Regulation of *Staphylococcus aureus* virulence. *Microbiology Spectrum* **6**: 1–34.

Jiang, W., Fang, L., and Inouye, M. (1996) The role of the 5'-end untranslated region of the mRNA for *cspA*, the major cold-shock protein of *Escherichia coli*, in cold-shock adaptation. *J Bacteriol* **178**: 4919–4925.

Jiang, W., Hou, Y., and Inouye, M. (1997) CspA, the major cold-shock protein of *Escherichia coli*, is an RNA chaperone. *J Biol Chem* **272**: 196–202.

Johansson, J., Mandin, P., Renzoni, A., Chiaruttini, C., Springer, M., and Cossart, P. (2002) An RNA thermosensor controls expression of virulence genes in *Listeria monocytogenes*. *Cell* **110**: 551–561.

Kaberdin, V.R., and Bläsi, U. (2006) Translation initiation and the fate of bacterial mRNAs. *FEMS Microbiol Rev* **30**: 967–979.

Katsowich, N., Elbaz, N., Pal, R.R., Mills, E., Kobi, S., Kahan, T., and Rosenshine, I. (2017) Host cell attachment elicits posttranscriptional regulation in infecting enteropathogenic bacteria. *Science* **355**: 735–739.

Katzif, S., Lee, E.-H., Law, A.B., Tzeng, Y.-L., and Shafer, W.M. (2005) CspA regulates pigment production in *Staphylococcus aureus* through a SigB-dependent mechanism. *J Bacteriol* **187**: 8181–8184.

Kelley, L.A., Mezulis, S., Yates, C.M., Wass, M.N., and Sternberg, M.J.E. (2015) The Phyre2 web portal for protein modeling, prediction and analysis. *Nat Protoc* **10**: 845–858.

Kim, S., Corvaglia, A.-R., Léo, S., Cheung, A., and Francois, P. (2016) Characterization of RNA Helicase CshA and its role in protecting mRNAs and Small RNAs of *Staphylococcus aureus* strain Newman. *Infection and Immunity* **84**: 833–844.

Klinkert, B., and Narberhaus, F. (2009) Microbial thermosensors. *Cell Mol Life Sci* **66**: 2661–2676.

Klinkert, B., Cimdins, A., Gaubig, L.C., Roßmanith, J., Aschke-Sonnenborn, U., and Narberhaus, F. (2012) Thermogenetic tools to monitor temperature-dependent gene expression in bacteria. *Journal of Biotechnology* **160**: 55–63.

Knox, J., Uhlemann, A.-C., and Lowy, F.D. (2015) *Staphylococcus aureus* infections: transmission within households and the community. *Trends in Microbiology* **23**: 437–444.

Knox, J., Uhlemann, A.-C., Miller, M., Hafer, C., Vasquez, G., Vavagiakis, P., *et al.* (2012) Environmental contamination as a risk factor for intra-household *Staphylococcus aureus* transmission. *PLoS ONE* **7**: e49900–.

Kortmann, J., and Narberhaus, F. (2012) Bacterial RNA thermometers: molecular zippers and switches. *Nature Publishing Group* **10**: 255–265.

Kouse, A.B., Righetti, F., Kortmann, J., Narberhaus, F., and Murphy, E.R. (2013) RNA-mediated thermoregulation of iron-acquisition genes in *Shigella dysenteriae* and pathogenic *Escherichia coli*. *PLoS ONE* **8**: e63781.

Krismer, B., Liebeke, M., Janek, D., Nega, M., Rautenberg, M., Hornig, G., *et al.* (2014) Nutrient limitation governs *Staphylococcus aureus* metabolism and niche adaptation in the human nose. *PLoS Pathog* **10**: e1003862.

Krismer, B., Weidenmaier, C., Zipperer, A., and Peschel, A. (2017) The commensal lifestyle of *Staphylococcus aureus* and its interactions with the nasal microbiota. *Nature Publishing Group* **15**: 675–687.

Kumar, S., Stecher, G., Suleski, M., and Hedges, S.B. (2017) TimeTree: A resource for timelines, timetrees, and divergence times. *Mol Biol Evol* **34**: 1812–1819.

Lasa, I., Toledo-Arana, A., and Gingeras, T.R. (2012) An effort to make sense of antisense transcription in bacteria. *RNA Biol* **9**: 1039–1044.

Lasa, I., Toledo-Arana, A., Dobin, A., Villanueva, M., de los Mozos, I.R., Vergara-Irigaray, M., *et al.* (2011) Genome-wide antisense transcription drives mRNA processing in bacteria. *Proc Natl Acad Sci USA* **108**: 20172–20177.

Lee, G., Hannett, N.M., Korman, A., and Pero, J. (1980) Transcription of cloned DNA from *Bacillus subtilis* phage SP01 requirement for hydroxymethyluracil-containing DNA by phage-modified RNA polymerase. *Journal of Molecular Biology* **139**: 407–422.

Lee, J.C. (1995) Electrotransformation of Staphylococci. *Methods Mol Biol* **47**: 209–216.

Lehnik-Habrink, M., Pförtner, H., Rempeters, L., Pietack, N., Herzberg, C., and Stülke, J. (2010) The RNA degradosome in *Bacillus subtilis*: identification of CshA as the major RNA helicase in the multiprotein complex. *Mol Microbiol* **77**: 958–971.

Lim, J., Thomas, T., and Cavicchioli, R. (2000) Low temperature regulated DEAD-box RNA helicase from the Antarctic archaeon, *Methanococcoides burtonii*. *Journal of Molecular Biology* **297**: 553–567.

Lindemann, J., Leiacker, R., Rettinger, G., and Keck, T. (2002) Nasal mucosal temperature during respiration. *Clin Otolaryngol Allied Sci* **27**: 135–139.

Lioliou, E., Sharma, C.M., Caldelari, I., Helfer, A.-C., Fechter, P., Vandenesch, F., *et al.* (2012) Global regulatory functions of the *Staphylococcus aureus* endoribonuclease III in gene expression. *PLoS Genet* **8**: e1002782.

Liu, C.-I., Liu, G.Y., Song, Y., Yin, F., Hensler, M.E., Jeng, W.-Y., *et al.* (2008) A cholesterol biosynthesis inhibitor blocks *Staphylococcus aureus* virulence. *Science* **319**: 1391–1394.

Liu, M.Y., Gui, G., Wei, B., Preston, J.F., Oakford, L., Yüksel, U., *et al.* (1997) The RNA molecule CsrB binds to the global regulatory protein CsrA and antagonizes its activity in *Escherichia coli*. *J Biol Chem* **272**: 17502–17510.

Loh, E., Kugelberg, E., Tracy, A., Zhang, Q., Gollan, B., Ewles, H., *et al.* (2013) Temperature triggers immune evasion by *Neisseria meningitidis*. *Nature* **502**: 237–240.

Loh, E., Righetti, F., Eichner, H., Twittenhoff, C., and Narberhaus, F. (2018) RNA thermometers in bacterial pathogens. *Microbiology Spectrum* **6**: 1–16.

Lorenz, C., Gesell, T., Zimmermann, B., Schoeberl, U., Bilusic, I., Rajkowitsch, L., *et al.* (2010) Genomic SELEX for Hfq-binding RNAs identifies genomic aptamers predominantly in antisense transcripts. *Nucleic Acids Research* **38**: 3794–3808.

Lünse, C.E., Schmidt, M.S., Wittmann, V., and Mayer, G. (2011) Carba-sugars activate the glmS-riboswitch of *Staphylococcus aureus*. *ACS Chem Biol* **6**: 675–678.

Madeira, F., Park, Y.M., Lee, J., Buso, N., Gur, T., Madhusoodanan, N., *et al.* (2019) The EMBL-EBI search and sequence analysis tools APIs in 2019. *Nucleic Acids Research* **47**: W636–W641.

Marchfelder, A., and Hess, W. (2012) *Regulatory RNAs in Prokaryotes*. Springer Science & Business Media, Vienna.

Mathy, N., Hébert, A., Mervelet, P., Bénard, L., Dorléans, A., Li de la Sierra-Gallay, I., *et al.* (2010) *Bacillus subtilis* ribonucleases J1 and J2 form a complex with altered enzyme behaviour. *Mol Microbiol* **75**: 489–498.

Max, K.E.A., Zeeb, M., Bienert, R., Balbach, J., and Heinemann, U. (2006) T-rich DNA single strands bind to a preformed site on the bacterial Cold Shock Protein *Bs*-CspB. *Journal of Molecular Biology* **360**: 702–714.

Max, K.E.A., Zeeb, M., Bienert, R., Balbach, J., and Heinemann, U. (2007) Common mode of DNA binding to cold shock domains. *FEBS Journal* **274**: 1265–1279.

Mayr, C. (2017) Regulation by 3′-untranslated regions. *Annu Rev Genet* **51**: 171–194.

Menendez-Gil, P., Caballero, C.J., Catalan-Moreno, A., Irurzun, N., Barrio-Hernandez, I., Caldelari, I., and Toledo-Arana, A. (2020) Differential evolution in 3′UTRs leads to specific gene expression in *Staphylococcus*. *Nucleic Acids Research* **48**: 2544–2563.

Menendez-Gil, P., Caballero, C.J., Solano, C., and Toledo-Arana, A. (2020) Fluorescent molecular beacons mimicking RNA secondary structures to study RNA Chaperone activity. In *RNA Chaperones*. Humana, New York, NY, New York, NY. pp. 41–58.

Michaux, C., Holmqvist, E., Vasicek, E., Sharan, M., Barquist, L., Westermann, A.J., *et al.* (2017) RNA target profiles direct the discovery of virulence functions for the cold-shock proteins CspC and CspE. *Proc Natl Acad Sci USA* **114**: 6824–6829.

Miller, L.G., and Diep, B.A. (2008) Clinical practice: colonization, fomites, and virulence: rethinking the pathogenesis of community-associated methicillin-resistant *Staphylococcus aureus* infection. *Clin Infect Dis* **46**: 752–760.

Morita, M.T., Tanaka, Y., Kodama, T.S., Kyogoku, Y., Yanagi, H., and Yura, T. (1999) Translational induction of heat shock transcription factor σ^{32}: evidence for a built-in RNA thermosensor. *Genes & Development* **13**: 655–665.

Mulhbacher, J., Brouillette, E., Allard, M., Fortier, L.-C., Malouin, F., and Lafontaine, D.A. (2010) Novel riboswitch ligand analogs as selective inhibitors of guanine-related metabolic pathways. *PLoS Pathog* **6**: e1000865–11.

Møller, T., Franch, T., Udesen, C., Gerdes, K., and Valentin-Hansen, P. (2002) Spot 42 RNA mediates discoordinate expression of the *E. coli* galactose operon. *Genes & Development* **16**: 1696–1706.

Nagai, H., Yuzawa, H., and Yura, T. (1991) Interplay of two cis-acting mRNA regions in translational control of sigma 32 synthesis during the heat shock response of *Escherichia coli*. *PNAS* **88**: 10515–10519.

Narberhaus, F. (2010) Translational control of bacterial heat shock and virulence genes by temperature-sensing mRNAs. *RNA Biol* **7**: 84–89.

Narberhaus, F., Waldminghaus, T., and Chowdhury, S. (2006) RNA thermometers. *FEMS Microbiol Rev* **30**: 3–16.

Narberhaus, F., Weiglhofer, W., Fischer, H.M., and Hennecke, H. (1996) The *Bradyrhizobium japonicum rpoH*$_1$ gene encoding a σ^{32}-like protein is part of a unique heat shock gene cluster together with *groESL*$_1$ and three small heat shock genes. *J Bacteriol* **178**: 5337–5346.

Nechooshtan, G., Elgrably-Weiss, M., Sheaffer, A., Westhof, E., and Altuvia, S. (2009) A pH-responsive riboregulator. *Genes & Development* **23**: 2650–2662.

Nocker, A., Hausherr, T., Balsiger, S., Krstulovic, N.P., Hennecke, H., and Narberhaus, F. (2001) A mRNA-based thermosensor controls expression of rhizobial heat shock genes. *Nucleic Acids Research* **29**: 4800–4807.

Novick, R.P. (2003) Autoinduction and signal transduction in the regulation of staphylococcal virulence. *Mol Microbiol* **48**: 1429–1449.

Opdyke, J.A., Kang, J.-G., and Storz, G. (2004) GadY, a small-RNA regulator of acid response genes in *Escherichia coli*. *J Bacteriol* **186**: 6698–6705.

Otaka, H., Ishikawa, H., Morita, T., and Aiba, H. (2011) PolyU tail of rho-independent terminator of bacterial small RNAs is essential for Hfq action. *Proc Natl Acad Sci USA* **108**: 13059–13064.

Oun, S., Redder, P., Didier, J.-P., Francois, P., Corvaglia, A.-R., Buttazzoni, E., *et al.* (2014) The CshA DEAD-box RNA helicase is important for quorum sensing control in *Staphylococcus aureus*. *RNA Biol* **10**: 157–165.

Owttrim, G.W. (2014) RNA helicases. *RNA Biol* **10**: 96–110.

Papenfort, K., and Vanderpool, C.K. (2015) Target activation by regulatory RNAs in bacteria. *FEMS Microbiol Rev* **39**: 362–378.

Peng, Y., Curtis, J.E., Fang, X., and Woodson, S.A. (2014) Structural model of an mRNA in complex with the bacterial chaperone Hfq. *Proc Natl Acad Sci USA* **111**: 17134–17139.

Phadtare, S., Alsina, J., and Inouye, M. (1999) Cold-shock response and cold-shock proteins. *Current Opinion in Microbiology* **2**: 175–180.

Phadtare, S., and Inouye, M. (1999) Sequence-selective interactions with RNA by CspB, CspC and CspE, members of the CspA family of *Escherichia coli*. *Mol Microbiol* **33**: 1004–1014.

Picard, F., Dressaire, C., Girbal, L., and Cocaign-Bousquet, M. (2009) Examination of post-transcriptional regulations in prokaryotes by integrative biology. *C R Biologies* **332**: 958–973.

Potts, A.H., Vakulskas, C.A., Pannuri, A., Yakhnin, H., Babitzke, P., and Romeo, T. (2017) Global role of the bacterial post-transcriptional regulator CsrA revealed by integrated transcriptomics. *Nat Commun* **8**: 1596.

Ren, G.-X., Guo, X.-P., and Sun, Y.-C. (2017) Regulatory 3′ untranslated regions of bacterial mRNAs. *Front Microbiol* **8**: 633–6.

Righetti, F., Nuss, A.M., Twittenhoff, C., Beele, S., Urban, K., Will, S., *et al.* (2016) Temperature-responsive *in vitro* RNA structurome of *Yersinia pseudotuberculosis*. *Proc Natl Acad Sci USA* **113**: 7237–7242.

Roux, C.M., DeMuth, J.P., and Dunman, P.M. (2011) Characterization of components of the *Staphylococcus aureus* mRNA degradosome holoenzyme-like complex. *J Bacteriol* **193**: 5520–5526.

Ruiz de los Mozos, I., Vergara-Irigaray, M., Segura, V., Villanueva, M., Bitarte, N., Saramago, M., *et al.* (2013) Base pairing interaction between 5′- and 3′-UTRs controls *icaR* mRNA translation in *Staphylococcus aureus*. *PLoS Genet* **9**: e1004001–18.

Sabnis, N.A., Yang, H., and Romeo, T. (1995) Pleiotropic regulation of central carbohydrate metabolism in *Escherichia coli* via the gene *csrA*. *J Biol Chem* **270**: 29096–29104.

Sachs, R., Max, K.E.A., Heinemann, U., and Balbach, J. (2012a) RNA single strands bind to a conserved surface of the major cold shock protein in crystals and solution. *RNA* **18**: 65–76.

Sachs, R., Max, K.E.A., Heinemann, U., and Balbach, J. (2012b) RNA single strands bind to a conserved surface of the major cold shock protein in crystals and solution. *RNA* **18**: 65–76.

Schaumburg, F., Mugisha, L., Kappeller, P., Fichtel, C., Köck, R., Köndgen, S., *et al.* (2013) Evaluation of non-invasive biological samples to monitor S*taphylococcus aureus* colonization in great apes and lemurs. *PLoS ONE* **8**: e78046–6.

Schrodinger, LLC. (2015) The PyMOL molecular graphics system, Version 1.8. Retrieved from https://pymol.org/.

Selinger, D.W., Saxena, R.M., Cheung, K.J., Church, G.M., and Rosenow, C. (2003) Global RNA half-life analysis in *Escherichia coli* reveals positional patterns of transcript degradation. *Genome Research* **13**: 216–223.

Serganov, A., and Nudler, E. (2013) A decade of riboswitches. *Cell* **152**: 17–24.

Shenhar, Y., Biran, D., and Ron, E.Z. (2012) Resistance to environmental stress requires the RNA chaperones CspC and CspE. *Environ Microbiol Rep* **4**: 532–539.

Shi, Y., Mowery, R.A., Ashley, J., Hentz, M., Ramirez, A.J., Bilgicer, B., *et al.* (2012) Abnormal SDS-PAGE migration of cytosolic proteins can identify domains and mechanisms that control surfactant binding. *Protein Science* **21**: 1197–1209.

Sifri, C.D., Begun, J., Ausubel, F.M., and Calderwood, S.B. (2003) *Caenorhabditis elegan*s as a model host for *Staphylococcus aureus* pathogenesis. *Infection and Immunity* **71**: 2208–2217.

Sledjeski, D.D., Gupta, A., and Gottesman, S. (1996) The small RNA, DsrA, is essential for the low temperature expression of RpoS during exponential growth in *Escherichia coli*. *EMBO J* **15**: 3993–4000.

Smirnov, A., Förstner, K.U., Holmqvist, E., Otto, A., Günster, R., Becher, D., *et al.* (2016) Grad-seq guides the discovery of ProQ as a major small RNA-binding protein. *Proc Natl Acad Sci USA* **113**: 11591–11596.

Toledo-Arana, A., Dussurget, O., Nikitas, G., Sesto, N., Guet-Revillet, H., Balestrino, D., *et al.* (2009) The *Listeria* transcriptional landscape from saprophytism to virulence. *Nature* **459**: 950–956.

Toledo-Arana, A., Merino, N., Vergara-Irigaray, M., Débarbouillé, M., Penadés, J.R., and Lasa, I. (2005) *Staphylococcus aureus* develops an alternative, *ica*-independent biofilm in the absence of the *arlRS* two-component system. *J Bacteriol* **187**: 5318–5329.

Toledo-Arana, A., Repoila, F., and Cossart, P. (2007) Small noncoding RNAs controlling pathogenesis. *Current Opinion in Microbiology* **10**: 182–188.

Tong, S.Y.C., Davis, J.S., Eichenberger, E., Holland, T.L., and Fowler, V.G. (2015) *Staphylococcus aureus* infections: epidemiology, pathophysiology, clinical manifestations, and management. *Clin Microbiol Rev* **28**: 603–661.

Treisman, J., Gönczy, P., Vashishtha, M., Harris, E., and Desplan, C. (1989) A single amino acid can determine the DNA binding specificity of homeodomain proteins. *Cell* **59**: 553–562.

Twittenhoff, C., Heroven, A.K., Mühlen, S., Dersch, P., and Narberhaus, F. (2020) An RNA thermometer dictates production of a secreted bacterial toxin. *PLoS Pathog* **16**: e1008184.

Uhlemann, A.-C., Knox, J., Miller, M., Hafer, C., Vasquez, G., Ryan, M., *et al.* (2011) The environment as an unrecognized reservoir for Community-Associated Methicillin Resistant *Staphylococcus aureus* USA300: A case-control study. *PLoS ONE* **6**: e22407–9.

Updegrove, T.B., Zhang, A., and Storz, G. (2016) Hfq: the flexible RNA matchmaker. *Current Opinion in Microbiology* **30**: 133–138.

Uppal, S., Akkipeddi, V.S.N.R., and Jawali, N. (2008) Posttranscriptional regulation of *cspE* in *Escherichia coli*: involvement of the short 5'-untranslated region. *FEMS Microbiol Lett* **279**: 83–91.

Ünal, C.M., and Steinert, M. (2014) Microbial peptidyl-prolyl *cis/trans* isomerases (PPIases): virulence factors and potential alternative drug targets. *Microbiol Mol Biol Rev* **78**: 544–571.

Valle, J., Echeverz, M., and Lasa, I. (2019) σ^B inhibits Poly-N-Acetylglucosamine exopolysaccharide synthesis and biofilm formation in *Staphylococcus aureus. J Bacteriol* **201**.

Valle, J., Toledo-Arana, A., Berasain, C., Ghigo, J.-M., Amorena, B., Penadés, J.R., and Lasa, I. (2003) SarA and not σ^B is essential for biofilm development by *Staphylococcus aureus*. *Mol Microbiol* **48**: 1075–1087.

Večerek, B., Moll, I., Afonyushkin, T., Kaberdin, V., and Bläsi, U. (2003) Interaction of the RNA chaperone Hfq with mRNAs: direct and indirect roles of Hfq in iron metabolism of *Escherichia coli*. *Mol Microbiol* **50**: 897–909.

Vincent, H.A., Henderson, C.A., Ragan, T.J., Garza-Garcia, A., Cary, P.D., Gowers, D.M., *et al.* (2012) Characterization of *Vibrio cholerae* Hfq provides novel insights into the role of the Hfq C-terminal region. *Journal of Molecular Biology* **420**: 56–69.

Vogel, J., and Luisi, B.F. (2011) Hfq and its constellation of RNA. *Nature Publishing Group* **9**: 578–589.

Waldminghaus, T., Gaubig, L.C., and Narberhaus, F. (2007) Genome-wide bioinformatic prediction and experimental evaluation of potential RNA thermometers. *Mol Genet Genomics* **278**: 555–564.

Waldminghaus, T., Heidrich, N., Brantl, S., and Narberhaus, F. (2007) FourU: a novel type of RNA thermometer in *Salmonella*. *Mol Microbiol* **65**: 413–424.

Wang, N., Yamanaka, K., and Inouye, M. (1999) CspI, the ninth member of the CspA family of *Escherichia coli*, is induced upon cold shock. *J Bacteriol* **181**: 1603–1609.

Waters, L.S., and Storz, G. (2009) Regulatory RNAs in bacteria. *Cell* **136**: 615–628.

Wattam, A.R., Davis, J.J., Assaf, R., Boisvert, S., Brettin, T., Bun, C., *et al.* (2017) Improvements to PATRIC, the all-bacterial bioinformatics database and analysis resource center. *Nucleic Acids Research* **45**: D535–D542.

Weber, G.G., Kortmann, J., Narberhaus, F., and Klose, K.E. (2014) RNA thermometer controls temperature-dependent virulence factor expression in *Vibrio cholerae*. *Proc Natl Acad Sci USA* **111**: 14241–14246.

Wertheim, H.F.L., Melles, D.C., Vos, M.C., van Leeuwen, W., van Belkum, A., Verbrugh, H.A., and Nouwen, J.L. (2005) The role of nasal carriage in *Staphylococcus aureus* infections. *Lancet Infect Dis* **5**: 751–762.

Wiemels, R.E., Cech, S.M., Meyer, N.M., Burke, C.A., Weiss, A., Parks, A.R., *et al.* (2017) An intracellular peptidyl-prolyl *cis/trans* isomerase is iequired for folding and activity of the *Staphylococcus aureus* secreted virulence factor nuclease. *J Bacteriol* **199**.

Wilkie, G.S., Dickson, K.S., and Gray, N.K. (2003) Regulation of mRNA translation by 5“- and 3-”UTR-binding factors. *Trends in Biochemical Sciences* **28**: 182–188.

Willimsky, G., Bang, H., Fischer, G., and Marahiel, M.A. (1992) Characterization of *cspB*, a *Bacillus subtilis* inducible cold shock gene affecting cell viability at low temperatures. *J Bacteriol* **174**: 6326–6335.

Wilson, D.N., and Nierhaus, K.H. (2005) Ribosomal proteins in the spotlight. *Crit Rev Biochem Mol Biol* **40**: 243–267.

Winkler, W.C., and Breaker, R.R. (2005) Regulation of bacterial gene expression by riboswitches. *Annu Rev Microbiol* **59**: 487–517.

Woodson, S.A., Panja, S., and Santiago-Frangos, A. (2018) Proteins that chaperone RNA regulation. *Microbiology Spectrum* **6**.

Xia, B., Ke, H., and Inouye, M. (2001) Acquirement of cold sensitivity by quadruple deletion of the *cspA* family and its suppression by PNPase S1 domain in *Escherichia coli*. *Mol Microbiol* **40**: 179–188.

Yakhnin, A.V., Baker, C.S., Vakulskas, C.A., Yakhnin, H., Berezin, I., Romeo, T., and Babitzke, P. (2013) CsrA activates *flhDC* expression by protecting *flhDC* mRNA from RNase E-mediated cleavage. *Mol Microbiol* **87**: 851–866.

Yamanaka, K., Fang, L., and Inouye, M. (1998) The CspA family in *Escherichia coli*: multiple gene duplication for stress adaptation. *Mol Microbiol* **27**: 247–255.

Zallot, R., Harrison, K.J., Kolaczkowski, B., and de Crécy-Lagard, V. (2016) Functional annotations of paralogs: A blessing and a curse. **6**: 39.

Zhang, Y., Burkhardt, D.H., Rouskin, S., Li, G.-W., Weissman, J.S., and Gross, C.A. (2018) A stress response that monitors and regulates mRNA structure is central to Cold Shock adaptation. *Molecular Cell* **70**: 274–286.e7.

Zuker, M. (2003) Mfold web server for nucleic acid folding and hybridization prediction. *Nucleic Acids Research* **31**: 3406–3415.

ANNEXES

Annex 1. Strains used in this study

Strains	Relevant characteristic(s)	BGR ID [a]	Source or reference [b]
Staphylococcus aureus			
15981	Wild type (WT) strain. MSSA clinical isolate; biofilm positive; PNAG-dependent biofilm matrix	8	(1)
Δ*cspA*	15981 strain with deletion of the *cspA* gene	83	(2)
Δ*cspB*	15981 strain with deletion of the *cspB* gene	1150	This study
Δ*cspC*	15981 strain with deletion of the *cspC* gene	195	This study
CspA^{3xF}	15981 strain expressing the 3xFLAG-tagged CspA protein from the chromosome	239	(2)
Δ*sigB*	15981 strain with deletion of the *sigB* operon	178	(1)
WT pCN51	15981 strain carrying the pCN51 plasmid	105	(2)
Δ*cspA* pCN51	15981 Δ*cspA* strain carrying the pCN51 plasmid	107	(2)
Δ*cspA* pCspA^{3xF}	15981 Δ*cspA* strain carrying the pCspA^{3xF} plasmid	268	(2)
Δ*cspA* pmA_CspB^{3xF}	15981 Δ*cspA* strain carrying the pmA_CspB^{3xF} plasmid	763	(3)
Δ*cspA* pmA_CspC^{3xF}	15981 Δ*cspA* strain carrying the pmA_CspC^{3xF} plasmid	761	(3)
Δ*cspA* pmA_CspA_L3_C^{3xF}	15981 Δ*cspA* strain carrying the pmA_CspA_L3_C^{3xF} plasmid	1650	This study
Δ*cspA* pmA_CspA_β4_C^{3xF}	15981 Δ*cspA* strain carrying the pmA_CspA_β4_C^{3xF} plasmid	1654	This study
Δ*cspA* pCspA_β5_C^{3xF}	15981 Δ*cspA* strain carrying the pmA_CspA_β5_C^{3xF} plasmid	1638	This study
Δ*cspA* pmA_CspC_L3β4_A^{3xF}	15981 Δ*cspA* strain carrying the pmA_CspC_L3β4_A^{3xF} plasmid	1622	This study
Δ*cspA* pmA_CspC_β5_A^{3xF}	15981 Δ*cspA* strain carrying the pmA_CspC_β5_A^{3xF} plasmid	1652	This study
Δ*cspA* pmA_CspA^{3XF}_P58E	15981 Δ*cspA* strain carrying the pmA_CspA^{3XF}_P58E plasmid	1704	This study
Δ*cspA* pmA_CspC^{3XF}_E58P	15981 Δ*cspA* strain carrying the pmA_CspC^{3XF}_E58P plasmid	1688	This study
Δ*cspA* pmA_CspB^{3XF}_D58P	15981 Δ*cspA* strain carrying the pmA_CspB^{3XF}_D58P plasmid	1729	This study
CspB^{3xF}	15981 strain expressing the 3xFLAG-tagged CspB protein from the chromosome	346	This study
CspC^{3xF}	15981 strain expressing the 3xFLAG-tagged CspC protein from the chromosome	240	This study
WT p5'UTR^{cspB}-gfp	15981 carrying the p5'UTR^{cspB}-gfp plasmid	1570	This study
WT p5'UTR^{cspC}-gfp	15981 carrying the p5'UTR^{cspC}-gfp plasmid	1398	This study
WT p5'UTR^{cspB}Δ24-gfp	15981 carrying the p5'UTR^{cspB}Δ24-gfp plasmid	1555	This study
WT p5'UTR^{cspC}Δ24-gfp	15981 carrying the p5'UTR^{cspC}Δ24-gfp plasmid	1429	This study

Continued in the following page

Annex 1. Continued

Strains	Relevant characteristic(s)	BGR ID [a]	Source or reference [b]
WT p5'UTR^{cspB}UAU47AA-gfp	15981 carrying the p5'UTR^{cspB}UAU47AA-gfp plasmid	1623	This study
WT p5'UTR^{cspB}C50G-gfp	15981 carrying the p5'UTR^{cspB}C50G-gfp plasmid	1579	This study
WT p5'UTR^{cspB}UU55AA-gfp	15981 carrying the p5'UTR^{cspB}UU55AA-gfp plasmid	1517	This study
WT p5'UTR^{cspC}UU48A-gfp	15981 carrying the p5'UTR^{cspC}UU48A-gfp plasmid	1415	This study
WT p5'UTR^{cspB}UU55AA+UU26AA-gfp	15981 carrying the p5'UTR^{cspB}UU55AA+UU26AA-gfp plasmid	1902	This study
ΔcspA p5'UTR^{cspB}-gfp	15981 Δ*cspA* strain carrying the p5'UTR^{cspB}-gfp plasmid	1571	This study
ΔcspA p5'UTR^{cspC}-gfp	15981 Δ*cspA* strain carrying the p5'UTR^{cspC}-gfp plasmid	1408	This study
ΔcspB p5'UTR^{cspB}-gfp	15981 Δ*cspB* strain carrying the p5'UTR^{cspB}-gfp plasmid	1572	This study
ΔcspC p5'UTR^{cspC}-gfp	15981 Δ*cspC* strain carrying the p5'UTR^{cspC}-gfp plasmid	1561	This study
ΔcspA CspB^{3xF}	15981 Δ*cspA* strain expressing the 3xFLAG-tagged CspB protein from the chromosome	1324	This study
ΔcspA CspC^{3xF}	15981 Δ*cspA* strain expressing the 3xFLAG-tagged CspC protein from the chromosome	725	This study
ΔcspA p5'UTR^{cspB}Δ24-gfp	15981 Δ*cspA* strain carrying the p5'UTR^{cspB}Δ24-gfp plasmid	1566	This study
ΔcspA p5'UTR^{cspB}C50G-gfp	15981 Δ*cspA* strain carrying the p5'UTR^{cspB}C50G-gfp plasmid	1928	This study
ΔcspA p5'UTR^{cspB}UU55AA-gfp	15981 Δ*cspA* strain carrying the p5'UTR^{cspB}C50G-gfp plasmid	1565	This study
ΔcspA p5'UTR^{cspC}Δ24-gfp	15981 Δ*cspA* strain carrying the p5'UTR^{cspC}Δ24-gfp plasmid	1516	This study
ΔcspA p5'UTR^{cspC}UU48A-gfp	15981 Δ*cspA* strain carrying the p5'UTR^{cspC}UU48A-gfp plasmid	1416	This study
ΔcspA p5'UTR^{cspB}UU55AA+UU26AA-gfp	15981 Δ*cspA* strain carrying the p5'UTR^{cspB}UU55AA+UU26AA-gfp plasmid	1749	This study
ΔcspB	15981 strain with deletion of the *cspB* gene	1150	This study
ΔcspC	15981 strain with deletion of the *cspC* gene	195	This study
ΔcspBC	15981 strain with deletion of the *cspB* and *cspC* genes	1251	This study
Δ24cspB	15981 strain with the first 24 nucleotides deletion of the *cspB* gene	1975	This study
Δ24cspC	15981 strain with the first 24 nucleotides deletion of the *cspC* gene	1987	This study

Continued in the following page

Annex 1. Continued

Strains	Relevant characteristic(s)	BGR ID [a]	Source or reference [b]
Δ24cspB^{3xF}	15981 strain including a deletion of the first 24 nucleotides of the *cspB* gene and expressing the 3xFLAG-tagged CspB protein from the chromosome	1991	This study
Δ24cspC^{3xF}	15981 strain including a deletion of the first 24 nucleotides of the *cspC* gene and expressing the 3xFLAG-tagged CspC protein from the chromosome	1992	This study
Δ24cspBC	15981 strain including the deletions of the first 24 nucleotides of *cspB* and *cspC* genes	1917	This study
Escherichia coli			
XL1-Blue	Strain used for cloning experiments	1	Stratagene
IMO1B	Strain used for cloning experiments	1837	(4)
WT pEW-5'UTR^{cspB}-gfp	IM01B strain carrying pEW-5'UTR^{cspB}-gfp plasmid	2013	This study

[a] Identification number of the strains stored at the Laboratory of Bacterial Gene Regulation.
[b] References:

1. Valle, J. (2003) SarA and not sigma B is essential for biofilm development by *Staphylococcus aureus*. *Mol Microbiol*, **48**, 1075–1087.
2. Caballero, C.J. (2018) The regulon of the RNA chaperone CspA and its auto-regulation in *S. aureus*. *Nucleic Acids Res*, **46**, 1345–1361.
3. Caballero, C.J. (2018). Functional analysis of the RNA chaperone CspA in *Staphylococcus aureus*. PhD Thesis. https://academica-e.unavarra.es/handle/2454/3220
4. MonK, IR. (2015) Complete bypass of restriction systems for Major Staphylococcus aureus lineages. *mBio*, **6**, 1066-1113

Annex 2. Plasmids used in this study

Plasmids	Relevant characteristic(s)	Source or reference [a]
pCN51	*E. coli-S. aureus* shuttle vector to express genes under the control of the P*cad* inducible promoter. Low copy number. Amp^R-Erm^R	(1)
pMAD_Δ*cspB*	pMAD plasmid containing the allele for deletion of the cspB coding region	This study
pMAD_Δ*cspC*	pMAD plasmid containing the allele for deletion of the cspC coding region	This study
$pCspA^{3xF}$	pCN51 plasmid expressing the *cspA* mRNA which encodes the 3xFLAG-tagged CspA protein	(2)
pmA_CspB^{3xF}	pCN51 plasmid expressing a chimeric *cspA* mRNA including codon substitutions to encode the 3xFLAG-tagged CspB protein	(2)
pmA_CspC^{3xF}	pCN51 plasmid expressing a chimeric *cspA* mRNA including codon substitutions to encode the 3xFLAG-tagged CspC protein	(2)
$pmA\_CspA\_L3\_C^{3xF}$	pCN51 plasmid expressing a chimeric *cspA* mRNA that encodes a modified 3xFLAG-tagged CspA including the loop 3 from CspC protein	This study
$pmA\_CspA\_\beta4\_C^{3xF}$	pCN51 plasmid expressing a chimeric *cspA* mRNA that encodes a modified 3xFLAG-tagged CspA including the β4 strand from CspC protein	This study
$pmA\_CspA\_\beta5\_C^{3xF}$	pCN51 plasmid expressing a chimeric *cspA* mRNA that encodes a modified 3xFLAG-tagged CspA including the β5 strand from CspC protein	This study
$pmA\_CspC\_L3\beta4\_A^{3xF}$	pCN51 plasmid expressing a chimeric *cspA* mRNA that encodes a modified 3xFLAG-tagged CspC including the loop 3 and the β4 strand from CspA protein	This study
$pmA\_CspC\_\beta5\_A^{3xF}$	pCN51 plasmid expressing a chimeric *cspA* mRNA that encodes a modified 3xFLAG-tagged CspC including the β5 strand from CspA protein	This study
pmA_CspA^{3XF}_P58E	pCN51 plasmid expressing a chimeric *cspA* mRNA including codon substitutions to encode the mutated 3xFLAG-tagged CspA P58E protein	This study
pmA_CspC^{3XF}_E58P	pCN51 plasmid expressing a chimeric *cspA* mRNA including codon substitutions to encode the mutated 3xFLAG-tagged CspC E58P protein	This study
pmA_CspB^{3XF}_D58P	pCN51 plasmid expressing a chimeric *cspA* mRNA including codon substitutions to encode the mutated 3xFLAG-tagged CspB D58P protein	This study
pMAD_*cspB*^{3xF}	pMAD plasmid containing the allele for insertion of the 3xFLAG at the C-terminus of the CspB protein	This study
pMAD_*cspC*^{3xF}	pMAD plasmid containing the allele for insertion of the 3xFLAG at the C-terminus of the CspB protein	This study
pHRG	High copy number plasmid containing the constitutive phyper promoter and *gfp* reporter gene	This study
$p5'UTR^{cspB}$-gfp	pHRG plasmid expressing the 5'UTR from *cspB* mRNA in frame with the green fluorescence protein GFP	This study
$p5'UTR^{cspC}$-gfp	pHRG plasmid expressing the 5'UTR from *cspC* mRNA in frame with the green fluorescence protein GFP	This study
$p5'UTR^{cspB}\Delta24$-gfp	pHRG plasmid expressing the 5'UTR from *cspB* mRNA where the first 24 nucleotides were deleted	This study
$p5'UTR^{cspC}\Delta24$-gfp	pHRG plasmid expressing the 5'UTR from *cspC* mRNA where the first 24 nucleotides were deleted	This study
$p5'UTR^{cspB}$UAU47AA-gfp	pHRG plasmid expressing the 5'UTR from *cspB* mRNA where the uridines and adenine at position 47-49 and 48, respctively were substituted by two adenines	This study
$p5'UTR^{cspB}$C50G-gfp	pHRG plasmid expressing the 5'UTR from *cspB* mRNA where the cytosine at position 50 was substituted by a guanine	This study

Continued in the following page

Annex 2. Continued

Plasmids	Relevant characteristic(s)	Source or reference [a]
p5'UTR^{cspB}UU55AA-gfp	pHRG plasmid expressing the 5'UTR from *cspB* mRNA where the uridines at position 55 and 56 were substituted by two adenines	This study
p5'UTR^{cspC}UU48A-gfp	pHRG plasmid expressing the 5'UTR from *cspC* mRNA where the uridines at position 48 and 49 were substituted by an adenine	This study
p5'UTR^{cspB}UU55AA+UU26AA-gfp	pHRG plasmid expressing the 5'UTR from *cspB* mRNA where the uridines at position 55 and 56 were substituted by two adenines and the uridines at position 26 and 27 were changed by two adenines	This study
pMAD_*Δ24cspB*	pMAD plasmid containing the allele for the first 24 nucleotides deletion of the *cspB* gene	This study
pMAD_*Δ24cspC*	pMAD plasmid containing the allele for the first 24 nucleotides deletion of the *cspB* gene	This study
pMAD_*Δ24cspB*^{3xF}	pMAD plasmid containing the allele for the first 24 nucleotides deletion of the *cspB*^{3xF} gene	This study
pMAD_*Δ24cspC*^{3xF}	pMAD plasmid containing the allele for the first 24 nucleotides deletion of the *cspC*^{3xF} gene	This study
pEW	*E. coli-S. aureus* shuttle vector to express genes under the control of the constitutive P*blaZ* promoter. Amp^{R}-Erm^{R}	(4)
pEW-5'UTR^{cspB}-gfp	pEW plasmid containing the *cspB* 5'UTR mRNA in frame with the green fluorescence protein GFP	This study

[a] References:

1. Charpentier, E. (2004) Novel cassette-based shuttle vector system for gram-positive bacteria. *Appl Environ Microbiol*, **70**, 6076-6085
2. Caballero, C.J. (2018). Functional analysis of the RNA chaperone CspA in *Staphylococcus aureus*. PhD Thesis. https://academica-e.unavarra.es/handle/2454/3220
3. Caballero, C.J. (2018) The regulon of the RNA chaperone CspA and its auto-regulation in *S. aureus*. *Nucleic Acids Res*, **46**, 1345–1361.
4. Menendez-Gil, P (2020). Differential evolution in 3'UTRs leads to specific gene expression in *Staphylococcus*. *Nucleic Acid Res*, **48**, 2544-2563

Annex 3. Oligonucleotides used in this study

Oligonucleotide name	Sequence [a]
Construction of pMAD plasmid for deletion of *cspB* gene	
CspB_A_EcoRI_v2	*GAATTC*GTTATAGAACACCATTGGAAG
CspB_B_SalI_v2	*GTCGAC*GTGACATATCGTTTAAACATG
CspB_C SalI	*GTCGAC*TCTTACAACATAAAACGACT
CspB_D BamHI	*GGATCC*TTAGTTGTTTATTGGAATTG
CspB_E_v2	AAATGAACATTCTAACGGAATAA
CspB_F	GTGTGAATTGTTCAATGTAACTTTA
Construction of pMAD plasmid for deletion of *cspC* gene	
CspC_A BglII	*AGAT*CTTTAGTTCGTCAAGGCTTGG
CspC_B SalI	*GTCGAC*ATTGAATACCTCCGTCGT
CspC_C SalI	*GTCGAC*TTTTAACTTATTCAAACAGTCC
CspC_D BamHI	*GGATCC*CTCAATAATTAATCAGTCTTAA
CspC_E	ATGCAAAGAAAATTGAAGTCGAG
CspC_F	TTCAGTAGACCCCAAAGCAT
Construction of pMAD plasmid for 24 deletion of *cspB* gene	
CspB_A EcoRI	*GAATTC*AACTTGGTATAACGTCATTG
CspB_D24_Izq	AAGACCAACTATACGCTCAT
CspB_D24_Drcha	ATGAGCGTATAGTTGGTCTTATTGTAGTGTATTTGTTTAGAATATCCT
CspB_D BamHI	GGATCCTTAGTTGTTTATTGGAATTG
Construction of pMAD plasmid for 24 deletion of *cspC* gene	
CspC_A BglII	*AGATCT*TTAGTTCGTCAAGGCTTGG
CspC_D24_Izq	AACTTTCATTATACACTTTT
CspC_D24_Drcha	AAAAGTGTATAATGAAAGTTATGTGAGTTATTTATATAGAATATTCTC
CspC_D BamHI	*GGATCC*CTCAATAATTAATCAGTCTTAA
Construction of pMAD plasmid for chromosomic 3xFLAG-labelling of the *cspB* gene	
cspB_A EcoRI	*GAATTC*AACTTGGTATAACGTCATTG
3xFcspB_B	TTATAATCACCGTCATGGTCTTTGTAGTCAACAGTTTGTACGTTAACTGC
3xFcspB_C	GACTACAAAGACCATGACGGTGATTATAAAGATCATGATATCGACTACAAA GATGACGACGATAAATAATCTTACAACATAAAACGACTCATTA
CspB_D BamHI	*GGATCC*TTAGTTGTTTATTGGAATTG
Construction of pMAD plasmid for chromosomic 3xFLAG-labelling of the *cspC* gene	
CspC_A BglII	*AGAT*CTTTAGTTCGTCAAGGCTTGG
3xFcspC_B	ACCGTCATGGTCTTTGTAGTCCATTTTAACTACGTTTGCAGCTT
3xFcspC_C	GACTACAAAGACCATGACGGTGATTATAAAGATCATGATATCGACTACAAA GATGACGACGATAAATAATTTTAACTTATTCAAACAGT
CspC_D BamHI	*GGATCC*CTCAATAATTAATCAGTCTTAA
Construction of plasmids expressing *csp* mRNAs	
CspA +1 BamHI	*GGATCC*TTCCATATTGCAAAGAATATTTGAGTG
CspA ter EcoRI	*GAATTC*CTATTGCAAACAATGTTGGTGATATAA
CspB_+1_BamHI	*GGATCC*AAGCTCGTGAATTAAATTGTAGTGTA
CspB_ter_EcoRI	*GAATTC*ATCATCGTGGTATCGTCTCATATT
CspC +1 BamHI	*GGATCC*AATAAAGAGCGTGAAGAAAAATGTG
CspC ter KpnI	*GGTACC*CCATTATATATTGTTAAATCTCCAAC
Construction of plasmid expressing 3xFLAG tagged CspB	
3xFcspB_B	TTATAATCACCGTCATGGTCTTTGTAGTCAACAGTTTGTACGTTAACTGC
3xFcspB_C	GACTACAAAGACCATGACGGTGATTATAAAGATCATGATATCGACTACAAA GATGACGACGATAAATAATCTTACAACATAAAACGACTCATTAT

Continued in the following page

Annex 3. Continued

Oligonucleotide name	Sequence [a]
Construction of plasmids expressing chimeric *cspA* mRNA and its variants	
CspA_ovl_dcha	GCAATTAACCAAGATGGTTAC
3xFLAG_NcoI_rv	*CCATGG*TTACTATTTATCGTCGTCATCTT
CspCA_ovl_izq	GATTTGTAACCATCTTGGTTAATTGCTGAAAAATGTACGAATACGTCACTA
CspA_L3_C_dcha	ATTCGTACATTTTTCAGCAATTGCTGAAGATGGTTACAAATCATTAGAAG
CspA_L3_C_izq	CAGCAATTGCTGAAAAATGTACGAATAC
CspA_Beta4_C_dcha	AGGTCAAAAAGTTGAGTTTGATATAGTTGAAGGCGACCGC
CspA_Beta4_C_izq	TATCAAACTCAACTTTTTGACCTTCTTCTAATGATTTGT
CspB_D58P	AACGTTTACAGCTTGTGGACCGCGTTGGCCT
Probe for Northen blot assays	
anti-GFP probe	TTATTTGTATAGTTCATCCATGCCATGTGTAATCCCAGCAGCTGTTACAAAC TCAAGAAGGACCATGTGG
anti_3xFLAG_probe	TTTATCGTCGTCATCTTTGTAGTCGATATCATGATCTTTATAATCACCGTCA TGGTCTTTGTAGTC
Synthesis of *cspB* 5'UTR mRNA	
T7_5UTRcspB_Fw	TAATACGACTCACTATAGGGACGTAATAAAAGCTCGTGAA
5UTR_CspB_RV_SpeI	ACTAGTTGTACCGTTATTCATATAGAAAACC
Synthesis of *cspC* 5'UTR mRNA	
T7_5UTRcspC_fw	TAATACGACTCACTATAGGGAAGTAATAAAGAGCGTGAAG
5'UTR_CspC_RV_SpeI	ACTAGTTGTACCGTTATTCATATTGAATACC
Construction of plasmids expressing 5'UTR *cspB and cspC* mRNA and its mutants	
5UTR_CspB_FW_EcoRI	*GAATTC*ACGTAATAAAAGCTCGTGAAT
5UTR_CspB_RV_SpeI	*ACTAGT*TGTACCGTTATTCATATAGAAAACC
5'UTR_cspC_FW_EcoRI	*GAATT*CAAGTAATAAAGAGCGTGAAGAAA
5'UTR_CspC_RV_SpeI	*ACTAGT*TGTACCGTTATTCATATTGAATACC
M5B_D24_EcoRI	*GAATTC*ATTGTAGTGTATTTGTTTAGAATATCC
M5B_50G_EcoRI	*GAATTC*ACGTAATAAAAGCTCGTGAATTAAATTGTAGTGTATTTGTTTAGAA TATGCTCTTTTTTAGTTATGAAT
M5B_2U552A_EcoRI	*GAATTC*ACGTAATAAAAGCTCGTGAATTAAATTGTAGTGTATTTGTTTAGAA TATCCTCTAATTTAGTTATGAAT
M5C_D24_EcoRI	*GAATTC*ATGTGAGTTATTTATATAGAATATTCTCCT
M5C_2U48A_EcoRI	*GAATTC*AAGTAATAAAGAGCGTGAAGAAAAATGTGAGTTATTTATATAGAAT AACTCCTTTTCATT
Construction of pMAD plasmid for 24 deletion of *cspB* gene	
CspB_A EcoRI	*GAATTC*AACTTGGTATAACGTCATTG
CspB_D24_Izq	AAGACCAACTATACGCTCAT
CspB_D24_Drcha	ATGAGCGTATAGTTGGTCTTATTGTAGTGTATTTGTTTAGAATATCCT
CspB_D BamHI	GGATCCTTAGTTGTTTATTGGAATTG
Construction of pMAD plasmid for 24 deletion of *cspC* gene	
CspC_A BglII	*AGATCT*TTAGTTCGTCAAGGCTTGG
CspC_D24_Izq	AACTTTCATTATACACTTTT
CspC_D24_Drcha	AAAAGTGTATAATGAAAGTTATGTGAGTTATTTATATAGAATATTCTC
CspC_D BamHI	*GGATCC*CTCAATAATTAATCAGTCTTAA

Continued in the following page

Annex 3. Continued

Oligonucleotide name	Sequence [a]
Construction of pMAD plasmid for chromosomic 3xFLAG-labelling of the *cspB* gene	
cspB_A EcoRI	*GAATTC*AACTTGGTATAACGTCATTG
3xFcspB_B	TTATAATCACCGTCATGGTCTTTGTAGTCAACAGTTTGTACGTTAACTGC
3xFcspB_C	GACTACAAAGACCATGACGGTGATTATAAAGATCATGATATCGACTACAAA GATGACGACGATAAATAATCTTACAACATAAAACGACTCATTA
CspB_D BamHI	*GGATCC*TTAGTTGTTTATTGGAATTG
Construction of pMAD plasmid for chromosomic 3xFLAG-labelling of the *cspC* gene	
CspC_A BglII	*AGAT*CTTTAGTTCGTCAAGGCTTGG
3xFcspC_B	ACCGTCATGGTCTTTGTAGTCCATTTTAACTACGTTTGCAGCTT
3xFcspC_C	GACTACAAAGACCATGACGGTGATTATAAAGATCATGATATCGACTACAAA GATGACGACGATAAATAATTTTAACTTATTCAAACAGT
CspC_D BamHI	*GGATCC*CTCAATAATTAATCAGTCTTAA
Construction of plasmids expressing 5'UTR *cspB and cspC* mRNA and its mutants	
5UTR_CspB_FW_EcoRI	*GAATTC*ACGTAATAAAAGCTCGTGAAT
5UTR_CspB_RV_SpeI	*ACTAGT*TGTACCGTTATTCATATAGAAAACC
5'UTR_cspC_FW_EcoRI	*GAATT*CAAGTAATAAAGAGCGTGAAGAAA
5'UTR_CspC_RV_SpeI	*ACTAGT*TGTACCGTTATTCATATTGAATACC
M5B_D24_EcoRI	*GAATTC*ATTGTAGTGTATTTGTTTAGAATATCC
M5C_D24_EcoRI	*GAATTC*ATGTGAGTTATTTATATAGAATATTCTCCT
M5B_C50G_EcoRI	*GAATTC*ACGTAATAAAAGCTCGTGAATTAAATTGTAGTGTATTTGTTTAGAA TATGCTCTTTTTTAGTTATGAAT
M5B_UU55AA_EcoRI	*GAATTC*ACGTAATAAAAGCTCGTGAATTAAATTGTAGTGTATTTGTTTAGAA TATCCTCTAATTTAGTTATGAAT
M5B_UAU47AA	*GAATTCACGTAATAAAAGCTCGTGAAT*TAAATTGTAGTGTATTTGTTTAGAA AACCTCTTTTTT
M5C_UU48A_EcoRI	*GAATTC*AAGTAATAAAGAGCGTGAAGAAAAATGTGAGTTATTTATATAGAAT AACTCCTTTTCATT
M5B_2U_26_2A	*GAATTC*ACGTAATAAAAGCTCGTGAATTAAAAAGTAGTGTATTTG
Probe for Northen blot assays	
anti-GFP probe	TTATTTGTATAGTTCATCCATGCCATGTGTAATCCCAGCAGCTGTTACAAAC TCAAGAAGGACCATGTGG
anti_3xFLAG_probe	TTTATCGTCGTCATCTTTGTAGTCGATATCATGATCTTTATAATCACCGTCA TGGTCTTTGTAGTC
Molecular beacon oligonucleotides	
CspB	CGTAATAAAAGCTCGTGAATTAAATTGTAGTGTATTTGTTTAGAATATCCTC TTTTTTAGTTATGAATTTGTTACA
CspC	AGTAATAAAGAGCGTGAAGAAAAATGTGAGTTATTTATATAGAATATTCTCC TTTTCATTTATGAATTTGTTACA
Synthesis of *cspB* 5'UTR mRNA	
T7_5UTRcspB_Fw	TAATACGACTCACTATAGGGACGTAATAAAAGCTCGTGAA
5UTR_CspB_RV_SpeI	ACTAGTTGTACCGTTATTCATATAGAAAACC
Synthesis of *cspC* 5'UTR mRNA	
T7_5UTRcspC_fw	TAATACGACTCACTATAGGGAAGTAATAAAGAGCGTGAAG
5'UTR_CspC_RV_SpeI	ACTAGTTGTACCGTTATTCATATTGAATACC

[a] Restriction enzymes sites and 3xFLAG sequences are indicated as italic or underlined letters, respectively

Annex 4. Codon modifications in the *cspA* mRNA to generate chimeric CSPs.

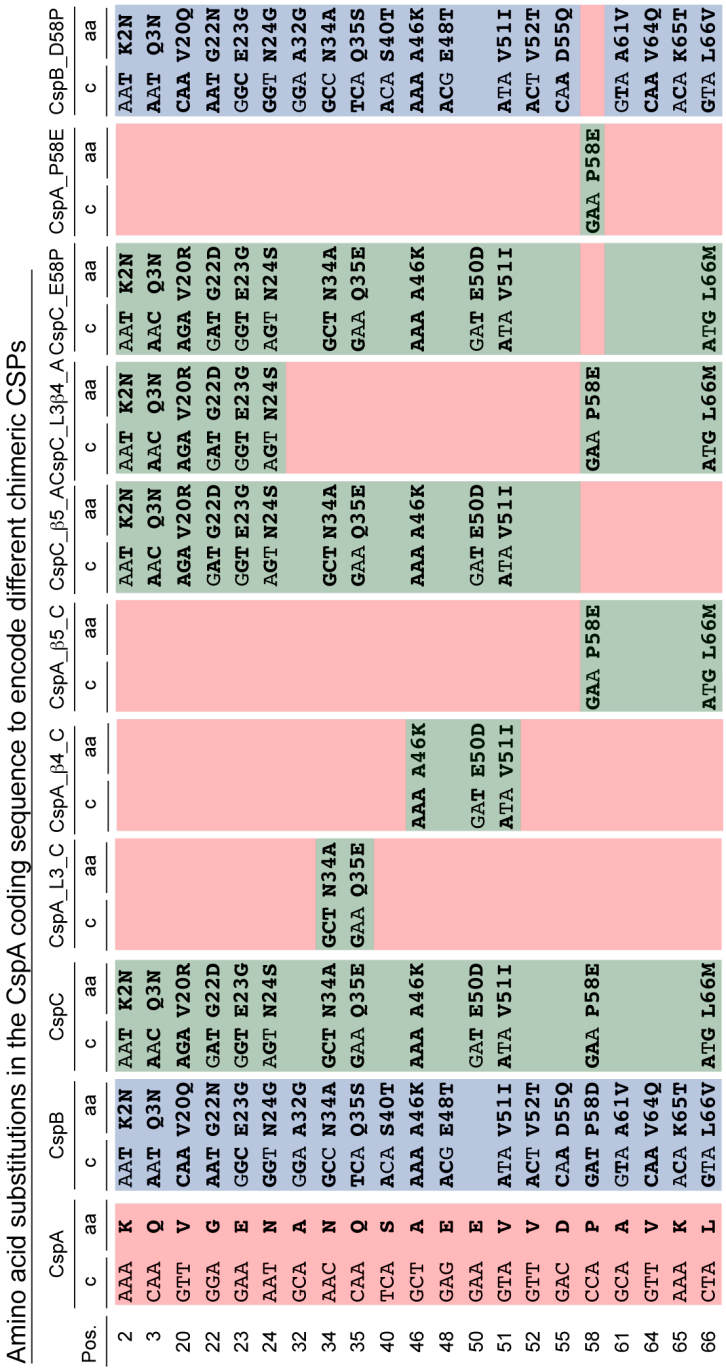

Adapted from Caballero, 2018. Only those codons (c) that were modified to include the indicated amino acid (aa) substitutions are represented. Red, blue and green colours represent protein regions from the CspA, CspB and CspC proteins, respectively. The corresponding amino acid positions (Pos) relative to the CspA ORF are also indicated.

Annex 5. Comparative analysis of CSP paralogs among staphylococcal species.

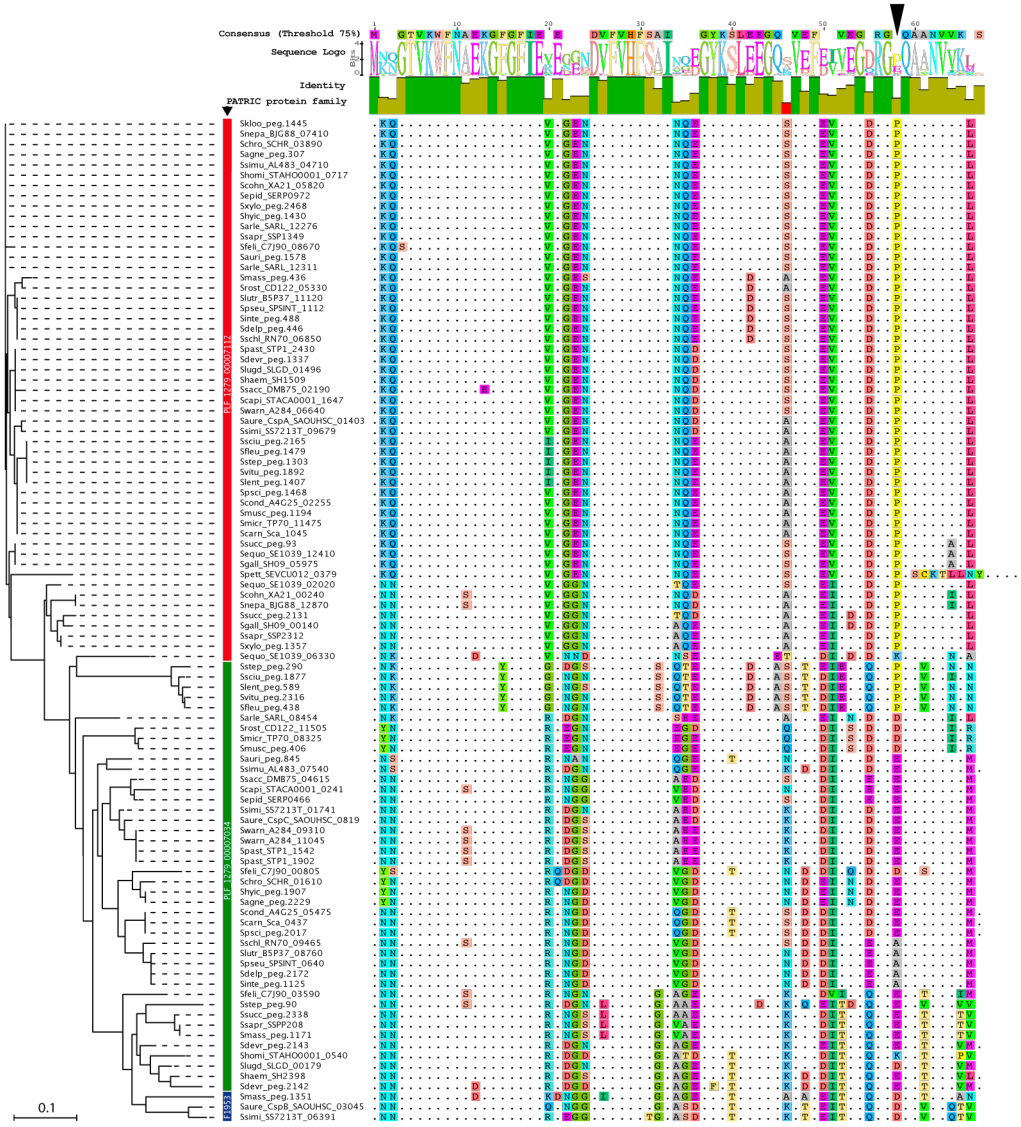

ClustalW analysis of CSP sequences revealed three main branches. Classification of CSPs according to PATRIC Protein family groups, which are based on sequence similarity over the entire protein length and the conserved genomic context, are represented by color bars (blue, PLF_1279_00001953; green, PLF_1279_00007034 and red, PLF_1279_00007112). The consensus sequence, sequence logo and protein identity plots are also indicated. Amino acid differences are highlighted. The black triangle indicates position 58. Sagne, *S. agnetis*; Sarle, *S. arlettae*; Saure, *S. aureus*; Sauri, *S. auricularis*; Scapi, *S. capitis*; Scarn, *S. carnosus*; Schro, *S. chromogenes*; Scohn, *S. cohnii*; Scond, *S. condimenti*; Sdelp, *S. delphini*; Sdevr, *S. devriesei*; Sepid, *S. epidermidis*; Sequo, *S. equorum*; Sfeli, *S. felis*; Sfleu, *S. fleurettii*; Sgall, *S. gallinarum*; Shaem, *S. haemolyticus*; Shomi, *S. hominis*; Shyic, *S. hycus*; Sinte, *S. intermedius*; Skloo, *S. kloosii*; Slent, *S. lentus*; Slugd, *S. lugdunensis*; Slutr, *S. lutrae*; Smass, *S. massiliensis*; Smicr, *S. microti*; Smusc, *S. muscae*; Snepa, *S. nepalensis*; Spast, *S. pasteuri*; Spett, *S. pettenkoferi*; Spsci, *S.*

pscifermentans; Spseu, *S. psudointermedius*; Srost, *S. rostri*; Ssacc, *S. saccharolyticus*; Ssapr, *S. saprophyticus*; Sschl, *S. schleiferi*; Ssciu, *S. sciuri*; Ssimi, *S. simiae*; Ssimu, *S. simulans*; Sstep, *S. stepanovicii*; Ssucc, *S. succinus*; Svitu, *S. vitulinus*; Swarn, *S. warneri*; Sxylo, *S. xylosus*.

Annex 6. Schematic representation of the *cspB/cspC* 5'UTR mutations.

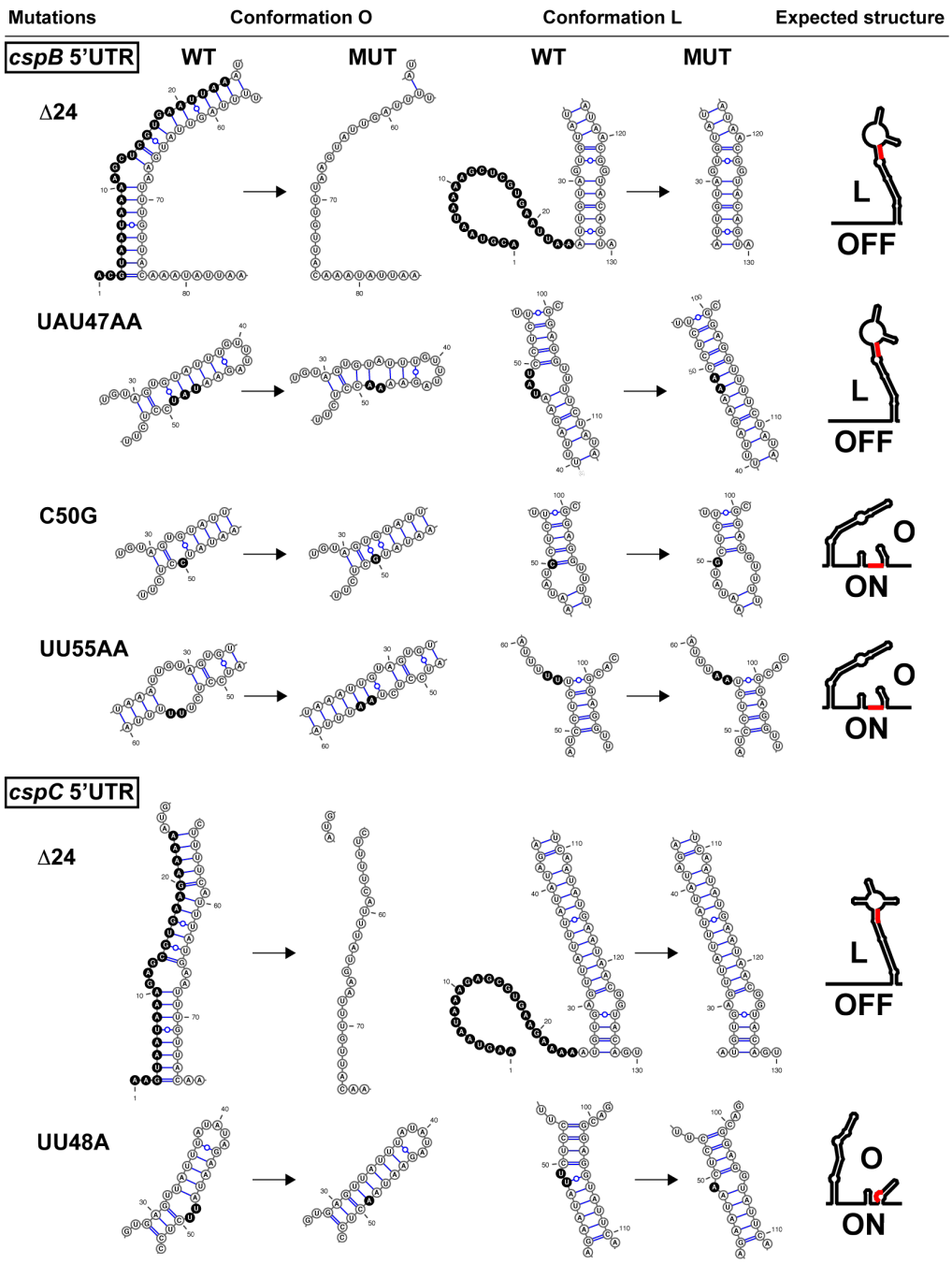

The wild type (WT) and mutated (MUT) structures are represented for conformations O and L. Mutated nucleotides were indicated in black. The expected mutated 5'UTR structure O or L (translation ON or OFF) is also showed.

Annex 7. Blastn comparative analysis showing the conservation of the *S. aureus* thermoswitch among different *Staphylococcus* species.

Staphylococcus species	Strain	Accession ID	Total CSPs	Thermo switch	Locus tag ID	*csp* genes including a thermoswitch / Sequence identity to *cspB* 5'UTR (%)			
S. aureus	NCTC 8325	NC_007795.1	3	2		*cspB*	100	*cspC*	85
S. argenteus	MSHR1132	NC_016941.1	3	2	SAMSHR1132_	*RS13405*	100	*RS03890*	85
S. schweitzeri	NCTC13712	NZ_LR134304.1	3	2	EL116_	*RS13645*	98	*RS04340*	87
S. simiae	NCTC13838	NZ_LT906460.1	3	2	CKV88_	*RS12300*	96	*RS03665*	85
S. succinus	14BME20	NZ_CP018199.1	3	2	BK815	*RS09355*	94	*RS08380*	75
S. devriesei	NCTC13828	UHCZ01000002	3	2	DYD94_	*RS10710*	89	*RS10715*	87
S. pasteuri	SP1	NC_022737.1	3	2	STP1_	*RS07870*	88	*RS09745*	83
S. warneri	NCTC11044	NZ_LR134269.1	3	2	EL082_	*RS11195*	88	*RS09370*	83
S. cornubiensis	NW1	FXUZ01000007	3	2	CCE82_	*RS08550*	88	*RS08575*	87
S. felis	ATCC 49168	NZ_CP027770.1	3	2	C7J90_	RS03590	87	*RS00805*	77
S. massiliensis	CCUG 55927	NZ_JH815593.1	3	2	A33S_	*RS0106390*	93	*RS0107335*	89
S. edaphicus	CCM 8730	MRZN01000034	3	1	BTJ66_	*RS13275*	94		
S. saprophyticus	ATCC 15305	NC_007352.1	3	1	SSP_	*RS12515*	93		
S. stepanovicii	NCTC13839	NZ_LT906462.1	3	1	CKV64_	*RS00450*	93		
S. petrasii	NCTC13835	UHDU01000001	2	1	DYD86_	*RS11030*	91		
S. haemolyticus	JCSC1435	NC_007168.1	2	1	SH_	*RS11570*	91		
S. lutrae	ATCC 700373	NZ_CP020773.1	2	1	B5P37_	*RS08760*	89		
S. pseudintermedius	HKU10-03	NC_014925.1	2	1	SPSINT_	*RS03305*	88		
S. delphini	NCTC12225	NZ_LR134263.1	2	1	EL101_	*RS10200*	88		
S. intermedius	NCTC 11048	UHDP01000003	2	1	DYA52_	*RS11680*	88		
S. lugdunensis	HKU09-01	NC_013893.1	2	1	SLGD_	*RS00875*	87		
S. hominis	C80	NZ_GL545254.1	2	1	HMPREF0798_	*RS00715*	87		
S. schleiferi	2317-03	NZ_CP010309.1	2	1	RN70_	*RS09475*	88		
S. fleurettii	FDAARGOS_682	NZ_CP046351.1	2	1	FOB90_	*RS10505*	88		
S. caprae	26D	NZ_CP031271.1	2	1	DWB96_	*RS10220*	84		
S. saccharolyticus	NCTC11807	UHDZ01000001	2	1	DYE57_	*RS09170*	83		
S. auricularis	NCTC12101	NZ_LS483491.1	2	1	DQL57_	*RS02425*	83		
S. epidermidis	ATCC 14990	NZ_CP035288.1	2	1	EQW00_	*RS09740*	83		
S. capitis	AYP1020	NZ_CP007601.1	2	1	ayp1020_	*RS00755*	83		
S. chromogenes	20B	NZ_CP031471.1	2	1	DWB92_	*RS09990*	81		
S. hyicus	ATCC 11249	NZ_CP008747.1	2	1	SHYC_	*RS09620*	80		
S. agnetis	908	NZ_CP009623.1	2	1	EP23_	*RS00105*	80		
S. rostri	DSM 21968	PPRF01000144	2	1	CD122_	*RS11505*	80		
S. muscae	ATCC 49910	NZ_CP027848.1	2	1	C7J88_	*RS09350*	80		
S. microti	DSM 22147	JXWY01000057	2	1	TP70_	*RS08325*	80		
S. equorum	KS1039	NZ_CP013114.1	2	1	SE1039_	*RS00970*	77		
S. nepalensis	JS11	NZ_CP017466.1	2	1	BJG89_	*RS13175*	78		
S. carnosus	TM300	NC_012121.1	2	1	SCA_	*RS02225*	76		
S. piscifermentans	NCTC13836	NZ_LT906447.1	2	1	CKV71_	*RS10125*	76		
S. condimenti	DSM 11674	NZ_CP015114.1	2	1	A4G25_	*RS05475*	76		
S. gallinarum	DSM 20610	JXCF01000001	2	1	SH09_	*RS00140*	75		
S. cohnii	532	LATV01000001	2	1	XA21_	*RS00240*	76		
S. xylosus	SMQ-121	NZ_CP008724.1	2	1	SXYLSMQ121_	*RS11945*	74		
S. pettenkoferi	VCU012	AGUA01000053	1	0					
S. kloosii	NCTC12415	UHDQ01000002	1	0					

Annex 8. Multiple sequence alignments of *csps* 5'UTRs from different *Staphylococcal* species.

The consensus sequence and sequence logo are shown. Blue and red arrows represent the nucleotides that form conformation O or L, respectively. Nucleotides were coloured in function of their degree of similarity as follows: dark green 100%, light green 80-99%, yellow 60-89% and white less that 60%. *Saure, S. aureus; Ssimi, S. simiae; Sschw, S. schweitzeri; Sarge, S. argenteus; Spast, S. pasteuri; Swarn, S. warneri; Scapi, S. capitis; Sepid, S. epidermidis; Ssacc, S. saccharolyticus; Scapra, S. caprae; Sagne, S. agnetis; Shyic, S. hycus; Schro, S. chromogenes; Smusc, S. muscae; Sfeli, S. felis; Sedap, S.*

edaphicus; Ssucc, S. succinus ; Sstep, S. stepanovicii; Smass, S. massiliensis; Scorn, S. cornubiensis; Sdelp, S. delphini; Sinte, S. intermedius; Spseu, S. pseudointermedius; Slutr, S. lutrae; Sfleu, S. fleurettii; Shomi, S. hominis; Smass, S. massiliensis; Sdevr, S. devriesei; Shaem, S. haemolyticus; Spetr, S. petrasii, Slugd, S. lugdunensis; Spast, S. pasteuri; Sauri, S. auricularis; Scarn, S. carnosus; Spsci, S. pscifermentans; Scond, S. condimenti; Scohn, S. cohnii; Snepa, S. nepalensis; Sgall, S. gallinarum; Ssapr, S. saprophyticus; Ssucc, S. succinus; Sequo, S. equorum; Sxylo, S. xylosus.

Annex 9. Prediction of putative mutually exclusive alternative structures in the 5'UTRs of *csp* genes from different bacteria.

Bacterial species	*csp* gene	5'UTR length (nt)[a]	Alternative structures
***Enterococcus faecalis* V583**	**(NC_004668)**		
	EF0781	116	
	EF1367	134	√
	EF1726	32	
	EF1991	117	√
	EF2925	109	
	EF2939	ND	
***Bacillus subtilis* 168**	**(NC_000964)**		
	cspC	115	
	cspB	119	√
	cspD	85	
***Clostridium perfringens* str. 13**	**(NC_003366)**		
	cspL		√
***Pseudomonas aeruginosa* PA14**	**(NC_008463)**		
	PA14_05960 (cspB)	151	√
	PA14_21760 (capB)	151	√
	PA14_30200 (cspD)	109	
	PA14_39180	ND	
	PA14_49410	ND	
	PA14_51840	ND	
***Salmonella* Typhimurium str. SL1344**	**(NC_016810)**		
	cspA	164	√
	cspB	145	√
	cspC	ND	
	cspD	87	
	cspE	43	
	cspH	23	

[a] 5'UTR length annotated using previous transcriptomic data (Lasa et al.,2012) ND: not determined.

IdAB
Instituto de Agrobiotecnología
Agrobioteknologiako Institutua

GOBIERNO DE ESPAÑA
MINISTERIO DE CIENCIA E INNOVACIÓN

CSIC
Consejo Superior de Investigaciones Científicas

Nafarroako Gobernua
Gobierno de Navarra

upna
Universidad Pública de Navarra
Nafarroako Unibertsitate Publikoa

erc
European Research Council
Established by the European Commission

European Commission

Horizon 2020
European Union funding
for Research & Innovation

upna
Universidad Pública de Navarra
Nafarroako Unibertsitate Publikoa